Variations of Calcium Isotopes (δ^{44}Ca) in Foraminifers Over the Past 24 Ma

Dissertation

zur Erlangung des Doktorgrades

der Mathematisch-Naturwissenschaftlichen Fakultät

der Christian-Albrechts-Universität

zu Kiel

vorgelegt von

Alexander Heuser

Kiel

2002

Referent: .....

Korreferent: .....

Tag der mündlichen Prüfung: .....

Zum Druck genehmigt: Kiel, den .....

Der Dekan

Hiermit erkläre ich an Eides statt, dass die vorliegende Abhandlung, abgesehen der Beratung durch meine akademischen Lehrer, nach Inhalt und Form meine eigene Arbeit darstellt. Ferner habe ich weder diese noch eine ähnliche Arbeit an einer anderen Abteilung oder Hochschule im Rahmen eines Prüfungsverfahrens vorgelegt.

Alexander Heuser

Contents

List of Tables

List of Figures

Abstract / Kurzfassung

Abstract

Calcium (Ca) isotopes show only little fractionation in nature ($\sim 6\,‰$) and mass spectrometric determination of calcium isotopic ratios is difficult (e.g. Russell et al., 1978). One of the goals of this thesis was to improve analytical precision of Ca isotope measurements. Measurements of Ca isotopes were carried out using a thermal ionization mass spectrometer (TIMS) using a two step dynamic mode (Heuser et al., 2002). In the first sequence masses 40, 41, 42 and 43 are measured simultaneously and in the second sequence the masses 44 and 48 are measured simultaneously. About 200 ng of Ca is needed for a single measurement. In order to correct for the fractionation during the measurement I added a $^{43}Ca/^{48}Ca$ double spike to the sample. For the correction of the added double spike I developed an iterative routine based on the algorithm of Compston and Oversby (1969). This new "multi-collector" technique improves sample throughput by a factor of 3 compared to "single-collector" measurements. The variations of Ca isotopes are presented as $\delta^{44}Ca$: $\delta^{44}Ca = (({}^{44}Ca/{}^{40}Ca)_{sample}/({}^{44}Ca/{}^{40}Ca)_{standard} - 1) \times 1000$ using the measured $^{44}Ca/^{40}Ca$ of NIST SRM 915a calcium carbonate as $({}^{44}Ca/{}^{40}Ca)_{standard}$.

The Ca isotope compositions of several different standard materials have been analyzed: natural CaF_2 (+1.41‰), IAPSO seawater salinity standard (+1.83 ‰) and Johnsen Matthey calcium carbonate Lots 4064 and 9912 (+0.58 and −11.46 ‰).

Measurements of $\delta^{44}Ca$ of foraminifers (*Orbulina universa*), cultured at different temperatures show a weak temperature dependent Ca isotope fractionation of 0.019 ‰ / °C (Gussone et al., in press) being in contrast to the study of Nägler et al. (2000) who reported a temperature dependent Ca isotope fractionation of *Globigerinoides sacculifer* of 0.24 ‰ / °C. This different fractionation behaviour can be attributed to a difference of the calcification process. In *O. universa* Ca is transported in a hydrated form (Ca^{2+}-aquocomplex). The relative mass difference between a $^{40}Ca^{2+}$-aquocomplex and a $^{44}Ca^{2+}$-aquocomplex with masses of about 500 amu is very small compared to the mass difference of pure $^{40}Ca^{2+}$- and $^{44}Ca^{2+}$-ions.

The $\delta^{44}Ca$ of four different foraminifera (*Globigerinoides trilobus, Globigerinoides ruber,*

Globigerinella spp. and *Globigerina bulloides*) were measured in order to reconstruct the δ^{44}Ca of seawater ($\delta^{44}Ca_{sw}$) of the past 24 Ma. The samples are from the western equatorial Pacific Ocean (ODP Leg 144, Sites 871 & 872) and from the southern Indian Ocean (ODP Leg 183, Site 1138).

The fractionation of Ca isotopes between foraminiferal calcite (cc) and seawater (sw) is expressed by the fractionation factor α ($\alpha = (^{44}Ca/^{40}Ca)_{cc}/(^{44}Ca/^{40}Ca)_{sw}$) and seawater temperature changes. Assuming a constant α, the $\delta^{44}Ca_{sw}$ can be reconstructed from the foraminiferal δ^{44}Ca. Changes of the seawater pH do not affect the fractionation between foraminiferal calcium carbonate and seawater of the studied foraminifera.

A plot of α-values and corresponding mixed layer water temperatures for the youngest foraminiferal samples suggests that *G. bulloides* and *G. trilobus* fractionate Ca isotopes independent of seawater temperature changes and *G. ruber/subquadratus* and *Globigerinella spp.* do fractionate Ca isotope depending on seawater temperature changes. This enables a reconstruction of $\delta^{44}Ca_{sw}$ using the *G. bulloides* and *G. trilobus* records and to reconstruct the temporal evolution of the western equatorial Pacific using the δ^{44}Ca records of *G. ruber/subquadratus* and *Globigerinella spp.*

The reconstructed $\delta^{44}Ca_{sw}$ records are in good agreement with previously published δ^{44}Ca data of marine carbonates (De La Rocha and DePaolo, 2000). As our sample series have a higher temporal resolution (∼1 Ma) some more details of the seawater δ^{44}Ca evolution can be seen. Additional to a minimum of $\delta^{44}Ca_{sw}$ at about 16 Ma, a minimum at about 4 Ma can be observed.

From the δ^{44}Ca of *G. ruber/subquadratus* and *Globigerinella spp.* we can estimate temperature changes while at the same time changes of the $\delta^{44}Ca_{sw}$ can be considered. The calculated temperatures of the two records vary between 28 to 31 °C over the studied time period. The most prominent feature of both trends is a cooling of about 1 to 2 °C between 4 and 1.5 Ma. During 15 and 7 Ma temperatures remained constant at about 29 °C. The evolution of temperatures between 24 and 15 Ma is ambiguous as the two records differ. The calculated temperatures are in general agreement with global benthic δ^{18}O data and local planktic δ^{18}O data giving further support to a temperature dependent Ca isotope fractionation of *G. ruber/subquadratus* and *Globigerinella spp.*

Although there are strong indications of a temperature dependent Ca isotope fractionation of *G. ruber/subquadratus* and *Globigerinella* an alternative model can be proposed assuming temperature independent Ca isotope fractionation of these two species. The calculated α-values from this study as well as data from literature suggest that α is species-specific. A change of the calcite precipitaion mechanism in the course of evolution of a foraminiferal

species could lead to a change of the fractionation factor. A change of the α-values of *Globigerinella spp.* and *G. ruber/subquadratus* between 3 and 1.5 Ma leads to a unique data set of the calculated $\delta^{44}Ca_{sw}$ of all four studied species.

Kurzfassung

Die Fraktionierung von Calcium-Isotopen in der Natur sind nur gering (~ 6 ‰) und konnten bisher nur ungen ügend genau massenspektrometrisch gemessen werden (z. B. Russell et al., 1978). Eines der Ziele der vorliegenden Arbeit war die Verbesserung der analytischen Genauigkeit und Geschwindigkeit von Calciumisotopenmessungen unter Verwendung moderner Massenspektrometer.

Die Messungen von Calcium-Isotopen wurden an einem Thermionen-Massenspektrometer (TIMS) durchgeführt (Heuser et al., 2002). Dabei erfolgte eine Messung in zwei Schritten: im ersten Schritt wurden die Massen 40, 41, 42 und 43 gemessen und im zweiten Schritt die Massen 44 und 48. Für eine Messung wurden rund 200 ng Calcium benötigt. Um die auftretende Fraktionierung während der Messungen zu korrigieren, wurde der Probe ein $^{43}Ca/^{48}Ca$-Doppelspike zugesetzt. Die Daten wurden im Anschluss an die Messung für den zugesetzten Calcium-Doppelspike korrigiert. Dafür wurde eine von mir angepasste iterative Routine, basierend auf dem Algorithmus von Compston und Oversby (1969), verwendet. Die hier verwendete "Multi-Kollektor"-Technik ermöglicht einen ca. dreimal größeren Probendurchsatz als bisherige Messmethoden. Die Variationen der Calcium-Isotopie werden als $\delta^{44}Ca$ angegeben $\delta^{44}Ca = ((^{44}Ca/^{40}Ca)_{sample}/(^{44}Ca/^{40}Ca)_{standard} - 1) \times 1000$, wobei das gemessene $^{44}Ca/^{40}Ca$ Verhältnis des Calcium-Karbonatstandards NIST SRM 915a als $(^{44}Ca/^{40}Ca)_{standard}$ verwendet wurde.

Im Rahmen dieser Arbeit wurde die Calciumisotopie verschiedener Standards bestimmt: natürlicher CaF_2 (+1,41‰), IAPSO Meerwasser-Salinitätsstandard (+1,82 ‰) und Calciumkarbonatstandards Johnsen Matthey Lots 4064 und 9912 (+0,58 und +11,46 ‰).

$\delta^{44}Ca$-Messungen von bei verschiedene Temperaturen gehälterten Foraminiferen *Orbulina universa* zeigen eine nur schwach ausgebildete Temperaturabhängigkeit des $\delta^{44}Ca$-Wertes von 0,019 ‰ / ℃ (Gussone et al., in press). Nägler et al. (2000) fanden dem gegenüber bei *Globigerinoides sacculifer* eine deutliche Temperaturabhängigkeit (0,24 ‰ / ℃). Dieses unterschiedliche Fraktionierungsverhalten kann darauf zurückgeführt werden, dass Calcium in *O. universa* als Ca^{2+}-Aquokomplex in die Zelle inkorporiert und transportiert wird. Der relative Massenunterschied zwischen einem $^{40}Ca^{2+}$-Aquokomplex und einem $^{44}Ca^{2+}$-

Aquokomplex mit Atommassen um 500 amu ist klein (1%), verglichen mit dem relativen Massenunterschied von 'reinen' $^{40}Ca^{2+}$- und $^{44}Ca^{2+}$-Ionen (10%).

Für die Rekonstruktion der Calcium-Isotopie von Meerwasser der letzten 24 Millionen Jahre wurde die Calcium-Isotopie an Proben von vier verschiedenen Foraminiferenspezies (*Globigerinoides trilobus, Globigerinoides ruber, Globigerinella spp.* und *Globigerina bulloides*) aus dem westlichen äquatorialen Pazifik (ODP Leg 144, Sites 871 & 872) und dem südlichen indischen Ozean (ODP Leg 183, Site 1138) gemessen.

Quantitativ wird die Fraktionierung von Calcium-Isotopen zwischen dem Calcit der Foraminiferenschalen (cc) und dem Meerwasser (sw) durch den Fraktionierungsfaktor α ($\alpha = (^{44}Ca/^{40}Ca)_{cc}/(^{44}Ca/^{40}Ca)_{sw}$) ausgedrückt. Aus den δ^{44}Ca Werten der Foraminiferenschalen kann das Meerwasser-δ^{44}Ca ($\delta^{44}Ca_{sw}$) unter der Annahme einer konstanten Fraktionierung berechnet werden. Andere Einflüsse auf das δ^{44}Ca der Foraminiferen als Temperatur, z. B. pH, können für die untersuchten Spezies in erster Näherung vernachlässigt werden.

Die graphische Darstellung der α-Werte mit den zugehörigen 'mixed layer' Meerwassertemperaturen der jüngsten Foraminiferenproben legt nahe, dass *G. bulloides* und *G. trilobus* Ca Isotope unabhängig von der Temperatur fraktionieren, während hingegen *G. ruber/subquadratus* und *Globigerinella spp.* Ca Isotope temperaturabhängig fraktionieren. Das ermöglicht zum einen die Rekonstruktion der Meerwasser Calciumisotopie mit Hilfe der *G. bulloides* und *G. trilobus* Daten und zum anderen eine Berechnung der Paläo-Meerwassertemperaturen des westlichen äquatorialen Pazifiks mit Hilfe der *G. ruber/subquadratus* und *Globigerinella spp.* Daten.

Die rekonstruierten $\delta^{44}Ca_{sw}$ Datensätze sind in guter Übereinstimmung mit den zuvor veröffentlichten Daten von marinen Karbonaten (De La Rocha und DePaolo, 2000). Im Vergleich zu der Untersuchung von De La Rocha und DePaolo (2000) sind hier mehr Details der $\delta^{44}Ca_{sw}$-Entwicklung erkennbar, da die zeitliche Auflösung der untersuchten Proben größer ist. Zusätzlich zu einem bekannten Minimum vor ca. 16 Ma kann ein zweites Minimum vor etwa 4 Ma beobachtet werden.

Von den *G. ruber/subquadratus* und *Globigerinella spp.* Daten können Temperaturänderungen unter gleichzeitiger Berücksichtigung der sich ändernden Meerwasser-Calciumisotopie abgeschätzt werden. Die ermittelten Temperaturen aus den beiden Datensätzen variieren zwischen 28°C und 31°C während der letzten 24 Ma. Besonders auffallend ist dabei eine Abkühlung zwischen 4 und 1,5 Ma von ca. 1 bis 2°C, die in beiden Datensätzen erkennbar ist. Zwischen 15 und 7 Ma lagen die Temperaturen konstant um 29°C. Die Entwicklung der Meerwassertemperaturen zwischen 24 und 15 Ma ist nicht eindeutig, da sich

die beiden Temperaturdatensätze in dieser Zeit deutlich unterscheiden. Ein weiteres Indiz für die temperaturabhängige Calcium Isotopenfraktionierung von *G. ruber/subquadratus* und *Globigerinella spp.* ist die Übereinstimmung der berechneten Temperaturen mit Sauerstoffisotopendaten, sowohl global als auch lokal.

Obwohl es starke Indizien für die temperaturabhängige Ca Isotopenfraktionierung von *G. ruber/subquadratus* und *Globigerinella spp.* gibt, kann eine alternative Erklärung der $\delta^{44}Ca_{cc}$ Daten, die davon ausgeht, dass es keine temperaturabhängige Fraktionierung bei den untersuchten Spezies gibt, nicht ausgeschlossen werden. Die berechneten Fraktionierungsfaktoren α von den Daten dieser Untersuchung und von publizierten Daten zeigen, dass die Fraktionierungsfaktoren spezies-spezifisch sind. Eine Änderung des Calcit-Präzipitationsmechanismus im Verlauf der Evolution einer Spezies kann zu einer Änderung des Fraktionierungsfaktors führen. Eine Änderung des α-Wertes von *Globigerinella spp.* und *G. ruber/subquadratus* zwischen 3 und 1,5 Ma führt zu einem einheitlichen $\delta^{44}Ca_{sw}$-Gesamtdatensatz aus den einzelnen Datensätzen der vier untersuchten Spezies.

References / zitierte Literaur

Compston W. and Oversby V. (1969) Lead Isotopic Analysis Using A Double Spike. *J. Geophys. Res.* **74**, 4338–4348.

De La Rocha C. L. and DePaolo D. J. (2000) Isotopic Evidence for Variations in the marine Calcium Cycle Over the Cenozoic. *Science* **289**, 1176–1178.

Gussone N., Eisenhauer A., Heuser A., Dietzel M., Bock B., Böhm F., Spero H. J., Lea D. W., Bijma J., Zeebe R. and Nägler T. F. (in press) Model for Kinetic Effects on Calcium Isotope Fractionation (δ^{44}Ca) in Inorganic Aragonite and Cultured Foraminifer (*Orbulina universa* and *Globigerinoides sacculifer*). *Geochim. Cosmochim. Acta.*

Heuser A., Eisenhauer A., Gussone N., Bock B., Hansen B. T., and Nägler Th. F. (2002) Measurement of Calcium Isotopes (δ^{44}Ca) Using a Multicollector TIMS Technique. *Int. J. Mass Spec.* **220**, 387–399.

Nägler Th. F., Eisenhauer A., Müller A., Hemleben C., and Kramers J. (2000) The δ^{44}Ca-temperature calibration on fossil and cultured *Globigerinoides sacculifer*: New tool for reconstruction of past sea surface temperatures. *Geochem. Geophys. Geosyst.* **1**, 2000GC000091.

Russell W. A., Papanastassiou D. A., and Tombrello T. A. (1978) Ca isotope fractionation on the Earth and other solar system materials. *Geochim. Cosmochim. Acta* **42**, 1075–1090.

1 Introduction and Goals

Calcium is the fifth most abundant element in the Earth's crust (including hydrosphere and biosphere) and has six stable naturally occurring isotopes with masses ranging from 40 to 48 atomic mass units (amu). Therefore, investigations on variations of calcium isotopes have been performed since the late1950's up to the end of the 1970's (e.g. Herzog et al., 1954; Backus, 1955; Backus et al., 1964; Corless, 1968; Stahl and Wendt, 1968; Coleman, 1971; Moore and Machlan, 1972; Russell et al., 1978). These early studies mainly focused on the search for calcium isotope variations in terrestrial (Artemov et al., 1966; Corless, 1968; Heumann and Luecke, 1973; Stahl, 1968; Stahl and Wendt, 1968) and extra-terrestrial samples (Backus et al., 1964; Russell et al., 1977, 1978) and the use of radiogenic ^{40}Ca (from the β^- decay of ^{40}K) as a geochronometer (Coleman, 1971; Heumann et al., 1977). A good overview of these early studies is given by Platzner (1997).

One major result of these early studies was that calcium isotope variations are very small compared to oxygen or carbon isotope variations. Mass spectrometers were not able to measure Ca isotopes with the required precision. A mile-stone was the work of Russell et al. (1978) who used a ^{42}Ca/^{48}Ca double spike. The use of a double spike improved the precision of mass spectrometric calcium isotope analysis. Differences in the ^{40}Ca/^{44}Ca of about 0.5 ‰ became clearly resolvable. However, the interest in calcium isotope variations disappeared. Through the 1980's up and the 1990's only a few investigations on calcium isotopes were published (Marshall and DePaolo, 1982; Niederer and Papanastassiou, 1984; Jungck et al., 1984; Marshall and DePaolo, 1989).

Recent advancements in mass spectrometry lead to a revivication of the interest in calcium isotope analysis. It was the study of Zhu and Macdougall (1998) showing that calcium isotope variations of foraminifers can be used as a proxy for paleo sea surface temperatures (SST) which led to the more detailed study of Nägler et al. (2000). Zhu and Macdougall (1998) also showed that the oceanic calcium isotope composition is not in steady state caused by an imbalance of Ca input and Ca output. This suggests the possibility to use δ^{44}Ca variations of seawater as a weathering proxy.

Widely used proxies for the reconstruction of past climate and environmental conditions are inter alia the oxygen isotope composition (δ^{18}O) and element/calcium ratios (e.g. Mg/Ca,

Sr/Ca, U/Ca) of biogenic (esp. foraminiferal) calcium carbonate. The major difficulties of the above proxies are:

(1) The variations are caused by more than one process: It is known that $\delta^{18}O$ variations of foraminifers are caused by temperature changes, changes in the volume of polar and continental ice sheets, changes of the seawater pH and changes of salinity (e.g. Billups and Schrag, 2002; Rohling and Bigg, 1998; Zeebe, 1999).

(2) Secondary factors affect Mg/Ca and Sr/Ca in foraminiferal calcium carbonate. These factors are: shell growth rate, pH and salinity, and species-specific effects (e.g. Delaney et al., 1985; Elderfield et al., 1996; Lea et al., 1990; Rosenthal et al., 1997).

(3) The original records/signals preserved in the foraminifers are altered through time by geochemical processes. Element/calcium ratios can be altered by diagenetic processes (especially recrystallization), secondary mineralizations of calcium carbonate and leaching/dissolution of calcium carbonates (e.g. Brown and Elderfield, 1996).

Calcium isotopes are less sensitive to alterations of the original record and variations of $\delta^{44}Ca$ of foraminifers are mainly caused by temperature variations (Nägler et al., 2000; Zhu and Macdougall; 1998) and secular changes of the seawater Ca isotopic composition.

The profit of a better knowledge of the secular variations of calcium isotopes in the oceans is twofold. (1) A neglect of secular changes can lead to over- and underestimations of temperature changes indicated by $\delta^{44}Ca$ variations of foraminifers. (2) Seawater $\delta^{44}Ca$ variations can be used as a proxy for continental weathering (Zhu and Macdougall, 1998; De La Rocha and DePaolo, 2000) as these variations are closely linked to the balance between Ca input and Ca output in the oceanic Ca cycle.

A reconstruction of the oceanic Ca cycle using Ca isotope variations can also lead to better models of the global carbon cycle as calcium carbonates ($CaCO_3$) are the main sink for oceanic Ca.

The major goals of this work were:

(1) Development of a method for precise and fast measurements of calcium isotopes by thermal ionization mass spectrometry (TIMS) using a $^{43}Ca/^{48}Ca$ double spike.

(2) Calibration of different calcium isotope standard materials (seawater, calcium carbonate and CaF_2) for inhouse use and for interlaboratory comparisons.

(3) Measurements of the calcium isotope composition of foraminiferal calcium carbonate to reconstruct the calcium isotope composition of seawater through the entire Miocene.

Chapter 2 presents a new TIMS multicollector method which I developed for the measurements of calcium isotopes. This method is now used for routine Ca isotope measurements at the GEOMAR research center, Kiel. The main advantage of this method is a higher

sample throughput compared to the previously used "single collector" method without a significant loss of precision. I have published this new method in the "International Journal of Mass Spectrometry" (Heuser et al., 2002).

Chapter 3 is a manuscript written by D. Hippler from Berne for publication in *Geo-Standards Newsletter*. To this comparative study of the δ^{44}Ca of different Ca standard materials I contributed about 60 % of the presented data from Kiel. The δ^{44}Ca values of NIST SRM 915a calcium carbonate, natural CaF_2, a seawater salinity standard (IAPSO), and two Johnsen Matthey calcium carbonate standards are presented and compared between the laboratories of Kiel, Berne and Strasbourg. The results show a good agreement between the laboratories and indicate that the multicollector measurements are as precise as single collector measurements.

In chapter 4 results of δ^{44}Ca measurements of cultured *O. universa* and inorganically precipitated aragonite are presented showing only a weak temperature dependent Ca isotope fractionation. This is in contrast to the previously published data of Nägler et al., (2000) who reported a strong temperature dependent Ca isotope fractionation (0.24 ‰/°C) for *Globigerinoides sacculifer*. A model is presented explaining the mechanisms which lead to the observed differences of temperature dependent Ca isotope fractionation. This manuscript was written by N. Gussone and is now accepted for publication in *Geochimica et Cosmochimica Acta*. I was involved in this study by numerous discussions, significant input to the development of the model and support of Ca isotope measurements.

In chapter 5, I present δ^{44}Ca ratios of four different foraminifera from the western equatorial Pacific Ocean (ODP Leg 144) and from the southern Indian Ocean (ODP Leg 183). I performed these measurements in order to reconstruct the δ^{44}Ca of seawater over the past 24 Ma. The samples were provided by Paul Pearson (Bristol, ODP Leg 144 samples) and by Florian Böhm (ODP Leg 183 samples). This is the first study comparing the δ^{44}Ca of different foraminifera over a time interval of 24 Ma. From the δ^{44}Ca of the foraminifers the δ^{44}Ca of the past seawater is reconstructed. Additionally it is possible to use the δ^{44}Ca data for a reconstruction of the evolution of seawater temperatures in the western equatorial Pacific.

In chapter 6, an alternative interpretation of the data of Chapter 5 is presented. Currently there is no direct evidence supporting this 'evolutionary' concept but it shows that other factors than temperature or seawater chemistry might be important to interpret fossil foraminiferal δ^{44}Ca records.

References:

Artemov Y., Knorre K., Strizhov V., and Ustinov V. (1966) $^{40}Ca/^{44}Ca$ and $^{16}O/^{18}O$ isotopic ratios in some calcerous rocks. *Geochem. Intern.* **3**, 1082–1086.

Backus M. M. (1955) Mass spectrometric determination o the relative isotopic abundance of calcium and the determination of geologic age. Ph.D. thesis, Massachusetts Institute of Technology.

Backus M. M., Pinson W., Herzog l., and Hurley P. (1964) Calcium isotope ratios in the Homestead and Pasamonte meteorites and a Devonian limestone. *Geochim. Cosmochim. Acta* **28**, 735–742.

Brown S. J. and Elderfield H. (1996) Variations in Mg/Ca and Sr/Ca ratios of planktonic foraminifera caused by postdepositional dissolution: Evidence of shallow Mg-dependent dissolution. *Paleoceanography* **11**, 543–551.

Corless J. (1968) Observations on the isotopic geochemistry of calcium. *Earth. Planet. Sci. Lett.* **4**, 475–478.

De La Rocha C. L. and DePaolo D. J. (2000) Isotopic Evidence for Variations in the Marine Calcium Cycle Over the Cenozoic. *Science* **289**, 1176–1178.

Elderfield H., Bertram C. J., and Erez J. (1996) A biomineralisation model for the incorporation of trace elements into foraminiferal calcium carbonate. *Earth. Planet. Sci. Lett.* **142**, 409–423.

Herzog L. F., Pinson W. H. Jr., Backus M. M., Strickland L., and Hurley P.M. (1954) Variations in isotopic abundances of strontium, calcium, and argon and related topics. Annual Progress Report for 1953-4, NYO 3934-II. Massachusetts Institute of Technology.

Heumann K. and Lieser K. (1973) Untersuchung von Isotopenfeinvariationen des Calciums in der Natur an rezenten Carbonaten und Sulfaten. *Geochim. Cosmochim. Acta* **37**, 1463–1471.

Heumann K., Schwabenbauer W., Stadler I., and Kubassek E. (1977) K/Ca-Altersbestimmungen an Kalifeldspäten. *Z. Naturforsch.* **32a**, 1333–1334.

Heumann K., Kubassek E., Schwabenbauer W., and Stadler I. (1979) Analytical Method for the K/Ca Age Determination of Geological Samples. *Fresen. Z. Anal. Chem.* **297**, 35–43.

Heuser A., Eisenhauer A., Gussone N., Bock B., Hansen B. T., and Nägler Th. F. (2002) Measurement of Calcium Isotopes ($\delta^{44}Ca$) Using a Multicollector TIMS Technique. *Int. J. Mass Spec.* **220**, 387–399.

Jungck M., Shimamura T., and Lugmair G. (1984) Ca isotope variations in Allende. *Geochim. Cosmochim. Acta* **48**, 2651–2658.

Lea D. W., Mashiotta T. A., and Spero H. J. (1999) Controls on magnesium and strontium uptake in planktonic foraminifera determined by live culturing. *Geochim. Cosmochim. Acta* **63**, 2369–2379.

Marshall B. D. and DePaolo L. J. (1982) Precise age determinations and petrogenetic studies using the K-Ca method. *Geochim. Cosmochim. Acta* **46**, 2537–2545.

Marshall B. D. and DePaolo L. J. (1989) Calcium isotopes in igneous rocks and the origin of granite. *Geochim. Cosmochim. Acta* **53**, 917–922.

Moore L.J. and Machlan L.A. (1972) High Accuracy Determination of Calcium in Blood Serum by Isotope Dilution Mass Spectrometry. *Anal. Chem.* **44**, 2291–2296.

Nägler T. F., Eisenhauer A., Müller A., Hemleben C. and Kramers J. (2000) The δ^{44}Ca-temperature calibration on fossil and cultured *Globigerinoides sacculifer*: New tool for reconstruction of past sea surface temperatures, *Geochem. Geophys. Geosyst.* **1**, 2000GC000091.

Niederer F. R. and Papanastassiou D. A. (1984) Ca isotopes in refractory inclusions. *Geochim. Cosmochim. Acta* **48**, 1279–1293. Platzner I. T. (1997) Modern Isotope Ratio Mass Spectrometry. John Wiley & Sons.

Rohling E. J. and Bigg, G.R. (1998): Paleosalinity and δ^{18}O: A critical assessment. *J.. Geophys. Res., C* **103**, 1307–1318

Rosenthal Y., Boyle E. A., and Slowey N. (1997) Temperature control on the incorporation of magnesium, strontium, fluorine and calcium into benthic foraminiferal shells from Little Bahama Bank: Prospect for thermocline paleoceanography. *Geochim. Cosmochim. Acta* **61**, 3633–3643.

Russell W. A., Papanastassiou D. A., and Tombrello T. A. (1978) Ca isotope fractionation on the Earth and other solar system materials. *Geochim. Cosmochim. Acta* **42**, 1075–1090.

Stahl W. (1968) Search for natural variations in calcium isotope abundances. *Earth. Planet. Sci. Lett.* **5**, 171–174.

Stahl W. and Wendt L. (1968) Fractionation of calcium isotopes in carbonate precipitation. *Earth. Planet. Sci. Lett.* **5**, 184–186.

Zeebe R. (1999) An explanation of the effect of seawater carbonate concentration on foraminiferal oxygen isotopes. *Geochim. Cosmochim. Acta* **63**, 2001–2007.

Zhu, P. and Macdougall J. (1998) Calcium isotopes in the marine environment and the oceanic calcium cycle, *Geochim. Cosmochim. Acta* **62**, 1691–1698.

2 Measurement of Calcium Isotopes (δ^{44}Ca) Using a Multicollector TIMS Technique

by

A. Heuser[1,2,*], A. Eisenhauer[1], N. Gussone[1], B. Bock[1], B.T. Hansen[3] and Th.F. Nägler[4]

[1] GEOMAR, Forschungszentrum für Marine Geowissenschaften, Wischhofstr. 1–3. 24148 Kiel, Germany

[2] Graduiertenkolleg "Dynamik globaler Kreisläufe im System Erde", Wischhofstr. 1–3, 24148 Kiel, Germany

[3] Göttinger Zentrum für Geowissenschaften, Goldschmidtstr. 3, 37077 Göttingen, Germany

[4] Institut für Geologie, Gruppe Isotopengeologie, Universität Bern, Erlacherstr. 9a, 3012 Bern, Switzerland

[*] Corresponding author. Tel.: +49-431-600-1404; Fax: +49-431-600-1400;
e-mail: aheuser@geomar.de

International Journal of Mass Spectrometry **220**: 387–399 (2002)

Abstract

We propose a new "multicollector technique" for the thermal ionization mass spectrometer (TIMS) measurement of calcium (Ca) isotope ratios improving average internal statistical uncertainty of the $^{44}Ca/^{40}Ca$ measurements by a factor of 2–4 and average sample throughput relative to the commonly used "peak jumping method" by a factor of 3. Isobaric interferences with potassium ($^{40}K^+$) and titanium ($^{48}Ti^+$) or positively charged molecules like $^{24}Mg^{19}F^+$, $^{25}Mg^{19}F^+$, $^{24}Mg^{16}O^+$ and $^{27}Al^{16}O^+$ can either be corrected or are negligible. Similar, peak shape defects introduced by the large dispersion of the Ca isotope system do not influence Ca isotope ratios. We use a $^{43}Ca/^{48}Ca$ double spike with an iterative double spike correction algorithm for precise isotope measurements.

Keywords: calcium isotope analysis; TIMS; multicollector; double spike correction

2.1 Introduction

Calcium (Ca) is the fifth most abundant element in the lithosphere and plays a major role in many geological and biological processes (e.g. [1, 2]). It has six naturally occurring stable isotopes with atomic mass units (amu) and abundances of ^{40}Ca (96.941 %), ^{42}Ca (0.647 %), ^{43}Ca (0.135 %), ^{44}Ca (2.086 %), ^{46}Ca (0.004 %) and ^{48}Ca (0.187 %). A good overview about previous investigations of possible isotope variations is given by Platzner [3]. Natural variations of the Ca-isotope ratios may be introduced by the beta-decay of the potassium isotope ^{40}K (half-life: 1.277×10^9 a) increasing the relative abundance of ^{40}Ca. The amount of this increase can be used to date igneous and metamorphic rocks [4–8]. Furthermore, Ca isotope variations can be introduced by kinetic fractionation due to diffusion and chemical exchange reactions. Nägler et al. [9] and Zhu and Macdougall [10] found a temperature dependence of the Ca-isotope fractionation during calcium carbonate ($CaCO_3$) precipitation. These authors observed that with increasing temperatures the heavier isotope (^{44}Ca) becomes enriched relative to ^{40}Ca [9]. However, this temperature controlled fractionation of Ca is different to the behavior of other stable isotope systems like oxygen ($\delta^{18}O$), carbon ($\delta^{13}C$) and boron ($\delta^{11}B$) [11] where the light isotopes become enriched relative to the heavier ones with increasing temperature. Most likely, the different behavior of Ca during temperature dependent fractionation is related to the fact that Ca is controlled by kinetic fractionation rather than by equilibrium fractionation [12]. This observation confirms measurements by Stahl and Wendt [13] who experimentally showed that the Ca-isotope variations during Rayleigh fractionation must be lower than about

1.5 ‰/amu. Heumann and Luecke [4] and later O'Neil [14] stated that major Ca isotope fractionation only occurs when materials with ion exchange capacity are involved and that fractionations are proportional to the mass-difference, that is δ^{48}Ca is about two times larger than δ^{44}Ca. As a consequence large isotope fractionation effects in an order of up to 22 ‰ can be observed during ion exchange processes [15–18]. Corless [19] suggested that variations of Ca isotope ratios in the order up about 10 ‰ (^{48}Ca/(total Ca)) can also be caused by kinetic isotope fractionation introduced by biological mediated processes.
It was Russell et al. [20–22] who first used a ^{42}Ca/^{48}Ca double spike for more accurate measurements of the calcium isotopic composition. They normalized the measured ^{44}Ca/^{40}Ca to a calcium fluorite standard (CaF_2) supposed to represent average bulk earth composition (δ^{44}Ca=[(^{44}Ca/^{40}Ca)$_{sample}$ / (^{44}Ca/^{40}Ca)$_{standard}$ − 1] × 1000). Generally, using the "peak jumping method" masses 40, 41, 42, 43, 44 and 48 were measured in sequence on a single faraday cup. Disadvantage of this time consuming method is the small sample throughput in combination with a reduced internal statistical precision [23]. Other mass spectrometers (diodelaser resonance ionization mass spectrometry [24] and multicollector ICPMS [25]) have also been tested for Ca isotope analysis. The main problem of the ICPMS measurements are isobaric interferences with the argon isotope $^{40}Ar^+$ on mass 40 or $^{12}C^{16}O_2{}^+$ on mass 44. Recent progress in the measurement of Ca isotopes using ICP-MS has recently been demonstrated by ([26–28]) by using collision or reaction cells to remove interferering $^{40}Ar^+$.
Here we present a new technique using a multi-collector TIMS (Finnigan MAT 262 RPQ+) in combination with a modified double spike technique improving the statistical uncertainties (internal reproducibility) of Ca isotope measurements and the average sample throughput. Multicollector techniques have been used previously for Ca isotope analysis [29, 30] but only for measuring masses 40–42 (first sequence) and 42–44 (second sequence) without using a double spike.

2.2 Experimental Methods and Mass Spectrometry

2.2.1 ^{43}Ca/^{48}Ca-spike solution

During the mass spectrometric measurement and chemical purification (ion exchange column chemistry and cleaning procedures) of a sample the calcium isotopes fractionate to a large extend [31–34]. In order to measure the original Ca isotope composition before any fractionation introduced by the measurements we apply the Ca double spike technique. This technique was originally introduced for Ca isotope measurements by Russell et al. [21]

Table 2.1: Ca spike concentration and isotope composition.

Isotope	Concentration (ng/g)
^{40}Ca	8.86
^{42}Ca	0.46
^{43}Ca	47.20
^{44}Ca	2.91
^{48}Ca	60.00

Isotope Ratio	Value
^{40}Ca/^{48}Ca	0.147729
^{42}Ca/^{48}Ca	0.007668
^{43}Ca/^{48}Ca	0.786624
^{44}Ca/^{48}Ca	0.048534
^{44}Ca/^{40}Ca	0.328537

who used a Ca double spike enriched in ^{42}Ca and ^{48}Ca. In contrast we use a spike enriched in ^{43}Ca and ^{48}Ca being those isotopes with the lowest natural abundance beside ^{46}Ca. A basic request is that the isotope composition of the spike has to be well known and that the spike material is depleted in ^{40}Ca and ^{44}Ca being the isotopes of interest (Tab. 2.1).

The ^{43}Ca/^{48}Ca double spike is added to the sample prior to chemical purification. In the mixture (spike + sample) most of the ^{43}Ca and ^{48}Ca comes from the spike whereas most of the ^{40}Ca and ^{44}Ca is from the sample. From the measured ^{40}Ca/^{48}Ca and ^{44}Ca/^{48}Ca and the knowledge of the ^{43}Ca/^{48}Ca ratio of the spike we can correct for all not naturally introduced fractionations of the Ca isotopes during chemical purification and mass-spectrometer measurement. Measured ^{44}Ca/^{40}Ca ratio have to be corrected for ^{44}Ca and ^{40}Ca introduced by the addition of the Ca spike solution. We adjusted the sample to spike ratio in a way that about 90 % of ^{48}Ca and ^{43}Ca originated from the spike. We found that this sample to spike ratio guaranteed most reliable Ca isotope measurements.

2.2.2 Sample preparation and sample loading

In order to perform the measurements we use three different Ca standards: (1) calcium carbonate powders (NIST SRM 915a, Johnson Matthey lot No. 4064 and lot No. 9912, also used by [21]), (2) an international seawater salinity standard (IAPSO) and (3) CaF_2 for the comparison with previous studies and for normalization procedures.

We mixed a Ca standard solution (1) with a concentration of about 500 $ng_{Ca}/\mu L$ from 250 mg of the NIST SRM915a standard which was dissolved in 4 mL of ultrapure 2 N HNO_3

and then further diluted with 196 mL ultrapure H_2O. The Johnson Matthey calcium carbonate standards have been dissolved in ultrapure HCl resulting in concentrations of about 220 $ng_{Ca}/\mu L$.

Furthermore, a seawater standard solution (2) was mixed from a 100 µL batch of the IAPSO seawater standard and about 12.66 mL of the $^{43}Ca/^{48}Ca$ double spike solution. This mixture was evaporated to dryness and then redissolved in 1 mL of ultrapure 2.5 N HCl. 500 µL of this solution were loaded onto ion exchange columns (length: 215 mm, diameter: 2 mm; cation exchange resin: Biorad AGW 50×8, 200–400 mesh) in order to extract the Ca-fraction. After rinsing the columns with 14 mL 2.5 N HCl the Ca-fraction was collected, evaporated and then redissolved in 50 µL 2.5 N HCl.

A CaF_2 (3) standard was prepared from a piece of natural fluorite dissolved in 6 N HCl and diluted with ultrapure H_2O to a concentration of about 100 $ng_{Ca}/\mu L$.

For the purpose of mass spectrometric Ca isotope measurements we added 30 µL of the double spike solution to 100 ng of Ca of the sample resulting in a spike to sample ratio of about 1 to 28. The mixture of spike and sample is evaporated to dryness and then redissolved in 1 to 2 µL of ultrapure 2.5 N HCl in order to guarantee complete chemical equilibrium.

For the TIMS measurements zone refined rhenium ribbon single filaments are used in combination with a Ta_2O_5-activator and the so called "sandwich-technique" following a method previously published by Birck [35]. About 0.5 µL Ta_2O_5 activator solution is first added on the filament and heated to near dryness at a current of about 0.7 A. Then 1 to 2 µL sample solution with concentrations of 200 to 400 $ng_{Ca}/\mu L$ were added on top of the activator solution and again heated close to dryness at 0.7 A. Another 0.5 µL of the activator were then loaded onto the filament and heated at 0.7 A to dryness. Finally, the filament was heated to 1.5 A and left there for about 20 s. Finally, the electrical current was increased until a weak red glow is visible followed by an immediate shut down of the electrical current. The activator solution stabilizes the signal intensity resulting in a precise measurement of the Ca isotopic composition of the sample/spike mixture.

2.2.3 TIMS multicollector measurement procedure

All Ca isotope measurements were carried out at the GEOMAR mass spectrometer facilities in Kiel, Germany and at the "Göttinger Zentrum für Geowissenschaften" (Göttingen, Germany). Both institutes are equipped with a Finnigan MAT262 RPQ+ mass spectrometer which are operated in positive ionization mode with a 10 kV acceleration voltage and a

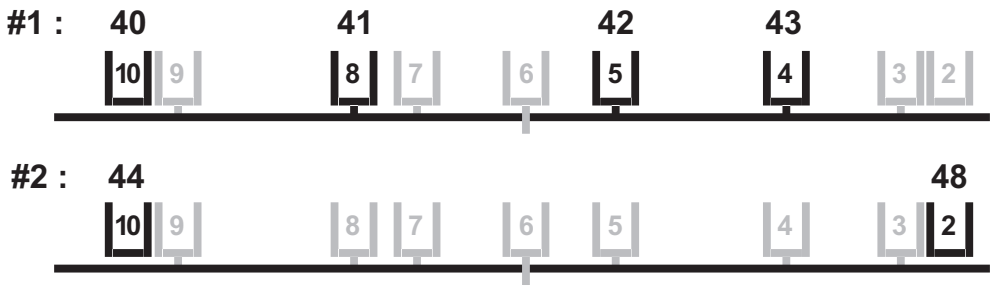

Figure 2.1: The cup configuration for Ca isotope measurement on a Finnigan MAT 262 RPQ+ mass spectrometer can be seen. In a first sequence $^{40}Ca^+$, $^{41}K^+$, $^{42}Ca^+$ and $^{43}Ca^+$ are measured. In a second sequence $^{44}Ca^+$ and $^{48}Ca^+$ are measured. Cup 6 is a fixed cup. Cup 10 is attached to cup 9 and cup 2 is attached to cup 3.

$10^{11}\,\Omega$ resistor for the faraday cups. The instruments are equipped with nine faraday cups (2–10) as detection system but can not account for the dispersion of the whole Ca isotope mass range from 40 to 48 amu, respectively.

The faraday cups are moveable and are arranged in a way to allow the simultaneous measurement of all Ca isotopes in two sequences. During the first sequence (1) the masses of 40, 41, 42, and 43 are measured simultaneously and during the second sequence (2) the masses 44 and 48 are measured seperately (Fig. 2.1, Tab. 2.2). Note, that with this arrangement of the cups it is also possible to measure the low intensity of ^{46}Ca in the second sequence using the ion counting system. Mass 41 is measured in order to monitor interfering $^{40}K^+$ ($^{40}K/^{41}K = 1.7384 \times 10^{-3}$).

To start the measurement, the filament is heated automatically to 2600 mA (corresponding to a temperature of about 1450 °C) at a rate of 200–240 mA/min. While heating up a cup gain calibration was carried out. After this first heating the signal was focussed and peak centering was performed. Then the filament was heated manually up to about 3000 mA (corresponding to about 1500–1580 °C). When the intensity of the ion beam reached 3–5×10^{-11} A on mass 40 data acquisition was started (temperatures at this point usually are 1500 to about 1600 °C). Before each block the baseline was recorded with closed beam valve (16 s integration time). Data acquisition summarizes 11 scans to one block. A minimum of 6 blocks corresponding to 66 scans was measured. Data acquisition was stopped when the 2σ-standard deviation ($2\sigma_{mean}$) of the $^{44}Ca/^{48}Ca$ and $^{40}Ca/^{48}Ca$ ratios was lower than 0.15 ‰.

A set of experiments were performed to find the ideal integration and idle times. The integration and idle times have been varied between 1 and 8 s. The experiments using 2 sec integration and 1 sec idle time show the highest $^{44}Ca/^{40}Ca$ ratios while longer integration

Table 2.2: Cup positions for Ca isotope multicollector measurements.

Cup #	distance from the center cup (mm)		Mass (amu)	
	GEOMAR, Kiel	GZG, Göttingen	1^{st}sequence	2^{nd}sequence
2	+28.36	+30.15	–	48
3	+25.15	+26.94	–	–
4	+19.07	+19.41	43	–
5	+3.15	+3.58	42	–
6	0.00	0.00	–	–
7	−10.42	−9.46	–	–
8	−12.23	−12.83	41	–
9	−25.33	−25.42	–	–
10	−27.17	−28.29	40	44

Note: Differences in cup positions between the two spectrometers are due to slightly different effective acceleration voltages. At both mass spectrometers cup 10 is attached to cup 9 and cup 2 is attached to cup 3 due to specific requirements. The distances between cup 9 to 10 and cup 2 to 3 are different for both machines. The largest possible distance for the outer cups 10 and 2 is about 30 mm relative to the fix center cup.

and idle times result in lower $^{44}Ca/^{40}Ca$ ratios (Fig. 2.2). Presumably, if the idle time is short (1 s), the ^{40}Ca signal is not completely disintegrated before recording the ^{44}Ca signal. In order to guarantee complete disintegration of the ^{40}Ca signal on the faraday cup we chose 4 seconds of integration and idle time for both sequences under measuring conditions. Table 2.3 shows a summary of the experimental conditions for Ca isotope analysis using TIMS.

2.2.4 Isobaric interferences and cluster-ions

The most obvious interference on the Ca isotope system arises from $^{40}K^+$ because in all isotope measurements carried out K was present to various extend. The isobaric interference of $^{40}K^+$ interfering with $^{40}Ca^+$ can be corrected by monitoring mass 41 ($^{40}K/^{41}K = 1.7384 \times 10^{-3}$). In general, the intensity on mass 41 is less than 10^{-14} A when measurement started. Thus, an interference correction is negligible because only signals in the order of 10^{-11} A on mass 40 would request a correction.

Further possible isobaric interference arise from magnesium fluoride (MgF^+). These molecular ions would interfere on masses 43 ($^{24}Mg^{19}F^+$) and 44 ($^{25}Mg^{19}F^+$). By monitoring ($^{26}Mg^{19}F^+$) at mass 45 detailed studies indicated no significant isobaric contributions on $^{43}Ca^+$ and $^{44}Ca^+$, respectively. Another group of isobaric interferences may arise from Mg- and Al-oxides interfering on mass 40 ($^{24}Mg^{16}O^+$) and 43 ($^{27}Al^{16}O^+$). These interferences

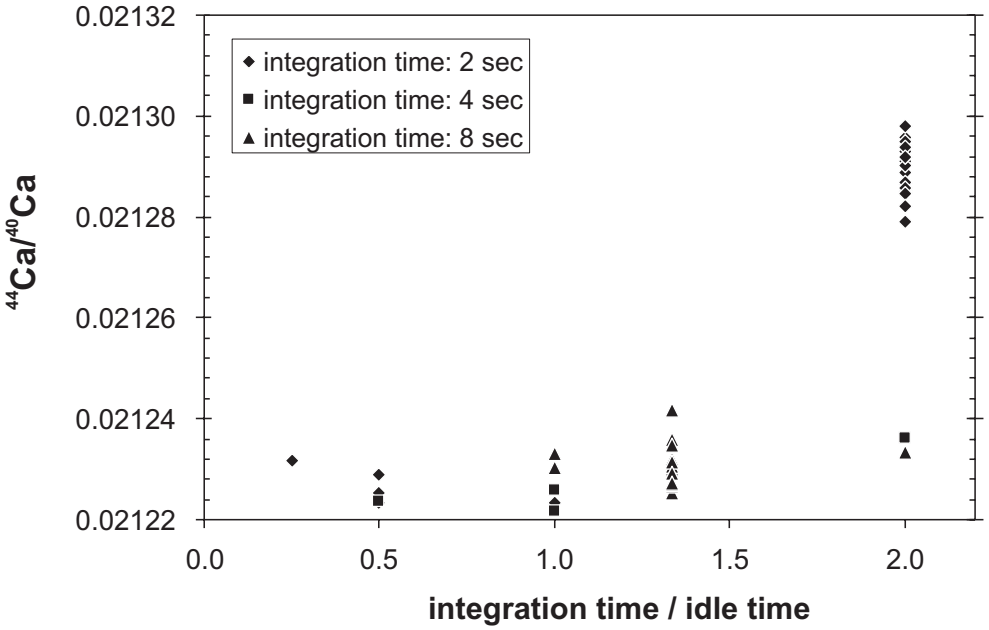

Figure 2.2: Set of measurements with different integration times and different integration to idle time ratios. The measurements with a 2 second integration time and 1 second idle time (integration time to idle time ratio = 2) show the highest $^{44}Ca/^{40}Ca$ ratios. However, increasing the idle time to 4 seconds results in lower $^{44}Ca/^{40}Ca$ ratios independent from the ratio of the integration time to idle time.

Table 2.3: Experimental conditions used for Ca isotope analysis by TIMS

Property	Setting
accelerating voltage	10 kV
amplifier resistor	$10^{11}\,\Omega$
source vacuum	$4\text{–}8 \times 10^{-8}$ mbar
analyzer vacuum	$5\text{–}9 \times 10^{-9}$ mbar
reference cup	10
cup gain calibration	before each sample
baseline	each block
	delay time: 10 s
	integration time: 16 s
	closed valve
peak centering	every 3rd block
data collection	blocks per run: ≥ 6
	scans per block: 11
	integration time: 4 s (both sequences)
	idle time: 4 s (both sequences)
analyzing temperature	1500–1580 °C

can not be monitored. However, Mg/Ca and Al/Ca ratios are generally low in our samples, therefore we consider possible interferences to be negligible. Interferences from $^{48}Ti^{+}$ and double charged $^{84}Sr^{2+}$, $^{86}Sr^{2+}$ and $^{88}Sr^{2+}$ (masses 42, 43 and 44) were not observed. Whereas no MgF^{+} has been observed some other fluorides like CaF^{+} (masses 59–67), SrF^{+} (masses 103–107) and BaF^{+} (masses 152–157) have been detected. The highest signals of CaF^{+} have been observed at temperatures of about 1500 °C with an intensity on mass 59 ($^{40}Ca^{19}F^{+}$) of about 80×10^{-14} A. Measurements showed that the CaF^{+} molecules (masses 61, 62, 63 and 67) decrease in several minutes to background levels which inhibited a quantitative determination of their Ca isotopic composition.

2.2.5 Peak shape defects

Fletcher et al. [29] reported peak shape defects using a wide-dispersion multi-collector mass spectrometer. They showed that the peak shapes from the outer cups are asymmetric limiting the range of measurable mass dispersion. We also found these peak-shape defects for the outer cups (Fig. 2.3) but the asymmetry is less pronounced than reported by Fletcher et al. [29]. By narrowing the aperture slits the asymmetry of the peak shapes can be reduced. However, measurements with and without the aperture slits do not show any significant influence on the Ca isotope ratios. Therefore, we conclude that the small peak shape defects observed are negligible.

2.3 Double Spike Correction

2.3.1 Ca Double Spike Data Reduction Algorithm

The results of the measurements have to be corrected for the added $^{43}Ca/^{48}Ca$ double spike. We use an iterative routine based on an algorithm presented by Compston and Oversby [36] and originally designed for lead isotope analysis. In this algorithm the linear fractionation terms have been replaced by terms which allow a correction following the exponential law. The use of the exponential law was proposed by Russell et al. [21] and later by Hart and Zindler [37] to be more suitable for fractionation correction of the Ca isotope system. (Fig. 2.5, equations (2) and (8)). The basic ideas are visualized in Fig. 2.4 where it is schematically illustrated that the measured Ca isotope ratios of the sample/spike mixture $(^{40}Ca/^{48}Ca)_{meas}$, $(^{43}Ca/^{48}Ca)_{meas}$, $(^{44}Ca/^{48}Ca)_{meas}$ do not plot on the ideal mixing line due to the mixing of spike and sample solution having different Ca isotope composition and due to isotope fractionation during mass spectrometer measurement.

This problem can be solved by an iterative method as it is visualized in the flow chart of

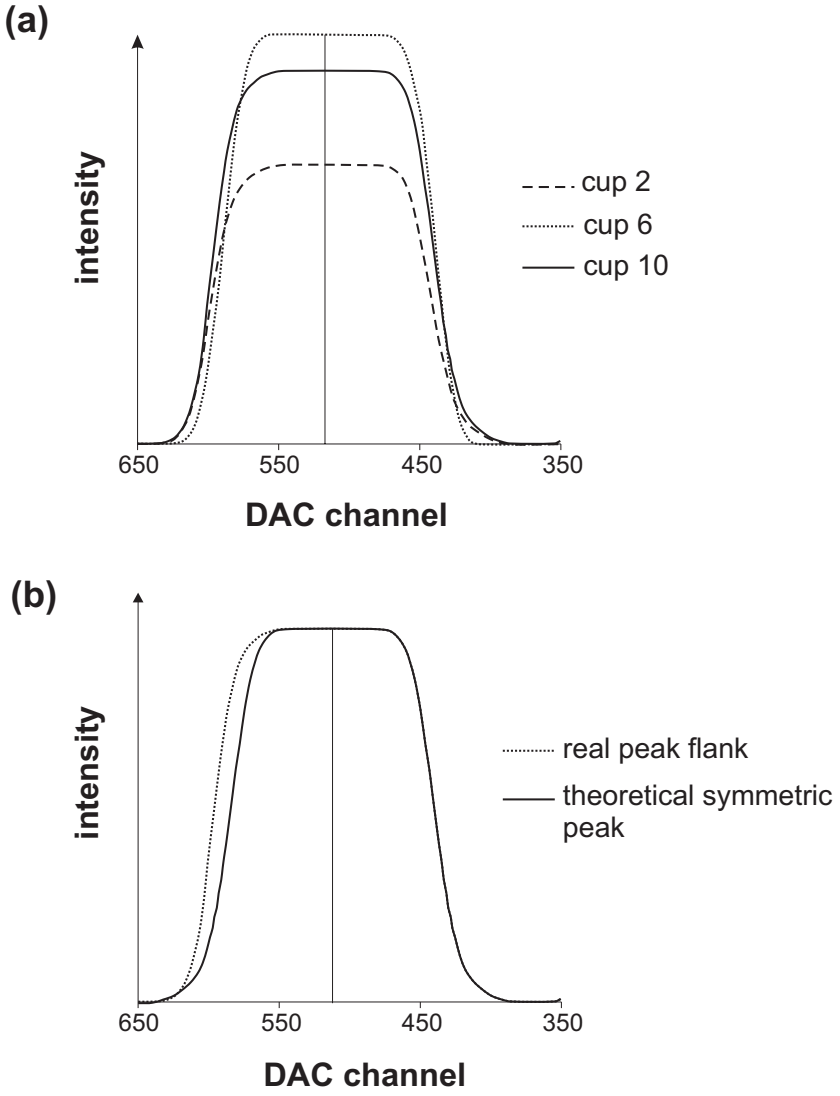

Figure 2.3: (a) The peak shapes of cup 6 and of the two outermost cups 2 and 10 are visualized. It can be seen that the peak shapes of the two outermost cups are asymmetric relative to cup 6. (b) Detailed comparison of expected vs. measured peak shape for cup 10. A peak shape defect can be seen resulting in an asymmetry at the high energy side.

Fig. 2.5. Iterative solutions to the "exponential double spike" problem have also been presented by [9, 38, 39] based on the routines of Compston and Oversby [36] or other routines [e.g. 40-42].

The algorithm presented in Fig. 2.5 starts with a first approximation of the spike to sample ratio Q (Q=$^{48}Ca_{sample}/^{48}Ca_{spike}$). Q can be calculated based on the measured $(^{40}Ca/^{48}Ca)_{meas}$ ratio ($Q_{48(40)}$ in equation (11)) and from the $(^{44}Ca/^{48}Ca)_{meas}$ ratio ($Q_{48(44)}$ in equation (12)). Note, that the $(^{40}Ca/^{48}Ca)_{sample}$ and $(^{44}Ca/^{48}Ca)_{sample}$ values in equation (11) and (12) for this first cycle of the algorithm correspond to either

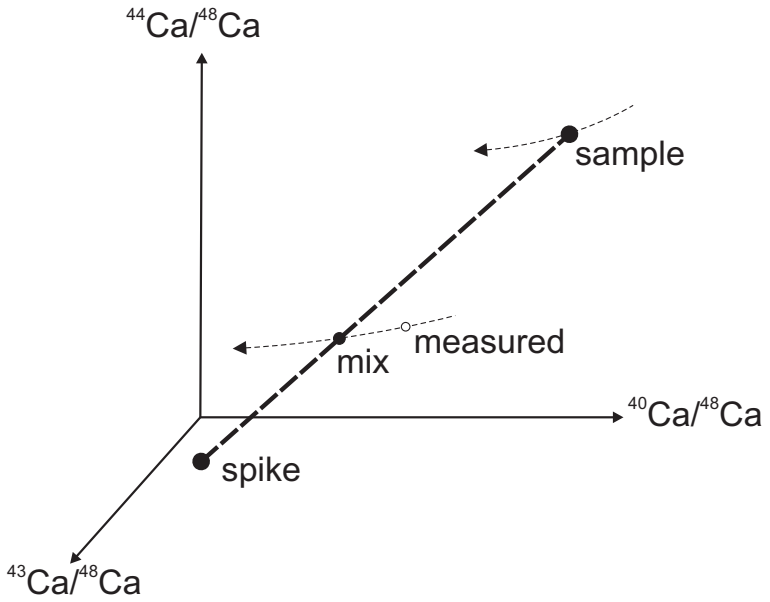

Figure 2.4: Three dimensional illustration of the Ca isotope composition of the spike, sample and the spike/sample mixture. Dotted lines represent fractionation curves. The values of the "mix" point has to be calculated from the "measured" point by an iterative approach. For calculation the well known Ca isotope ratios of the "spike" are used and for the "sample" ratios as start parameters the previously published values of Russell et al. [21] are adopted

the $^{40}Ca/^{48}Ca$ and $^{44}Ca/^{48}Ca$ [18]of a Ca standard or to the measured $^{40}Ca/^{48}Ca$ and $^{44}Ca/^{48}Ca$ of the unspiked sample. Of course, calculated $Q_{48(40)}$ and $Q_{48(44)}$ are different but serve as base for the first approximation (equation (1)) of the $^{43}Ca/^{48}Ca$ ratio ($(^{43}Ca/^{48}Ca)_{calc}$). Q_{48} is the arithmetic mean of $Q_{48(40)}$ and $Q_{48(44)}$ (equation (13)). Then, a first approximation of the fractionation factor β can be estimated (equation (2)) from the calculated $(^{43}Ca/^{48}Ca)_{calc}$ and the measured $(^{43}Ca/^{48}Ca)_{meas}$ ratios. From the equations (3) and (4) fractionation factor β allows to calculate improved values of $(^{40}Ca/^{48}Ca)_{calc}$ and $(^{44}Ca/^{48}Ca)_{calc}$ from $(^{40}Ca/^{48}Ca)_{meas}$ and $(^{44}Ca/^{48}Ca)_{meas}$. In equation (5) a first approximation $(^{40}Ca/^{44}Ca)_{calc}$ and from equation (7) a first estimate of the anticipated $(^{44}Ca/^{40}Ca)_{sample-new}$ can be calculated. Comparison of $(^{44}Ca/^{40}Ca)_{sample}$ and $(^{44}Ca/^{40}Ca)_{sample-new}$ in equation (8) allows the calculation of a fractionation factor (fu) and a new estimate of the $(^{44}Ca/^{48}Ca)_{sample-new}$ ratio (equation (9)) and the $(^{40}Ca/^{48}Ca)_{sample-new}$ ratio (equation (10)). With the latter values algorithm will start again at equation (11) and (12). The iterations converge rapidly already after about 4 to 5 cycles the difference between $Q_{48(40)}$ and $Q_{48(44)}$ becomes lower than about 10^{-6} and calculations can be terminated.

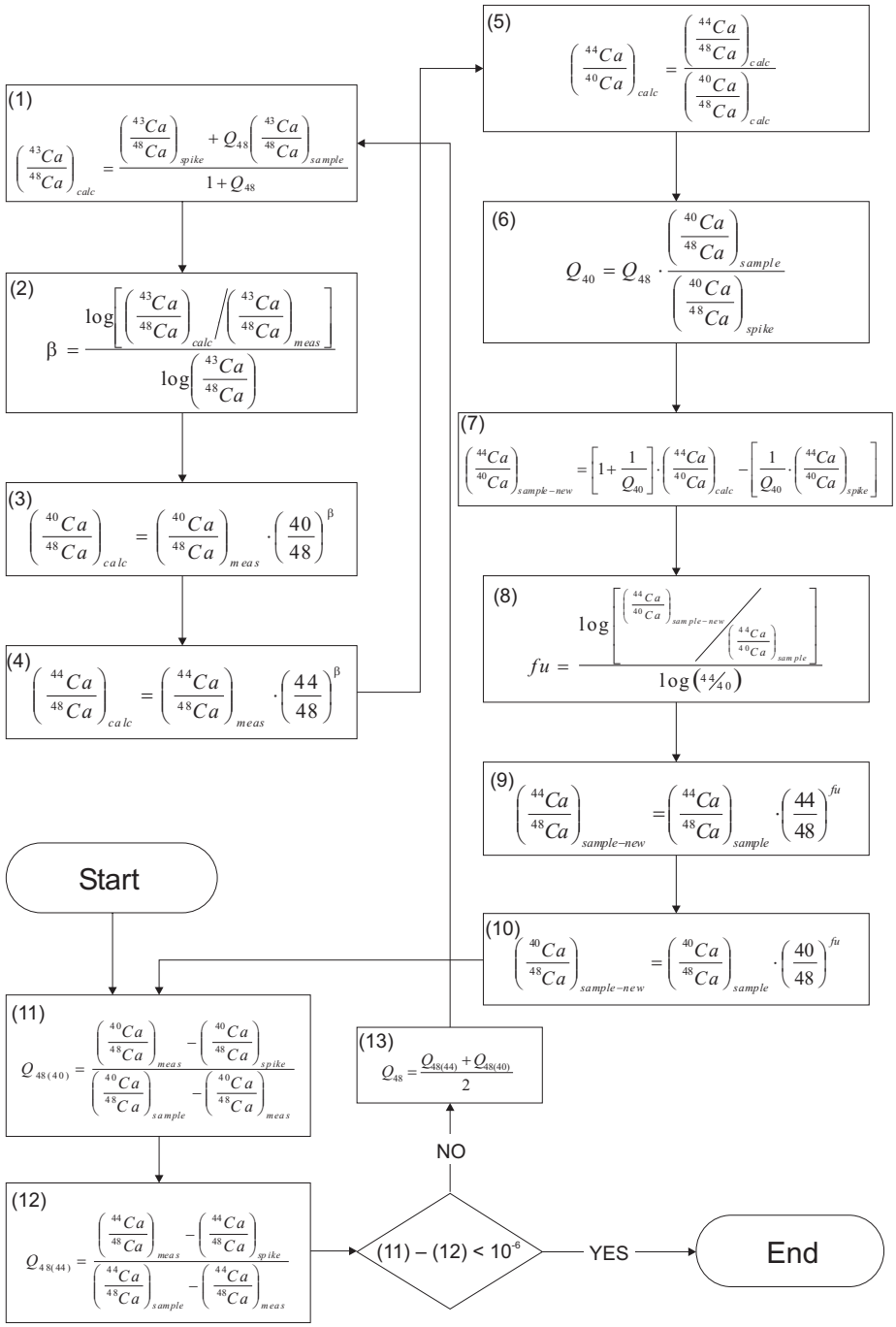

Figure 2.5: Flow chart of the numerical algorithm applied to determine the original $(^{44}Ca/^{40}Ca)_{sample}$ ratio from the $(^{40}Ca/^{48}Ca)_{meas}$ and $(^{44}Ca/^{48}Ca)_{meas}$ ratios. meas = measured Ca isotope ratios of the spike/sample mixture; spike = Ca isotope ratios of the pure spike; sample = Ca isotope ratios of the pure sample or a standard material; calc = calculated Ca isotope ratios after first fractionation correction; sample-new = Ca isotope ratios after a second fractionation correction being the "sample" values for the next cycle.

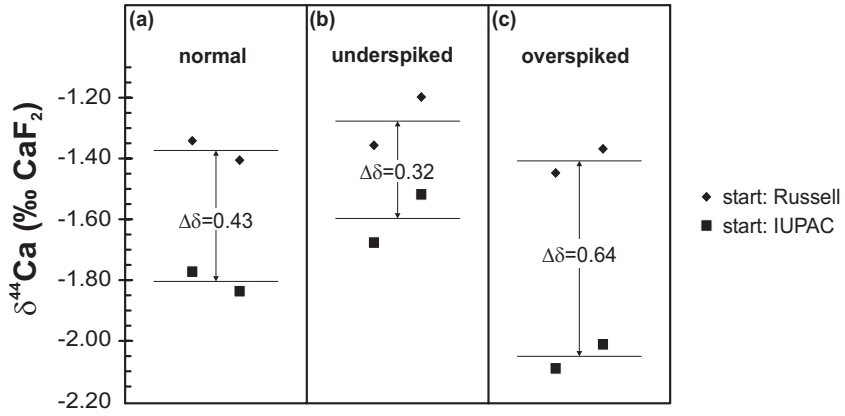

Figure 2.6: Calculation of $^{44}Ca/^{40}Ca$ with different starting values for the $(^{40}Ca/^{48}Ca)_{sample}$, $(^{43}Ca/^{48}Ca)_{sample}$ and $(^{44}Ca/^{48}Ca)_{sample}$ in the Ca double spike correction algorithm. Squares represent IUPAC values [44] and diamonds represent the Ca isotope ratios presented by Russell et al. [21]. In general the $\delta^{44}Ca$ values based on the IUPAC Ca isotope ratios tend to be lower than those of the Russell values and show deviations associated with the sample to spike ratio.

2.3.2 Start Values for the Iterative Ca Double Spike Correction

As described in the previous section (2.3.1) the values of the $(^{40}Ca/^{48}Ca)_{sample}$, $(^{43}Ca/^{48}Ca)_{sample}$ and $(^{44}Ca/^{48}Ca)_{sample}$ in our double spike correction algorithm can either be the $^{40}Ca/^{48}Ca$, $^{43}Ca/^{48}Ca$ and $^{44}Ca/^{48}Ca$ ratios of a standard or of the unspiked (pure) sample. A set of experiments was performed in order to find an optimal "standard" isotopic composition as starting values for the $(^{40}Ca/^{48}Ca)_{sample}$, $(^{43}Ca/^{48}Ca)_{sample}$ and $(^{44}Ca/^{48}Ca)_{sample}$ for carbonate samples.

Two different batches of the NIST carbonate standard have been prepared, one with a spike to sample ratio about 30 % larger (overspiked) than usual and a second batch with a spike to standard ratio about 30 % less (underspiked) than usual. All $^{44}Ca/^{40}Ca$ results were calculated using the $^{40}Ca/^{48}Ca$, $^{43}Ca/^{48}Ca$ and $^{44}Ca/^{48}Ca$ isotope ratios published by Russell et al. [21] ("Russell values") or using the Ca isotope composition published by Moore and Machlan [43] and defined by the IUPAC ("IUPAC values") as the natural Calcium isotope composition [44] (Fig. 2.3.2).

The $\delta^{44}Ca$ values for the underspiked (b), the normal spiked (90 % of the ^{43}Ca and ^{48}Ca originated from the spike) (a) and the overspiked (c) measurements are in the same range using the "Russell values" ($\delta^{44}Ca \approx -1.3$ ‰). Using the "IUPAC values" for the normal spiked standard a shift ($\Delta\delta$) of about 0.43 ‰ towards lighter values is observed. This shift is smaller for the underspiked standard measurements ($\Delta\delta = 0.32$ ‰) but larger for the overspiked standard measurements ($\Delta\delta = 0.64$ ‰). Therefore we suggest to use the Ca isotope ratios previously published [21] as standard isotopic composition being the start

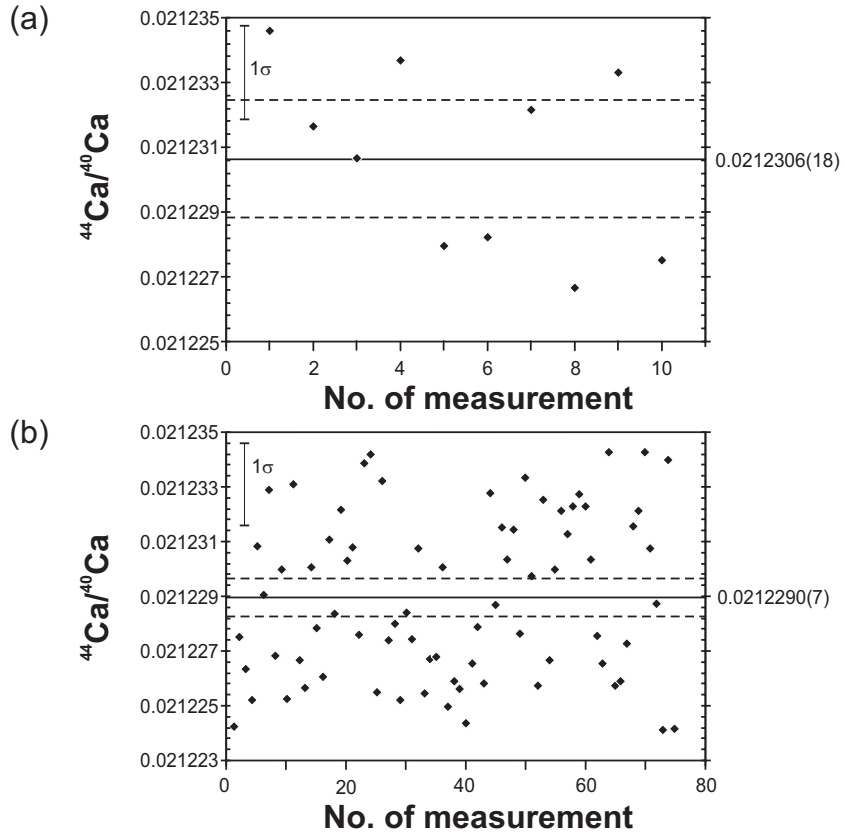

Figure 2.7: Comparison of $^{44}Ca/^{40}Ca$ NIST SRM 915a measurements performed with the "peak jumping method"(a) and the "multicollector technique" (b). Dotted lines represent 2 standard deviations of the mean ($2\sigma_{mean}$).

values in our Ca double spike correction algorithm.

2.4 Results and Discussion

2.4.1 "Peak Jumping" Versus "Multicollector Isotope Measurements"

In Fig. 2.7 we compare $^{44}Ca/^{40}Ca$ isotope ratio measurement performed by the common "peak jumping method" with the new "multicollector technique". During peak jumping masses 40, 42, 43, 44 and 48 have been measured on a fixed Faraday cup (cup 6) with 4 sec integration and 4 sec idle times. The baseline was recorded at the end of each block with closed beam valve. Similar to the multicollector method 11 scans have been recorded as a block. Fig. 2.7 shows the $^{44}Ca/^{40}Ca$ ratio for (a) the "multicollector measurements" and (b) the "peak jumping measurements" of the NIST SRM 915a. We found that the internal reproducibility for the $^{40}Ca/^{48}Ca$ and $^{44}Ca/^{48}Ca$ ratios of a multicup measurement is generally better than about 0.15 ‰, whereas for the single cup measurements statistical

uncertainties vary to larger extend from 0.090 ‰ to 0.304 ‰. Most likely, the latter observation reflects the enhanced sensitivity of the "peak jumping" method to fluctuations of the beam intensity. Using the "peak jumping method" about 3–4 samples can be measured during one day. However, applying the "multicollector technique" the sample throughput per day is at least 3 times higher.

The results for the $^{44}Ca/^{40}Ca$ ratio determined by the single cup measurements range from 0.021226 to 0.021235 and the values of the multicup measurements are in a range from 0.021224 to 0.021235. Within the statistical uncertainty the mean value of the single cup measurements ($^{44}Ca/^{40}Ca$ = 0.0212306(18), $\delta^{44}Ca_{CaF_2} = -1.35$ ‰) is in accord with the mean value of the multicup measurements ($^{44}Ca/^{40}Ca$ = 0.0212290(07), $\delta^{44}Ca_{CaF_2} = -1.43$ ‰). Note, that the mean value calculated from the multicup measurements are more precise because of the larger number of available measurements. The average deviation of one single measurement from the mean value standard deviation (variance: $1\,\sigma = 0.000003$) is similar for both techniques. As our $^{43}Ca/^{48}Ca$ double spike is not calibrated for the determination of the absolute $^{44}Ca/^{40}Ca$ ratio the above values do not represent the true isotopic composition of the NIST SRM 915a calcium carbonate standard. In order to further verify our new multicollector technique we also measured the two Johnson Matthey $CaCO_3$ standards. Using our new technique we were able to confirm earlier results by Russell et al. [21] that there is a difference of 12 ‰ between these two standards.

2.4.2 Reproducibility of δ^{44}Ca

We also used our new multicollector technique for repeated measurements of the CaF_2-standard and the NIST SRM 915a carbonate standard. Fig. 2.8a shows the results of about 120 measurements of CaF_2 and fig. 2.8b of nearly 90 measurements of the NIST standard. The long term mean of all $^{44}Ca/^{40}Ca$ measurements of the CaF_2-standard is used for normalization of the δ^{44}Ca values. The average δ^{44}Ca value of the CaF_2 measurements is (0.00 ± 0.05) ‰ and the δ^{44}Ca value of the NIST standard is (-1.45 ± 0.05) ‰. The given statistical uncertainty represent 2σ deviation of the mean ($2\sigma_{mean}$).

The δ^{44}Ca values of the CaF_2 have a 1σ standard deviation of 0.25 ‰. However, the values vary within a relatively wide range between −0.7 ‰ and +0.8 ‰. The 1s standard deviation of the last 30 measurements is 0.35 ‰while it is 0.18 ‰ for the first 90 measurements. The reasons for this pejoration of the external reproducibility remains unclear. Contamination of either the standard solution, the double spike solution or the Ta_2O_5 activator solution should lead to a noticeable shift in the δ^{44}Ca values in one direction and not to the observed

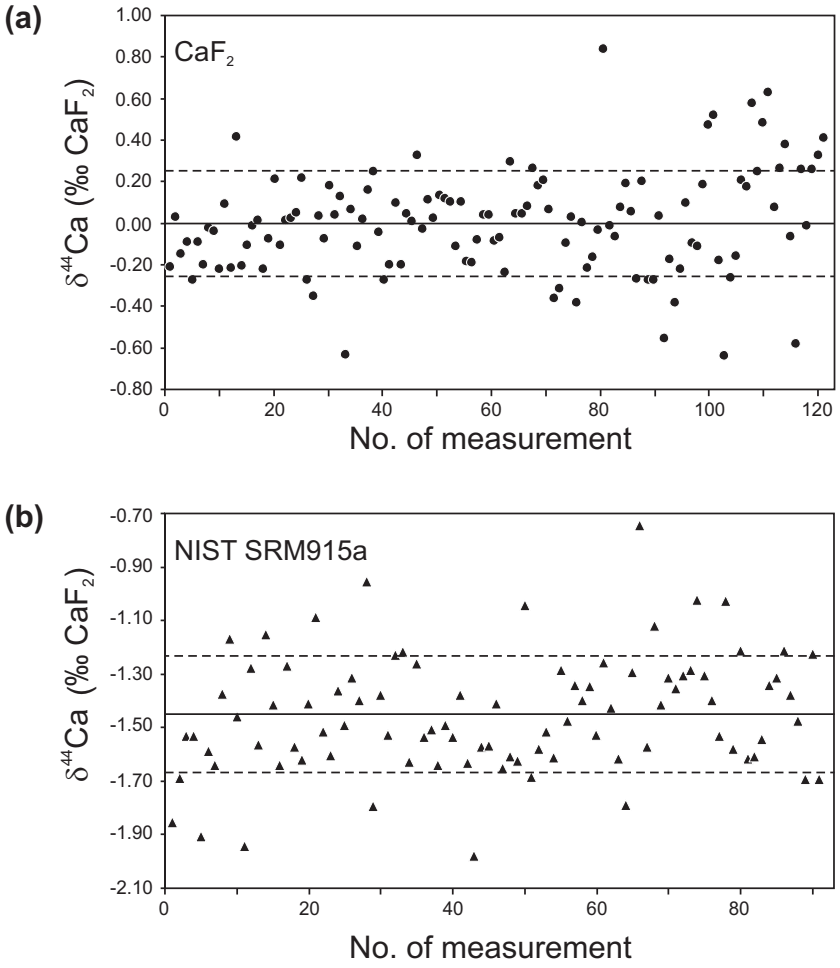

Figure 2.8: δ^{44}Ca values of (a) CaF_2 and (b) NIST SRM 915a measurements. Note, all δ^{44}Ca values are normalized to the long term measurements of the $^{44}Ca/^{40}Ca$ ratio of the CaF_2 standard. Solid lines represent mean δ^{44}Ca ratios and dashed lines represent the 1s standard deviation.

pejoration of the reproducibility.

The range of the δ^{44}Ca values of the NIST SRM 915a measurements vary between $-2.0\,‰$ and $-0.8\,‰$. However, the 1σ standard deviation of all measurements is $0.22\,‰$. Opposite to the CaF_2 measurements the range of the δ^{44}Ca values is not changing significantly during the measurement period. The reason for this is that we did not measure NIST in the time interval we observed the increase in 1s standard deviation of the CaF_2 measurements.

Acknowledgements

Financial support to A Heuser was provided by the Graduiertenkolleg “Dynamik globaler Kreisläufe” from the “Deutsche Forschungsgemeinschaft, DFG” (GRK 171) by the state government of Schleswig-Holstein and a grant (Ei272/5-3) from the DFG. This study was

also supported by a grant to A. Eisenhauer (Ei272/12-1) from the "Deutsche Forschungsgemeinschaft, DFG". Comments by S. Galer and an anonymous reviewer improved the manuscript.

References

[1] R.P. Rubin, G.B. Weiss, J.W.J. Putney, Calcium in Biological Systems, Plenum Publishing Corporation, New York, 1985

[2] E.T. Degens, Chem. Geol. 25 (1979) 257–269

[3] I.T. Platzner, Modern Isotope Ratio Mass Spectrometry, John Wiley & Sons, Chicester, 1997

[4] K. Heumann, W. Luecke, Earth Planet. Sci. Lett. 20 (1973) 341–346

[5] K. Heumann, H. Klöppel, Z. Naturforsch. 34b (1979) 1044–1045

[6] B.D. Marshall, L.J. DePaolo, Geochim. Cosmochim. Acta 46 (1982) 2537–2545

[7] B.D. Marshall, L.J. DePaolo, Geochim. Cosmochim. Acta 53 (1989) 917–922

[8] T.F. Nägler, I.M. Villa, Chem. Geol. 169 (2000) 5–16

[9] T.F. Nägler, A. Eisenhauer, A. Müller, C. Hemleben, J. Kramers, Geochem. Geophys. Geosyst. 1 (2000) 2000GC000091

[10] P. Zhu, J. Macdougall, Geochim. Cosmochim. Acta 62 (1998) 1691-1698

[11] N. Gussone, A. Eisenhauer, A. Heuser, M. Dietzel, B. Bock, F. Böhm, H. Spero, D.W. Lea, J. Bijma, R. Zeebe, Th.F. Nägler, Geochim. Cosmochim. Acta (in press)

[12] J.R. O'Neil, R.N. Clayton, T.K. Mayeda, J. Chem. Phys. 31 (1969) 5547–5558

[13] W. Stahl, L. Wendt, Earth. Planet. Sci. Lett. 5 (1968) 184-186

[14] J.R. O'Neil, in: J.W. Valley, J.R. O'Neil, H.P. Taylor, (Eds.), Reviews of Mineralogy. Stable Isotopes in High Temperature Geological Processes, Mineralogical Society of America, 1986, pp. 561–570.

[15] K. Heumann, Z. Naturforsch. 27b (1972) 492-497

[16] K. Heumann, H.-P. Schiefer, Angew. Chem.-Int. Ed. 19 (1980) 406–407

[17] K. Heumann, H.-P. Schiefer, Z. Naturforsch. 36b (1981) 566–570

[18] W.A. Russell, D.A. Papanastassiou, Anal. Chem. 50 (1978) 1151–1154

[19] J. Corless, Earth Planet. Sci. Lett. 4 (1968) 475–478

[20] W.A. Russell, D.A. Papanastassiou, T. Tombrello, S. Epstein, Proc. Eighth Lun. Sci. Conf., Geochim. Cosmochim. Acta Suppl. 8 (1977) 3791–3805

[21] W.A. Russell, D.A. Papanastassiou, T.A. Tombrello, Geochim. Cosmochim. Acta 42 (1978) 1075–1090

[22] W.A. Russell, D.A. Papanastassiou, Anal. Chem. 50 (1978) 1151–1154

[23] J.L. Skulan, D.J. DePaolo, T.L. Owens, Geochim. Cosmochim. Acta 61 (1997) 2505–2510

[24] K. Wendt, K. Blaum, B. A. Bushaw, F. Juston, W. Nörtershäuser, N. Trautmann, B. Wiche, Fresen. Z. Anal. Chem. 359 (1997) 361–363

[25] L. Halicz, A. Galy, N. Belshaw, R. O'Nions, J. Anal. At. Spec. 14 (1999) 1835–1838

[26] V.I. Baranov, S.D. Tanner, J. Anal. At. Spec. 14 (1999) 1133

[27] I. Feldmann, N. Jakubowski, D. Stuewer, Fresen. J. Anal. Chem. 365 (1999) 415

[28] S.F. Boulyga, J.S. Becker, Fresen. J. Anal. Chem. 370 (2001) 618–623

[29] I. Fletcher, A. Maggi, K. Rosman, N. Naughton, Int. J. Mass. Spec. Ion Proc. 163 (1997) 1–17

[30] D.R. Nelson, M.T. McCulloch, Chem. Geol. (Isot. Geosci.) 79 (1989) 275–293

[31] K. Heumann, K. Lieser, H. Elias, in: K. Ogata, T. Hayakawa, (Eds.), Recent Developments in Mass Spectrometry, University of Tokyo Press, Tokyo, 1970

[32] K. Heumann, K. Lieser, Z. Naturforsch. 27b (1972) 126–133

[33] K. Heumann, K. Lieser, Geochim. Cosmochim. Acta 37 (1973) 1463–1471

[34] K. Heumann, H. Klöppel, G. Sigl, Z. Naturforsch. 37b (1982) 786–787

[35] J. Birck, Chem. Geol. 56 (1986) 73–83

[36] W. Compston, V. Oversby, J. Geophys. Res. 74 (1969) 4338–4348

[37] S. Hart, A. Zindler, Int. J. Mass. Spec. Ion Proc. 89 (1989) 287–301

[38] C. Siebert, T.F. Nägler, J.D. Kramers, Geochem. Geophys. Geosyst. 2 (2001) 2000GC000124

[39] M. F. Thirlwall, Chem. Geol. 184 (2002) 255–279

[40] B. Hamelin, G. Manhes, F. Albarede, Allègre C.J., Geochim. Cosmochim. Acta 49 (1985) 173–182

[41] N. Gale, Chem. Geol. 6 (1970) 305-310

[42] C. Johnson, B. Beard, Int. J. Mass. Spec. 193 (1999) 87–99

[43] L.J. Moore, L.A. Machlan, Anal. Chem. 44 (1972) 2291–2296

[44] Commission on Atomic Weights and Isotopic Abundances, Pure Appl. Chem. 70 (1998) 217–236

3 Comparison of Ca Isotope Standards and Seawater and a Convenient Way to Relate Ca isotopic data sets

by

D. Hippler[1], A.D. Schmitt[2], N. Gussone[3], A. Heuser[3], P. Stille[2], A. Eisenhauer[3] and Th.F. Nägler[1]

[1] Isotopengeologie, Mineralogisch-petrographisches Institut, Universität Bern, Erlacherstrasse 9a, CH-3012 Bern, Switzerland.

[2] Centre de Géochemie de la Surface (CNRS) - EOST, 1 rue Blessig, F-67084 Strasbourg Cedex Strasbourg, France

[3] GEOMAR, Forschungszentrum für Marine Geowissenschaften, Wischhofstr. 1–3, D-24148 Kiel, Germany.

submitted to *Geostandards Newsletter*

Abstract

A compilation of δ^{44}Ca data sets of different calcium standard material is presented, based on measurements in three different laboratories (Institute of Geological Sciences, Berne; Centre de Géochimie de la Surface, Strasbourg; GEOMAR, Kiel) to support the establishment of a Ca isotope reference. Samples include a series of international and internal Ca-standard material, such as NIST SRM 915a, IAPSO, seawater, two calcium carbonates and a CaF_2 standard. The deviations in δ^{44}Ca for selected pairs of standards have been defined, and are consistent within statistical uncertainties in all three laboratories. The focus has been put on the pair seawater and NIST SRM 915a, i.e. an important geological reservoir and an international available pure Ca standard. The difference of δ^{44}Ca of seawater to NIST 915a is defined as 1.88 ± 0.04 ‰. The conversion of NIST SRM 915a related values to seawater can be described by the simplified equation $\delta^{44}Ca_{Sa/Sw} = \delta^{44}Ca_{Sa/NIST} - 1.88$. We suggest referring Ca isotope data to average seawater as common reservoir, while using NIST SRM 915a as secondary standard.

3.1 Introduction

Calcium (Ca) is an abundant element both in marine and in terrestrial systems (Broecker & Peng, 1982). Previous investigations have shown that calcium isotopes are a powerful tool for studying geological, biological and climate-related processes (Skulan et al., 1997; Zhu & McDougall, 1998; Skulan & DePaolo, 1999; Nägler et al., 2000; de la Rocha & DePaolo, 2000). The significance of calcium isotope data for oceanography has recently been demonstrated (Nägler et al., 2000; de la Rocha & DePaolo, 2000).

Applying high precision mass-spectrometric methods and a double spike technique relatively small natural fractionation of calcium isotopes can be resolved (Russell et al., 1978). The latter represents a reconnaissance study on the determination of calcium isotopic fractionation in meteoritic and terrestrial samples. Further work deals with the biological control of the calcium isotopic abundance and its significance for biochemistry (Skulan et al., 1997; Skulan & DePaolo, 1999). Studies on cultured and natural single species planktonic foraminifera has shown that temperature-dependent biological fractionation occurs. Based on these investigations calcium isotopes are established as an alternative sea-surface temperature proxy (Zhu & McDougall, 1998; Nägler et al., 2000). Further the calcium isotope ratio of modern seawater is homogeneous in worldwide oceans within analytical uncertainties (Zhu & McDougall, 1998; De La Rocha & DePaolo, 2000; Schmitt et al., 2001). This is expected in view of the long residence time of calcium (1Ma; Broecker &

Peng, 1982) compared to the mixing time of ocean water of about 1.5 kyr (cf. Broecker & Peng, 1982). In addition, the knowledge of Ca isotopic composition of seawater, river, terrestrial and biological samples has made it possible to use Ca isotopes as a tool for quantifying the marine calcium cycle (Zhu & McDougall, 1998; De La Rocha & DePaolo, 2000).

Most problematic remains the comparison of data from different laboratories. In order to be able to compare the Ca isotope data of different laboratories, a common Ca isotopic standard is necessary. Previous studies dealing with Ca isotopes refer mostly to Ca salts as laboratory standards. Russell et al. (1978) gave a precisely defined reference value for the $^{42}Ca/^{44}Ca$ ratio of 0.31221 ± 0.00002 deduced from two Ca terrestrial standards, two lunar samples and four meteorites. Skulan et al (1997) normalized the unspiked sample to this $^{42}Ca/^{44}Ca$ standard value. They also set an arbitrary but reasonable value for their $^{44}Ca/^{40}Ca$ ultrapure $CaCO_3$ standard ratio of 0.0217 and referred all data to this value. Therefore, quite different isotopic composition values for seawater, which is the only common and comparable sample for several Ca isotope studies, have been published (Schmitt et al., 2001). Russell et al. (1978) and Nägler and Villa (2000) used natural fluorite as a Ca standard free of technical or biological isotopic fractionation. In order to avoid the problem of interlaboratory bias Zhu & McDougall (1998) and Schmitt et al. (2001) proposed to use seawater as a common standard.

Seawater is largely available and represents a major natural Ca reservoir. However, the inconvenience is that Ca isotope measurements of seawater require a calcium separation technique prior to analyses. The $CaCO_3$ reference powder of the National Institute of Standards NIST SRM 915a, used by Halicz et al. (1999), would be an alternative and is proposed here as future reference standard. However, it is not related to a geological reservoir.

An interlaboratory Ca-workshop in autumn 2001 held at the GEOMAR research institute in Kiel, Germany, encouraged us to compile our data about international and internal standard material. The main goal of this study is twofold: (a) Several standards (including seawater) used in previous studies (Russell et al., 1978; Skulan et al., 1997; Zhu & McDougall, 1998; Nägler et al., 2000; Schmitt et al., 2001) are to be cross-calibrated; (b) the Ca isotope fractionation between seawater and NIST SRM 915a should be defined. The latter calibration allows the use of the convenient NIST SRM 915a standard during measurements periods while referencing the results to the Ca seawater reservoir. The cooperation of the three institutes at Berne, Strasbourg and Kiel enables calibrations independent of laboratory specific biases.

3.2 Sample material

NIST SRM 915a is a Ca standard provided by the National Institute of Standards, USA. Aliquots of Johnson Matthey Ca carbonate standards Lot. 9912 and Lot. 4064 were provided by courtesy of Dr. A. Papanastassiou. These standards have been previously measured at the CALTECH by Russell et al. (1978). An extreme technical fractionation has been observed for Lot. 4064. These standards are included to link our data to Russell et al. (1978). Because of their wide isotopic range ($\sim 12\,‰$ δ^{44}Ca) they would also magnify systematic interlaboratory offsets, if present. A solution obtained from a natural fluorite (CaF_2) sample is used as a standard in Berne (Nägler et al., 2000) and Kiel and is added for comparison. IAPSO standard seawater, batch P135 is a reference seawater material from the "Ocean Scientific International" and is used at Geomar as seawater reference. Various seawater samples were taken from different localities and depths. Seawater samples measured in Berne are listed in the Appendix. For seawater samples from Strasbourg see Schmitt et al. (2001).

3.3 Methods

All three laboratories used ^{43}Ca/^{48}Ca double spikes. Absolute isotope ratios defined with the double spike technique are dependent on the spike calibration procedure and standard normalization. Thus we present our data as per mil differences relative to a given standard, in line with previous publications. The isotopic composition of calcium is expressed in the δ-notation (δ^{44}Ca), with the heavy isotope in the numerator analog to light stable isotope (e.g. δ^{18}O):

$$\delta^{44}Ca = [(^{44}Ca/^{40}Ca)_{sample}/(^{44}Ca/^{40}Ca)_{normal} - 1] \cdot 1000 \qquad (3.1)$$

Besides natural mass-related variations the calcium isotopic composition differs due to the production of ^{40}Ca from the radioactive decay of ^{40}K. Unspiked runs are used as monitor for possible input of radiogenic calcium. In all analyses of unspiked standards there were no detectable amounts of radiogenic calcium. This result is in line with the findings of previous publications for Ca dominated samples (Zhu & McDougall, 1998; Russell et al., 1978).

Details of analytical techniques are given elsewhere (Nägler et al., 2000; Schmitt et al., 2001) The method of seawater purification in Berne is described in the Appendix.

3.4 Results and Discussion

The compiled results of different standard measurements are presented in Table 3.1. Uncertainties given are at the 2σ level. Data sets of Bern and Kiel are normalized to the CaF_2-standard, whereas the data set of Strasbourg is referred to an average value of ocean water. When referred to the same standard, values of all three laboratories are identical within analytical uncertainties, precluding any interlaboratory bias. Table 3.2 shows the relative deviations in δ^{44}Ca of two pairs of selected standards relative to each other. The deviations are defined for seawater and NIST SRM 915a and for the two Johnson Matthey (Lot. 4064 and 9912) standards. Uncertainties reflect the 2σ standard error propagated from Table 3.2. Propagated errors for the difference of the two Johnson Matthey standards are larger due to the limited number of analyses. The weighted average of the difference between seawater and NIST SRM 915a is defined to be 1.88 ± 0.04 ‰ and 11.84 ± 0.16 ‰ for the two Johnson Matthey standards. Again the results of all three laboratories are identical within uncertainties. Further the deviation of both Johnson Matthey standards measured by Russell et al. (1978; $\delta^{44}\text{Ca} = 11.80$ ‰) is equal to the weighted average of the three laboratories.

Present and previous measurements at Berne, Geomar and Strasbourg of Ca isotopic composition of modern seawater, including IAPSO support earlier observations of Ca-isotopic homogeneity between the world oceans and within different water depths. Therefore, as suggested by Schmitt et al. (2001) and Zhu & McDougall (1998), Ca isotopic data can be related to seawater as geological reference.

Analog to the equations given by Stosch (2002; Gl.192) for oxygen isotopes the theoretic conversion of δ^{44}Ca-values related primary to NIST SRM 915a in δ^{44}Ca-values related to seawater could be correctly described in the following manner:

$$\delta^{44}Ca_{Sa/Sw} = [(10^{-3}\delta^{44}Ca_{Sa/NIST} + 1)(10^{-3}\delta^{44}Ca_{NIST/Sw} + 1) - 1] \cdot 10^{-3} \qquad (3.2)$$

The subscripted indices in the formula correspond to the deviation sample-seawater ($\delta^{44}\text{Ca}_{Sa/Sw}$) and sample-NIST SRM 915a ($\delta^{44}\text{Ca}_{Sa/NIST}$). As listed in Table 3.3 the favorable value to describe the relation between NIST SRM 915a and seawater ($\delta^{44}\text{Ca}_{NIST/Sw}$) is defined to be the weighted average of -1.88 ± 0.04 ‰.

Table 3.1: The δ^{44}Ca ratios of different standards

	Bern[1]				Kiel[2]				Strasbourg[3]			
	δ^{44}Ca	1	2	n	δ^{44}Ca	1	2	n	δ^{44}Ca	1	2	n
NIST SRM 915a	−1.47	± 0.19	± 0.07	8	−1.41	± 0.30	± 0.03	109	−1.89	± 0.08	± 0.06	2
CaF2	0.00	± 0.19	± 0.04	29	0.00	± 0.29	± 0.03	88				
Johnson Matthey Lot.4064	−12.69	± 0.19		1	−12.78	± 0.29		1	−13.49	± 0.34	± 0.24	2
Johnson Matthey Lot. 9912	−0.87	± 0.19		1	−0.83	± 0.18	± 0.10	3	−1.42	± 0.15	± 0.09	3
Mean seawater	0.48	± 0.11	± 0.06	4	0.41	± 0.13	± 0.06	5	0.00	± 0.17	± 0.04	15

1: Uncertainties are listed as 2σ st.deviation; for single analysis the external standard reproducibility is given
2: This column reflects the 2σ st.deviation of the mean
n: number of analyses
δ^{44}Ca values of Bern and Kiel are normalized to CaF_2-standard
δ^{44}Ca values of Strasbourg are normalized to seawater
[1] measured on a modified single cup AVCO mass spectrometer (Nägler et al., 2000) now equipped with a Thermolinear ion source
[2] measured on a Finnigan MAT 262 RPQ+
[3] measured on a VG sector thermal ionisation mass spectrometer (Schmitt et al., 2001)

Table 3.2: Relative differences of δ^{44}Ca of standards

	Bern		Kiel		Strasbourg		weighted average	weighted error	Russell et al.(1978)
Δ (Seawater - NIST 915a)	1.95	± 0.09	1.82	± 0.07	1.89	± 0.07	1.88	± 0.04	
Δ (Johnson Matthey Lot. 4064 - 9912)	11.82	± 0.27	11.95	± 0.34	12.07	± 0.25	11.84	± 0.16	11.80

Uncertainties are the 2s st. error propagated from Table 3.1
Propagated errors for Johnson Matthey standards are larger due to limited number of analyses (see Table 3.1)
Data of Russell et al. (1978) for reasons of comparison.

Table 3.3: The δ^{44}Ca ratios of modern seawater measured at the Institute of Geological Sciences, Berne

Location	Sample	Depth	δ^{44}Ca	2σ st.dev
Indian Ocean (Southern Arabian Sea)	24 CTD	Surface	0.52	± 0.12
Atlantic Ocean (S. England)	ATL-OC	Surface	0.42	± 0.15
Pacific Ocean (North Rift Zone)	52 CTD	1637 m	0.45	± 0.15
IAPSO standard seawater (batch P135)	IAPSO	Surface	0.54	± 0.19

Uncertainties reflect the 2σ standard error of the measurement
δ^{44}Ca values of modern seawater are normalized to CaF_2-standard
Sample ATL-OC was previously measured by Schmitt et al. (2001)

Within the existing analytical precision, equation (3.2) can accurately be approximated by

$$\delta^{44}Ca_{Sa/Sw} = \delta^{44}Ca_{Sa/NIST} - 1.88 \tag{3.3}$$

It is recommended here to use NIST SRM 915a regularly as secondary standard and refer data to seawater composition applying formula [3.3].

3.5 Summary and Conclusion

A set of Ca-standard materials provides consistent δ^{44}Ca ratios within statistical uncertainties in three European laboratories (Berne, GEOMAR, Strasbourg). In particular, the relative deviation of δ^{44}Ca of two pairs of standards (seawater-NIST, Johnson Matthey Lot. 4064-9912) to each other shows very good correspondence, the latter being further compatible with previous results of Russell et al. (1978). Therefore, no bias correction is necessary and the Ca isotope data of the three laboratories are directly comparable with each other when expressed in δ^{44}Ca notation.
Seawater and NIST SRM 915a are potential common calcium reference materials. The difference of δ^{44}Ca of seawater to NIST SRM 915a is accurately defined as 1.88 ± 0.04 ‰. The simplified descriptive equation for this relation is $\delta^{44}\mathrm{Ca}_{Sa/Sw} = \delta^{44}\mathrm{Ca}_{Sa/NIST} - 1.88$. We propose to use this relation in further studies to refer Ca isotope data to average seawater as common reservoir, while using NIST SRM 915a as secondary standard.

Acknowledgements

We are greatly indebted to D.A. Papanastassiou for providing standard material. D.H. and T.F.N. wish to thank Igor Villa for fruitful discussions. Ca Isotope work at Bern is

supported by the Swiss National Science Foundation (grants 21-61644.00 and 21-60987.00). The work of N. Gussone, A. Heuser and A. Eisenhauer are supported by the grant from the "Deutsche Forschungsgemeinschaft, DFG (Ei272/12-1)".

References

W.S. Broecker and T.-H. Peng (1982) Tracers in the Sea, 690pp, New York, Eldigo Press.

C.L. De La Rocha and D.J. DePaolo (2000) Isotopic evidence for variations in the marine Calcium cycle over the Cenozoic, Science, 289: 1176–1178.

L. Halicz, A. Galy, N.S. Belshaw and R.K. O'Nions (1999) High-precision measurements of calcium isotopes in carbonates and related materials by multiple collector inductively coupled plasma mass-spectrometry (MC-ICP-MS), Journal of Analytical Atomic Spectrometry, 14: 1835–1838.

Th.F. Nägler, A. Eisenhauer, A. Müller, C. Hemleben and J. Kramers (2000) The δ^{44}Ca-temperature calibration on fossil and cultured *Globigerinoides sacculifer*: New tool for reconstruction of past sea surface temperatures, Geochemistry Geophysics Geosystems, 1, 2000GC000091.

Th.F. Nägler and I.M. Villa (2000) In pursuit of the ^{40}K branching ratios: K-Ca and ^{39}Ar-^{40}Ar dating of gem silicates, Chemical Geology, 169: 5–16.

W.A. Russell, D.A. Papanastassiou and T.A. Tombrello (1978) Ca isotope fractionation on the earth and other solar system materials, Geochimica et Cosmochimica Acta, 42: 1075–1090.

A.-D. Schmitt, G. Bracke, P. Stille and B. Kiefel (2001) The Calcium isotope composition of modern seawater determined by Thermal Ionisation Mass Spectrometry, Geostandards Newsletter, 25: 267–275.

J. Skulan, D.J. DePaolo and T.L. Owens (1997) Biological control of calcium isotopic abundances in the global calcium cycle, Geochimica et Cosmochimica Acta, 61: 2505–2510.

J. Skulan and D.J. DePaolo (1999) Calcium isotope fractionation between soft and mineralized tissues as a monitor of Calcium use in vertebrates, PNAS, 96: 13709–13713.

H.-G. Stosch (2002) Isotopengeochemie, Version 2.3.5 (April 2002) http://129.13.109.66/WWW_only/html/ftp.html

P. Zhu and J.D. MacDougall (1998) Calcium isotopes in the marine environment and the oceanic calcium cycle, Geochimica et Cosmochimica Acta, 62: 1691–1698.

Appendix: Purification of seawater samples in Bern

5 µL seawater was processed through chemical separation. A $^{43}Ca/^{48}Ca$ double spike was added to the samples prior to purification of Ca. microcolumns containing 10 µL AP-MP-50 (200–400 mesh) cation exchange resin and a HCl chemistry were used. This is necessary to remove remaining interfering elements such as potassium and strontium that might act as potential isobaric interferences. The chemical efficiency for Ca is close to 100%. Total procedural blanks in our work were below 1 ng and therefore have a negligible effect on the isotopic data.

4 Model for Kinetic Effects on Calcium Isotope Fractionation (δ^{44}Ca) in Inorganic Aragonite and Cultured Planktonic Foraminifera

by

N. Gussone[1], A. Eisenhauer[1,*], A. Heuser[1,2], M. Dietzel[3], B. Bock[1], F. Böhm[1], H.J. Spero[4], D.W. Lea[5], J. Bijma[6], R. Zeebe[6] and Th.F. Nägler[7]

[1] GEOMAR, Forschungszentrum für Marine Geowissenschaften, Wischhofstr. 1–3, D-24148 Kiel, Germany.

[2] Graduierten Kolleg "Dynamik globaler Kreisläufe im System Erde", GEOMAR Forschungszentrum für marine Geowissenschaften, Wischhofstr. 1–3, 24148 Kiel, Germany.

[3] Institut für Technische Geologie und Angewandte Mineralogie, Technische Universität Graz, A-8010 Graz, Rechbauerstrasse 12, Austria

[4] University of California, Davis, Department of Geology, One Shield Avenue, Davis, CA 95616, U.S.A.

[5] University of California, Department of Geological Sciences, Santa Barbara, CA 93106, U.S.A.

[6] Alfred Wegener Institut für Polar und Meeresforschung, Kolumbuskai 1, D-27515 Bremerhaven, Germany.

[7] Isotopengeologie, Mineralogisch-petrographisches Institut, Universität Bern, Erlachstrasse 9a, CH-3012 Bern, Switzerland.

[*] Corresponding author, fon:49-431-600-2282, fax:49-431-600-2928

aeisenhauer@geomar.de

Geochimica et Cosmochimica Acta, in press

Abstract

The calcium isotope ratios ($\delta^{44}\mathrm{Ca} = (({}^{44}\mathrm{Ca}/{}^{40}\mathrm{Ca})_{sample}/({}^{44}\mathrm{Ca}/{}^{40}\mathrm{Ca})_{standard} - 1) \times 1000$) of *Orbulina universa* and of inorganically precipitated aragonite are positively correlated to temperature. The slopes of 0.019 and 0.015 ‰ °C^{-1}, respectively, are a factor of 13 and 16 times smaller than the previously determined fractionation from a second foraminifera, *Globigerinoides sacculifer*, having a slope of about 0.24 ‰ °C^{-1} (Nägler et al., 2000). The observation that δ^{44}Ca is positively correlated to temperature is opposite in sign to the oxygen isotopic fractionation (δ^{18}O) in calcium carbonate ($CaCO_3$). These observations are explained by a model which considers that Ca^{2+}-ions forming ionic bonds are affected by kinetic fractionation only whereas covalently bound atoms like oxygen are affected by kinetic and equilibrium fractionation. From thermodynamic consideration of kinetic isotope fractionation it can be shown that the slope of the enrichment factor α(T) is mass dependent. However, for *O. universa* and the inorganic precipitates the calculated mass of about 520 ± 60 and 640 ± 70 amu (atomic mass unit) is not compatible with the expected ion mass for ^{40}Ca and ^{44}Ca. To reconcile this discrepancy we propose that Ca diffusion and δ^{44}Ca isotope fractionation at liquid/solid transitions involves Ca^{2+}-aquocomplexes ($Ca[H_2O]_n{}^{2+} \cdot m\,H_2O$) rather than pure Ca^{2+}-ion diffusion. From our measurements we calculate that such a hypothesized Ca^{2+}-aquocomplex correlates to a hydration number of up to 25 water molecules (490 amu). For *O. universa* we propose that their biological mediated Ca isotope fractionation resembles fractionation during inorganic precipitation of $CaCO_3$ in seawater. In order to explain the different Ca isotope fractionation in *O. universa* and in *G. sacculifer* we suggest that the latter species actively dehydrates the Ca^{2+}-aquocomplex before calcification takes place. The very different temperature response of Ca isotopes in the two species suggests that the use of δ^{44}Ca as a temperature proxy will require careful study of species effects.

4.1 Introduction

The important role of calcium (Ca) in biological processes is based on its chemical versatility which is related to its highly adaptable coordination geometry, its divalent charge, modest binding energies, fast reaction kinetics and its inertness in redox reactions (cf. Williams, 1989; Williams, 1974). It was suggested that changes in the calcium concentration, together with changes in seawater alkalinity and pH, were a major driving force for the onset of biomineralization and the alternating mineralogy of marine carbonate precipitation observed throughout Earth's history. However, there are only a few data sets that

link seawater concentrations or calcium isotope ratios to Earth's biological evolution (cf. De La Rocha and DePaolo, 2000; Arp et al., 2001; Wallmann, 2001; Stanley and Hardie, 1998; Kempe and Degens, 1985; Degens, 1979).

Natural fractionation of Ca isotopes in surface processes is reported to be relatively small (cf. Heumann et al., 1970; Heumann and Lieser, 1972; Heumann et al., 1982; Stahl and Wendt, 1968) requiring high analytical precision to be resolved. Russell et al. (1978) first combined modern high-precision mass spectrometry with the application of the Ca double spike technique in order to determine isotope fractionation in terrestrial and cosmic materials. Skulan et al. (1997, 1999) focused their attention on the biological control of the Ca isotopic composition. They analyzed Ca from various marine organisms and concluded that Ca isotope fractionation is relatively uniform in magnitude among vastly different organisms and that Ca becomes isotopically lighter when it moves through food chains. Zhu and MacDougall (1998) suggested that Ca isotope data from foraminifera of a given species may significantly vary with ocean water temperature and/or depth and showed that there is a 0.6 ‰ difference in the δ^{44}Ca ratios between *G. sacculifer* from the Holocene and the last glacial maximum (LGM) of the equatorial Pacific (Zhu and MacDougall, 1998). Utilizing recent estimates of sea surface temperature change since the Last Glacial Maximum (Lea et al., 2000), this 0.6 ‰ difference would reflect a temperature change of about 3 °C. A more systematic study of δ^{44}Ca-temperature relationships in the cultured planktonic foraminifera Globigerinoides sacculifer, demonstrated a clear temperature dependence over a temperature range from 19.5 to 29.5 °C (Nägler et al., 2000). The calculated δ^{44}Ca-temperature slope of about 0.24 ‰ °C^{-1} was similar to the observations of Zhu and MacDougall (1998). Further, Nägler et al. (2000) found a 0.7 ‰ difference in δ^{44}Ca of fossil *G. sacculifer* between Holocene and LGM core sections of equatorial Atlantic core GeoB1112. Thus, a significant temperature dependence of δ^{44}Ca has been established for *G. sacculifer*. The magnitude of the temperature sensitivity is similar to that for oxygen isotope ratios (δ^{18}O) although the positive slope for δ^{44}Ca is opposite in sign compared to other stable isotope systems like oxygen (O), carbon (C) and boron (B) where isotope fractionation is inversely related to temperature (Zeebe and Wolf-Gladrow, 2001).

In a further study, De La Rocha and DePaolo (2000) used an intertidal benthic foraminifer, *Glabratella ornatissima*, to establish a δ^{44}Ca-temperature relationship. Although the authors claim that this species does not display a temperature relationship, in our opinion the small temperature range (8.5–10.8 °C) used for calibration and the scatter of their data do not allow for a definitive conclusion.

The discrepant statements concerning temperature controlled δ^{44}Ca isotope fractionation

reflect the absence of a thermodynamic model describing temperature dependent inorganic or biologically mediated δ^{44}Ca fractionation. In order to address this problem, we systematically investigated the temperature dependent δ^{44}Ca fractionation of inorganically precipitated aragonite and of another cultured planktonic foraminifera, *O. universa*, and compared the results with the earlier measurements on cultured *G. sacculifer*.

4.2 Materials and Methods

4.2.1 Inorganic precipitation of aragonite: experimental setup

The setup for inorganic precipitation of aragonite is described in detail in Dietzel and Usdowski (1996). The experimental set up consists of two bottles: a 0.5 l polyethylene (PE) bottle, containing 35 g solid $NaHCO_3$ which is saturated with CO_2 gas from a tank with a pressure of 1 atmosphere. The inner bottle is surrounded by a 5 l container filled with a Ca-Mg-Cl solution (Ca: 0.01 mol/l; Mg: 0.02 mol/l) and selected trace metals. The concentrations of Ca, Mg and Cl and the Ca : Mg : Cl ratios in the solutions used for the inorganic precipitation of aragonite, were chosen to gain pure aragonite precipitation and are different from modern seawater. In particular, the solutions contained no sulfate, although in seawater about 10 % of the solved Ca is complexed by sulfate ions. The issue here is to gather first order information on the kinetics of inorganic Ca isotope fractionation and its temperature dependence, rather than to investigate the complexities of the open ocean environment. Reagent grade chemicals (Merck p.a.) and pure gases (Messer-Griesheim CO_2: 99.995 vol.%) were used for the experiments. Only about 2 % of the dissolved Ca was precipitated, so that the isotopic composition and concentration of Ca remained nearly constant during the experiment.

When CO_2 diffuses through the PE walls, $CaCO_3$ precipitates as aragonite within the Ca-Mg-Cl solution. Each experiment was terminated when about 100 mg of $CaCO_3$ were precipitated. At temperatures of 10 °C and 50 °C (± 0.3 °C) about 20 days and about 2 days were needed for the precipitation of about 100 mg aragonite, respectively. The aragonite was grown at a pH of 9.0, which was kept constant during the entire experiment in order to prevent the formation of brucite. The entire experiment was carried out in an inert N_2-atmosphere. After termination of each experiment the precipitated solids were removed from the outer solution by filtration through a 0.2 µm membrane filter under nitrogen atmosphere. Some additional solids were mechanically removed from the outside of the 0.5 l bottle. The solids were washed with double distilled water until the remaining solution was chloride free and dried at 30 °C. The mineralogical composition of the solids was identified

by X-ray diffraction (goniometer type Philips PW 1130/1370) and infrared spectroscopy (Perkin Elmer FTIR 1600) at the University of Göttingen, Germany.

4.2.2 Culture Experiments (O. universa)

Foraminifers were maintained in laboratory cultures between 10.5 °C and 29.3 °C (± 0.2 °C) at either the Wrigley Institute for Environmental Science on Santa Catalina Island (California, USA) or at the Isla Magueyes Marine Laboratory on Puerto Rico. Orbulina universa were collected by scuba divers and were grown in 0.8 µm filtered sea water using standard procedures (Spero, 1998; Spero et al., 1997). All analyzed specimens were collected as 'juvenile' pre-sphere individuals. The complete precipitation of the spherical chamber which was used for δ^{44}Ca analysis occurred under controlled conditions in the laboratory. For the temperature calibration Orbulina universa were cultured in ambient seawater. The pH drops with increasing temperature due to the temperature dependent dissociation constants. However, the pH-values varied only between about 8.1–8.3. For studying the effect of CO_3^{2-}-changes on the δ^{44}Ca, *O. universa* was cultured at 22 °C in seawater containing 137–530 µmol kg^{-1} CO_3^{2-}.

4.2.3 Sample Preparation and δ^{44}Ca-measurements

For determination of the Ca isotope composition about 1 mg of aragonite or 5 to 40 µg of foraminiferal test calcite were dissolved in 2.5 N ultrapure HCl. An isotopically well defined ^{43}Ca/^{48}Ca double spike was added to an aliquot of the solution to correct for isotope fractionation in the mass-spectrometer during the course of the Ca isotope analysis. The sample-spike mixture was dried and recovered in about 2 µL 2.5 N HCl and then loaded with a Ta_2O_5-activator solution using the "sandwich-technique" (activator-sample-activator) onto a previously outgassed single filament (zone refined rhenium). After evaporating to dryness the filament with the sample/spike mixture was briefly glowed.
Measurements of the isotopic composition of Ca were performed on a Finnigan MAT 262 RPQ+ thermal ionization mass spectrometer at GEOMAR research center in Kiel, Germany. The mass-spectrometer was operated in positive ionization mode with a 10 kV acceleration voltage and a 10^{11} Ω resistor for the faraday cups. A stable ion-beam of about 3 to 5 V on mass 40 is achieved at about 1550 to 1580 °C. Data acquisition is performed in two steps because the dispersion of our mass-spectrometer does not account for the mass range from 40 to 48 amu (atomic mass units). In the first step masses 40, 41, 42, 43 and in a second step 44 and 48 are measured simultaneously. During data acquisition ^{41}K

was continuously monitored for correction of isobaric interferences on mass 40, although we found that this interference or any other possible isobaric interferences are negligible. In order to calculate the "true" $^{44}Ca/^{40}Ca$ ratio of the carbonate sample the measured isotope ratios have to be corrected for the added $^{43}Ca/^{48}Ca$ double spike. This correction is carried out using the mathematical algorithm of Compston and Oversby (1969) slightly modified by adopting an exponential mass fractionation law. The isotope variations of Ca are expressed as δ^{44}Ca-values ($\delta^{44}Ca=((^{44}Ca/^{40}Ca)_{sample}/(^{44}Ca/^{40}Ca)_{standard}$ -1)×1000), where the measured $^{44}Ca/^{40}Ca$ ratios are normalized relative to the $^{44}Ca/^{40}Ca$ ratio of a CaF_2-standard solution ($^{44}Ca/^{40}Ca$: 0.021208; (Russell et al., 1978)). Such a normalization procedure was previously used by Nägler et al. (2000) and Russell et al. (1978). More details of our analytical method are given in Heuser et al. (2002). In order to monitor our long-term reproducibility we repeatedly measured two internal standards, natural CaF_2 and calcium carbonate (NIST SRM 915a). Our 95 measurements of the CaF_2 standard show a mean $^{44}Ca/^{40}Ca$-ratio of 0.0212594 ± 0.0000005 ($2\sigma_m$). All measurements of samples and standard materials are normalized to this value. As our $^{43}Ca/^{48}Ca$ double spike is not calibrated for the determination of the absolute $^{44}Ca/^{40}Ca$ ratio the above values do not represent the true isotopic composition of the CaF_2 standard. 105 measurements of NIST SRM 915a show a mean δ^{44}Ca value of -1.450 ± 0.025 ‰ ($2\sigma_m$). The mean 2σ-reproducibility of our samples is about 0.12 ‰ (ranging from 0.03 to 0.2 ‰) determined by repeated aliquot measurements of various sample materials. In order to improve the statistical significance of a single δ^{44}Ca-measurement all samples were measured at least twice.

4.3 Results

The δ^{44}Ca values of *O. universa* and the inorganically precipitated aragonite are presented in Table 4.1. From Figure 4.1 it can be seen that the values of the inorganic precipitates and of *O. universa* are generally lower than their corresponding bulk solution. Furthermore, the δ^{44}Ca-ratios of all carbonates are positively correlated to temperature although the temperature sensitivity of the previously measured *G. sacculifer* (Nägler et al., 2000) is a factor of about 13 and 16, respectively, larger than that of *O. universa* and the precipitates.

Precipitates:	$\delta^{44}Ca_{arag-fluid} = 0.015 \cdot T(°C) - 2.23$	$\delta^{44}Ca_{fluid} = -0.3$ ‰
O. universa:	$\delta^{44}Ca_{calcite-fluid} = 0.019 \cdot T(°C) - 0.96$	$\delta^{44}Ca_{fluid} = +0.5$ ‰
G. sacculifer:	$\delta^{44}Ca_{calcite-fluid} = 0.24 \cdot T(°C) - 8.00$	$\delta^{44}Ca_{fluid} = +0.5$ ‰

Table 4.1: δ^{44}Ca-values of cultured *O. universa* and inorganically grown aragonite

sample	T (°C)	$\delta^{44}Ca_{CaCO_3}$	α(T)	CO_3^{2-} (μmol kg^{-1})	light
O. universa	10.5	−0.71	1.00121	amb	
O. universa	10.5	−0.73	1.00123	amb	
O. universa	12.9	−0.69	1.00119	amb	
O. universa	12.9	−0.74	1.00124	amb	
O. universa	16.2	−0.72	1.00122	amb	
O. universa	18	−0.63	1.00113	amb	
O. universa	18	−0.65	1.00115	amb	
O. universa	21	−0.58	1.00108		hl
O. universa	21	−0.69	1.00119		hl
O. universa	22	−0.57	1.00107	156	
O. universa	23.3	−0.56	1.00106	amb	hl
O. universa	23.3	−0.46	1.00096	amb	hl
O. universa	27	−0.44	1.00094	amb	hl
O. universa	27	−0.40	1.00090	amb	hl
O. universa	27	−0.45	1.00095	amb	hl
O. universa	29.2	−0.64	1.00114	190	hl
O. universa	29.3	−0.33	1.00083		hl
O. universa	29.3	−0.36	1.00086		hl
O. universa	29.3	−0.41	1.00091		hl
O. universa	29.3	−0.46	1.00096		ll
O. universa	29.3	−0.43	1.00093		ll
O. universa	22	−0.54	1.00104	324	
O. universa	22	−0.58	1.00108	260	
O. universa	22	−0.64	1.00114	242	
O. universa	22	−0.70	1.00120	242	
O. universa	22	−0.46	1.00096	324	
O. universa	22	−0.54	1.00104	220	
O. universa	22	−0.58	1.00108	220	
O. universa	22	−0.65	1.00115	530	
O. universa	22	−0.55	1.00105	137	
Aragonite	10	−2.07	1.00178		
Aragonite	10	−2.10	1.00180		
Aragonite	10	−2.18	1.00188		
Aragonite	10	−2.01	1.00171		
Aragonite	19	−1.94	1.00164		
Aragonite	19	−1.91	1.00162		
Aragonite	19	−1.98	1.00168		
Aragonite	30	−1.83	1.00153		
Aragonite	30	−1.81	1.00152		

Table 4.1: continued

sample	T (°C)	$\delta^{44}Ca_{CaCO_3}$	α(T)	CO_3^{2-} (μmol kg^{-1})	light
Aragonite	30	−1.77	1.00147		
Aragonite	30	−1.73	1.00143		
Aragonite	30	−1.84	1.00154		
Aragonite	30	−1.86	1.00156		
Aragonite	30	−1.68	1.00138		
Aragonite	30	−1.72	1.00142		
Aragonite	40	−1.54	1.00124		
Aragonite	40	−1.62	1.00132		
Aragonite	40	−1.60	1.00130		
Aragonite	40	−1.61	1.00131		
Aragonite	40	−1.60	1.00130		
Aragonite	40	−1.65	1.00135		
Aragonite	50	−1.54	1.00125		
Aragonite	50	−1.52	1.00123		
Aragonite	50	−1.58	1.00128		
Aragonite	50	−1.46	1.00116		
Aragonite	50	−1.43	1.00113		
Aragonite	50	−1.57	1.00128		
Aragonite	50	−1.58	1.00128		

Note: δ^{44}Ca value of the seawater was determined to be +0.5 ‰. The δ^{44}Ca for the bulk solution ($CaCl_2$) of the aragonite was determined to be −0.3 ‰. hl: high light; ll: low light; amb: ambient CO_3^{2-} content of seawater.

In contrast to the δ^{18}O system which becomes isotopically lighter with increasing temperature, the δ^{44}Ca values increase with increasing temperature (Fig. 4.2). Figure 4.3 shows the enrichment factors of *G. sacculifer, O. universa* and the aragonite as a function of the inverse temperature ($\alpha(T) = (^{44}Ca/^{40}Ca)_{fluid}/(^{44}Ca/^{40}Ca)_{solid}$). From logarithmic fits to our isotope and temperature data, the calculated initial enrichment factors α_0 and slopes (ξ) are presented in Table 4.2 and discussed below.

In order to investigate the influence of the CO_3^{2-} concentration on the Ca isotope fractionation we cultured *O. universa* at 22 °C in seawater containing CO_3^{2-} concentrations between 137 and 530 µmol kg^{-1}. Figure 4.4 shows, that our data do not show any significant relationship between the CO_3^{2-}-concentration (and hence pH) and their corresponding δ^{44}Ca values in *O. universa*.

Table 4.2: Initial values (α_0) and slopes (ξ) for the enrichment factor α(T)

	α_0	ξ
Precipitates	0.997	1.37
O. universa	0.996	1.64
G. sacculifer	0.932	21.6

Note: α_0 and ξ values are calculated initial values and slopes for the enrichment factor $\alpha(\mathrm{T}) = \alpha_0 \cdot exp^{(-\xi)}$. The slope ξ corresponds to $\mathrm{E} / \mathrm{k}{\cdot}\mathrm{T}$ (E = energy, k = Boltzman constant,T = absolute temperature).

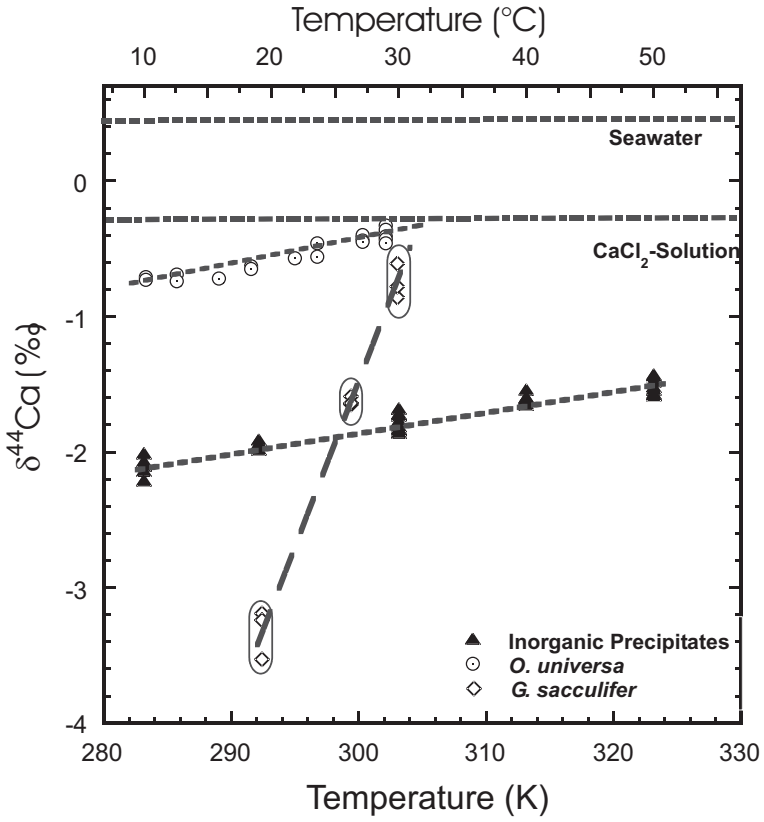

Figure 4.1: The δ^{44}Ca values of the inorganic precipitates and *O. universa* correlate with temperature. All carbonate samples are isotopically lighter than the corresponding bulk solution from which they precipitated. For comparison we show the δ^{44}Ca values for *G. sacculifer* (Nägler et al., 2000). The δ^{44}Ca ratios of *G. sacculifer* show an about 13 and 16 times steeper slope than *O. universa* and the inorganic precipitates, respectively.

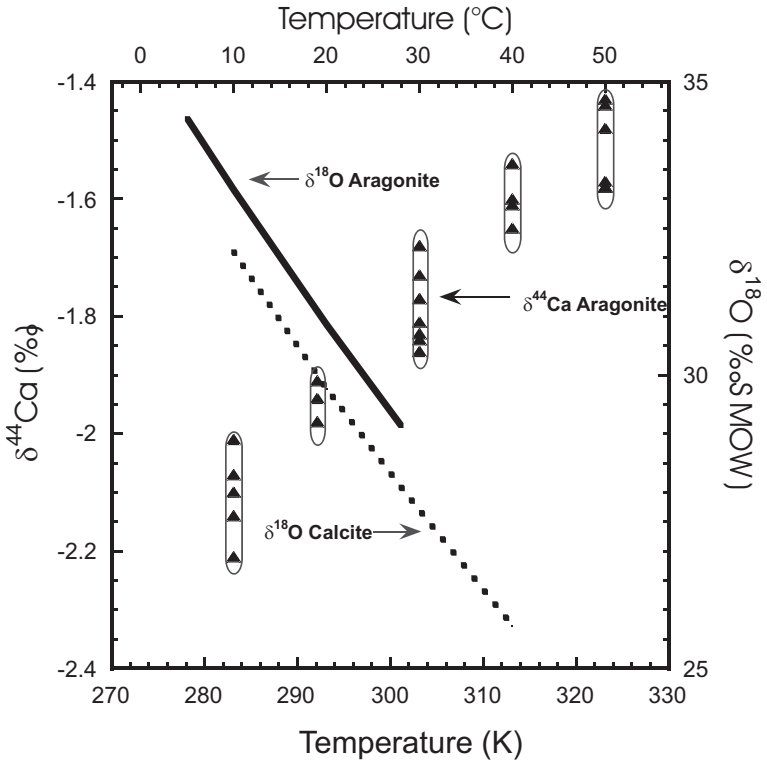

Figure 4.2: Comparison of the experimentally determined temperature dependence for δ^{44}Ca of inorganic aragonite and the temperature dependence of δ^{18}O in isotopic equilibrium for aragonite (Böhm et al., 2000) and for calcite (Kim and Neil, 1997).

4.4 Discussion

4.4.1 Calcium Diffusion and Isotope Fractionation

In order to understand the opposite fractionation behavior of the $^{18}O/^{16}O$ and the $^{44}Ca/^{40}Ca$ isotope systems two possible isotope fractionation processes have to be taken into account: (1) equilibrium isotope fractionation due to the vibrational characteristics of the light and heavy isotopes related to covalent atomic bonding and (2) kinetic isotope fractionation due to the different transport reaction characteristics of light and heavy isotopes during diffusion across the boundary layer between a solution and a solid (cf. O'Neil, 1986; O'Neil et al., 1969; Bigeleisen and Mayer, 1947; Urey, 1947). Kinetic isotope fractionation occurs at any boundary layer from one phase to another (e.g. liquid/solid, liquid/enzyme) because lighter isotopes always tend to diffuse faster than heavier isotopes which results in an enrichment of the lighter isotopes in the product phase. In contrast, equilibrium fractionation occurs as a consequence of covalent atomic bonding. During molecule formation the incorporation of heavier isotopes is preferred because covalent atomic bonds formed with heavier isotopes show larger bonding energies and, hence, are more stable

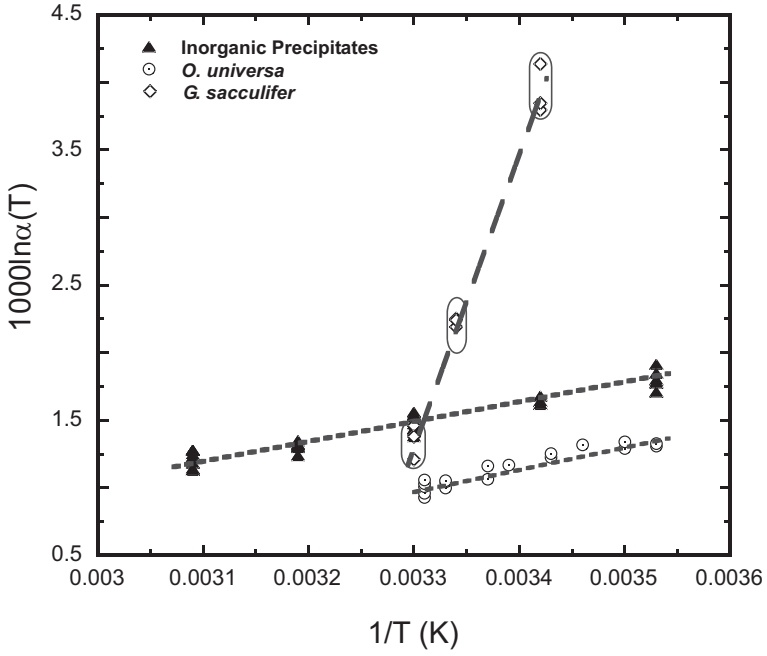

Figure 4.3: The enrichment factor $1000 \ln \alpha(\mathrm{T})$ is shown as a function of the inverse temperature ($\alpha(\mathrm{T}) = (^{44}\mathrm{Ca}/^{40}\mathrm{Ca})_{bulksolution}/(^{44}\mathrm{Ca}/^{40}\mathrm{Ca})_{carbonate}$). Although there is a slight offset between *O. universa* and the inorganic precipitates, it can be seen that the slopes of the enrichment factors $1000 \ln \alpha(\mathrm{T})$ are quite similar. In contrast, the slope of the enrichment factor of *G. sacculifer* is steeper by a factor of 13 and 16, respectively.

than covalent bonds formed with lighter isotopes (cf. O'Neil, 1986; O'Neil et al., 1969). As a consequence of the covalent bonding with C and H atoms the δ^{18}O ratios of the dissolved carbonate species CO_2, HCO_3^- and CO_3^{2-} always tend to be heavier than the δ^{18}O composition of the surrounding bulk solution (e.g. seawater). For example at 19 °C the isotope fractionation of H_2O versus CO_2(aq), HCO_3^-, and solid $CaCO_3$ is about 58 ‰, 34 ‰, and 29 ‰, respectively (Zeebe, 1999).

In contrast, elements like Ca tend to form ionic rather than covalent bonds in carbonate crystals (O'Neil, 1986). Therefore, Ca isotope fractionation is only affected by kinetic isotope fractionation and not by equilibrium fractionation because no vibration bonding modes are active (O'Neil et al., 1969). In general, at fluid-solid interactions both kinetic and equilibrium fractionation processes are temperature dependent. At lower temperatures equilibrium fractionation tends to enrich the heavier isotope in the more stable molecules whereas kinetic fractionation tends to enrich the lighter isotopes in the product phase. Consequently, isotope systems like δ^{18}O controlled by equilibrium fractionation are an inverse function of temperature whereas isotope systems like δ^{44}Ca, controlled by kinetic fractionation, are positively related to temperature (Figure 4.3). Increasing temperature

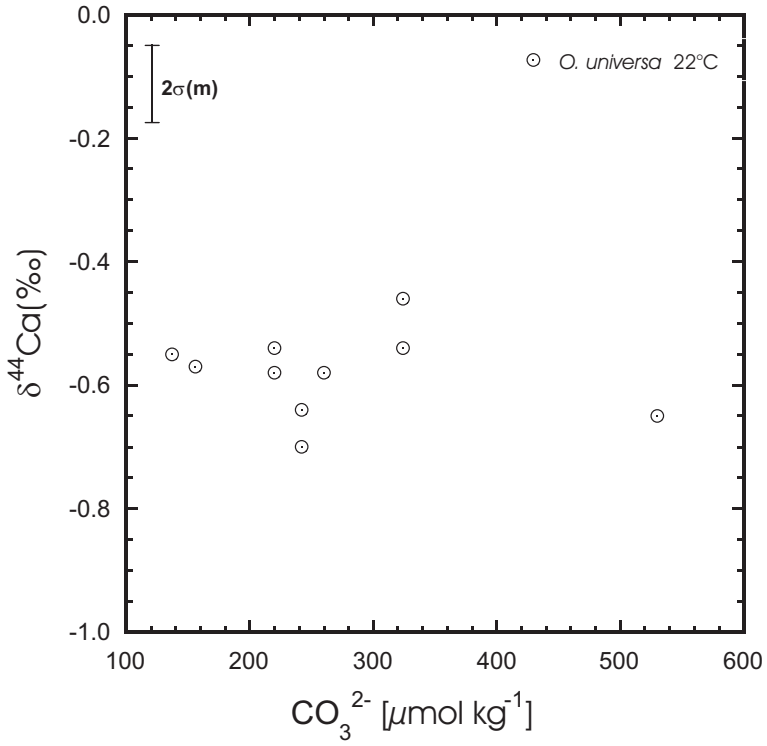

Figure 4.4: The δ^{44}Ca values are plotted as a function of the CO_3^{2-} concentration. Although the CO_3^{2-}-concentration has been varied by almost a factor of 4, there is no indication of a pH dependence of the δ^{44}Ca ratios in *O. universa*.

diminishes the isotope fractionation contrast between the reactants in the bulk solution and the product (e.g. $CaCO_3$).

4.4.2 Kinetic Effects on the Isotope Fractionation–Temperature Relation

It is generally accepted that diffusion across a liquid-solid boundary to and along a crystal growth surface is mass dependent because the diffusion velocities of the lighter isotopes are faster than those of the heavier isotopes. Therefore, the enrichment of the lighter isotope in the $CaCO_3$ crystal relative to the bulk solution as a function of temperature can be described by an enrichment factor α(T). Equation (4.1) and (4.2) in the appendix show that the slope of the enrichment factor α(T) is a function of the ratio of the mass difference (Δm) between the heavy and the light isotope and the reduced isotope mass (m). These equations clearly show that kinetic isotope fractionation is most efficient for low masses at low temperatures. For relatively high masses and high temperatures the enrichment factor approaches unity as expected for kinetic isotope fractionation (see appendix).
These thermodynamic considerations can be used to identify processes responsible for our measured δ^{44}Ca data. In the case of an exclusive kinetic fractionation of ^{40}Ca and ^{44}Ca

it can be predicted, that the slopes for α(T) of the precipitates and two investigated foraminiferal species should be similar. From 4.2 it can be seen that the slopes of the enrichment factors for *O. universa* and the inorganic precipitates are similar. However, a major difference exists between inorganic precipitates, *O. universa* and *G. sacculifer*. The slope of α(T) for *G. sacculifer* is steeper by a factor of 13 relative to *O. universa* and a factor of 16 relative to the precipitates (Table 4.2). From equation (4.2) it follows that the slope of the enrichment factor α(T) is controlled by the (Δm/m)-ratio. Relatively low (Δm/m)-ratios correspond to relatively shallow slopes for α(T) whereas relatively large (Δm/m)-ratios correspond to steep slopes for α(T). The observation of shallower slopes for the inorganic precipitates and *O. universa* apparently indicate that Ca speciation with atomic masses much larger than pure Ca atoms (e.g. 40 and 44 amu) must control the diffusion velocity in *O. universa* and the inorganic precipitates. The similarity of the slopes of *O. universa* and the inorganic precipitates indicates that an inorganic or thermodynamic process has to be involved in order to explain their similarity. This process cannot be simple Rayleigh fractionation because the latter effect is closely related to equilibrium fractionation and not to kinetic isotope fractionation as it is the case for the Ca-isotope system. Furthermore, the difference in Ca isotope fractionation behavior between *O. universa* and *G. sacculifer* indicates that their specific $CaCO_3$ precipitation mechanisms must be considerably different. Thus, a combination of inorganic transport mechanisms and kinetically controlled biochemical calcification processes has to be involved in order to explain the observed phenomena. In the section below we will first focus on a model for Ca^{2+} diffusion into a $CaCO_3$ crystal. Then, we will discuss different calcification models for *O. universa* and *G. sacculifer*.

From the assumption that Ca is diffusing as pure Ca^{2+}-ion in *G. sacculifer* we can estimate from the different slopes of the enrichment factors that the apparent atomic mass of the diffusing species in *O. universa* and the inorganic precipitates correspond to a weight of about 520 ± 60 and 640 ± 70 amu, respectively. Masses of several hundred amu cannot reflect the motion of a single Ca^{2+}-ion or any other known inorganic Ca species within *O. universa* and the inorganic precipitates. Such large masses usually reflect either organic molecules or metal complexes (e.g. Ca^{2+}-aquocomplexes, Bockris and Reddy, 1973; Langmuir, 1997). Most likely, the influence of large organic molecules is negligible for the inorganic precipitates. Therefore, we hypothesize that these calculated masses reflect the motion and diffusion of Ca^{2+}-ion complexes (Ca^{2+}-aquocomplex) in *O. universa* and the inorganic precipitates. From the calculated masses of about 520 (*O. universa*) and 640 amu (precipitates) we calculate hydration numbers (the number of water molecules associated

with a single Ca^{2+}-ion) of about 27 ± 4 and 33 ± 5.

In general, ion complexes are dissolved species that exist because of the association of a cation with an anion or with neutral molecules like water (Langmuir, 1997). Most trace metals and many major elements are transported in water in complexed form. Estimates of the number of water molecules associated with each cation (hydration number) are difficult to obtain, and the results vary with the technique used for determination. Koneshan et al. (1998) calculated first shell hydration numbers of 4 water molecules associated with a lithium ion and 7 water molecules associated with a potassium ion. Hydration numbers increase with increasing ionic size, as in the sequence $Li^+ < Na^+ < K^+ < Rb^+ < Cs^+$.

Recent work suggests, that the first hydration shell of a Ca^{2+}-aquocomplex consists of 8 water molecules ($Ca\,[H_2O]_8{}^{2+}$, 184 amu) (Jalilehvand et al., 2001; Koneshan et al., 1998) although in earlier publications between 6 to 10 water molecules are reported (Kaufman Katz et al., 1996; Langmuir, 1997; Spångberg et al., 2000). Modeling and experimental results indicate a strongly bound, clearly defined inner hydration shell, and a more weakly bound second shell (Jalilehvand et al., 2001; Koneshan et al., 1998). Molecules of the second shell are bound by hydrogen bondings to the water molecules of the first hydration shell. The number of waters that may occupy the second hydration sphere varies depending on the model selected from 11 to 18 (Jalilehvand et al., 2001). The concept of strongly bound first shell and weakly bound second shell molecules is also supported by the findings that the residence time of a water molecule in the first shell ($Ca[H_2O]_8{}^{2+}$) of a Ca^{2+}-aquocomplex is about 40 times longer than in the second shell. The residence times of water molecules in the second shell of a Ca^{2+} are in the same order of magnitude as the residence times of water molecules in the first shell of alkali cations (Koneshan et al., 1998).

An atomic mass around 520 amu (*O. universa*) is compatible with the maximum value for a hydration number of about 25 which has recently been reported by Spångberg et al. (2000), Jalilehvand et al. (2001) and Koneshan et al. (1998). Values of more than 600 amu (inorganic aragonite) exceed the empirically determined and accepted hydration number for a Ca^{2+}-aquocomplex. Apparently higher hydration numbers might be caused by additional complexation with anions. This is also appealing because the mineral surface is charged and the electrostatic repulsion is reduced by ion-pairing the hydrated cation.

For example, in seawater $\sim 10\,\%$ of the dissolved Ca^{2+} is bound to $SO_4{}^{2-}$ forming a $CaSO_4{}^0 \cdot n\,H_2O$ complex (Byrne, 2002). However, in our experiments, the inorganic aragonite was precipitated from a sulfate free solution. Therefore, at least for our inorganically precipitated aragonite, complexation with $SO_4{}^{2-}$ can be ruled out. Other anions like Cl^- or carbonate species may play a role in this case.

We note, that the hypothesized fractionation processes involving hydrated and de-hydrated Ca^{2+}-ions presented here have yet not been tested by experiments. We therefore consider our interpretation preliminary pending future confirmation.

4.4.3 Ca^{2+}-Transport and Fractionation in O. universa and G. sacculifer

In order to reconcile our δ^{44}Ca-data we suggest that the δ^{44}Ca fractionation involved is similar in Orbulina and inorganic aragonite although their calcification mechanisms are different. For *G. sacculifer*, a metabolic process is suggested that actively dehydrates the Ca^{2+}-aquocomplex before calcification. Differences between *G. sacculifer* and *O. universa* have already been reported concerning Ca storage within the cytoplasm (Ca-pools). Anderson and Faber (1984) hypothesized that *G. sacculifer* stores significant amounts of Ca in its cytoplasm prior to deposition. In contrast, Lea et al. (1995) found little evidence for a substantial Ca pool in *O. universa*. Both observations are in accord with our δ^{44}Ca data because Ca storage requests enzymatically mediated Ca-transport which is performed more favorably in dehydrated ionic form than in complexed form. In contrast, the absence of Ca storage in *O. universa* points to a calcification process closer to inorganic $CaCO_3$ precipitation.

Following a model for imperforate foraminifer originally presented by ter Kuile (1991), we propose for *O. universa* that seawater is incorporated into vesicles within the cytoplasm by the process of vacuolization. Precipitation of $CaCO_3$ needles (Hemleben et al., 1986) is then triggered in the vesicles either by actively increasing the pH in the vesicle or by the removal of calcium carbonate precipitation inhibiting ions like Mg^{2+} or ${PO_4}^{3-}$ (Swart, 1983). In the vesicle, $^{44}Ca/^{40}Ca$ fractionation occurs during the formation of the amorphous carbonate $CaCO_3$ which closely resembles the precipitation of inorganic $CaCO_3$.

Following a model for perforate foraminifer (ter Kuile, 1991) we further propose that dehydration of the Ca^{2+}-aquocomplex occurs anywhere at the transition from seawater to the cytoplasm of *G. sacculifer*. Presumably, regulated cell membranes ("Voltage Operated Ca^{2+}-Channels" (VOC)) are involved with the dehydration of the Ca^{2+}-aquocomplex. It is well known that such Ca^{2+}-VOCs show a high selectivity for Ca^{2+} and are more selective for Ca^{2+} by a factor of 1000 than for other cations like Na^+ and K^+ (cf. Aidley and Stanfield, 1996, Tsien and Tsien, 1990). After dehydration of the Ca^{2+}-aquocomplex by passing the channels the pure Ca^{2+}-ions become attached to transport enzymes within the cytoplasm (ter Kuile, 1991). Kinetic $^{44}Ca/^{40}Ca$ fractionation then occurs at the phase transition of the Ca ions from the channels to the transport enzymes and the adsorption

onto their ligands. Ca is either stored in Ca-pools (Anderson and Faber, 1984) or transported by these enzymes directly to the site of calcification (ter Kuile, 1991).
While our working hypothesis presented here is able to reconcile the observation, and is in line with the above mentioned species dependent biological/metabolic processes, it is clear that further studies will have to investigate parameters like varying precipitation rates, pH changes or chemical composition of the culture solution.

4.5 Summary and Conclusions

A. The temperature dependent fractionation characteristics of δ^{44}Ca and δ^{18}O are opposite since δ^{44}Ca ratios in $CaCO_3$ are controlled by kinetic isotope fractionation only.

B. The slope of the enrichment factor α(T) of the inorganic precipitates and *O. universa* reflects the occurrence, transport and diffusion of Ca^{2+}-aquocomplexes in seawater. Our δ^{44}Ca data reveal atomic masses which reflect the motion of heavy Ca^{2+}-aquocomplexes. These heavy complexes are less sensitive to temperature dependent kinetic isotope fractionation than pure Ca^{2+}-ions.

C. Ca isotope fractionation in *G. sacculifer* indicates dehydration of the Ca^{2+}- aquocomplex and transport in its pure ionic form presumably during biological mediated processes.

D. A major conclusion of this study is that the results for *G. sacculifer* cannot be generalized to other species. For paleoceanographic applications it will be necessary to carefully study different species to elucidate their response to temperature as well as to other environmental influences.

Acknowledgements

This study is supported by a grant of the "Deutsche Forschungsgemeinschaft (DFG)" to A. Eisenhauer (Ei272/12-1, CAESAR). The U.S. National Science Foundation supported this studies with grants to H.J. Spero (OCE-9729203) and to D.W. Lea (OCE-9729327). Ca isotope work in Bern (Switzerland) is supported by SNF grant 21-61644 to Th.F. Nägler. H.J. Spero acknowledges the Hanse Institute for Advanced Studies, Delmenhorst, Germany for fellowship support. We also thank the research staff of the Wrigley Institute for Environmental Studies and the Isla Magueyes Marine Laboratory, Puerto Rico for assistance

in the field. In particular, we appreciate the help of D.R. Cole, A. Paytan and T. Esat who significantly helped to improve the manuscript by constructive comments and helpful suggestions.

References

Aidley D. J. and Stanfield P. R. (1996) Ion Channels. Cambridge University Press.

Anderson O. R. and W. W. Faber jr. (1984) An estimation of calcium carbonate deposition rate in a planktonic foraminifer *Globigerinoides sacculifer* using ^{45}Ca as a tracer: a recommended procedure for improved accuracy. *J. Foraminiferal Res.* **14**, 303–308.

Arp G., Reimer A., and Reitner J. (2001) Photsynthesis-Induced Biofilm Calcification and Calcium Concentrations in Phanerozoic Oceans. *Science* **292**, 1701–1704.

Bigeleisen J. and Mayer M.G. (1947) Calculation of equilibrium constants for isotopic exchange reactions. *J. Chem. Phys.* **15**, 261–267.

Bockris J. O. and Reddy A. K. N. (1973) Modern Electrochemistry. Plenum Press.

Böhm F., Joachimski M. M., Dullo W.-C., Eisenhauer A., Lehnert H., Reitner J., and Wörheide G. (2000) Oxygen isotope fractionation in marine aragonite of coralline sponges. *Geochim. Cosmochim. Acta* **64**, 1695–1703.

Byrne, R. H. (2002) Inorganic speciation of dissolved elements in seawater: the influence of pH on concentration ratios. *Geochem. Trans.* **3**, 11–16

Compston W. and Oversby V. (1969) Lead isotopic analysis using a double spike. *J. Geophys. Res.* **74**, 4338–4348.

Degens E. T. (1979) Why do organism calcify? *Chem. Geol.* **25**, 257–269.

Dietzel M. and Usdowski E. (1996) Coprecipitation of Ni^{2+}, Co^{2+}, and Mn^{2+} with galena and covellite, and of Sr^{2+} with calcite during crystallization via diffusion of H_2S and CO_2 through polyethylene at 20 °C: Power law and Nernst law control of trace elements partitioning. *Chem. Geol.* **131**, 55–65.

Hemleben C., Anderson O. R., Berthold W., and Spindler M. (1986) Calcification and Chamber Formation in Foraminifera: A brief overview. In *Biomineralization in Lower Plants and Animals* (ed. B. S. C. Leadbeater and R. Riding), pp. 237–249. The Systematics Association.

Heumann K. G., Klöppel H., and Sigl G. (1982) Inversion der Calcium- Isotopenseparation an einem Ionenaustauscher durch Veränderung der LiCl- Elektrolytkonzentration. *Z. Naturforsch.* **37b**, 786–787.

Heumann K. G. and Lieser K.H. (1972) Untersuchung von Calciumisotopieeffekten bei heterogenen Austauschgleichgewichten. *Z. Naturforsch.* **27b**, 126–133.

Heumann K. G., Lieser K. H., and Elias H. (1970) Difficulties in Measuring the Isotopic Abundances of Calcium with a Mass Spectrometer. In *Recent Developments in Mass Spectroscopy* (ed. K. Ogata and T. Hayakawa), pp. 457–459. University of Tokyo Press

Heuser A., Eisenhauer A., Gussone N., Bock B., Hansen B. T., and Nägler Th. F. (2002) Measurement of Calcium Isotopes (δ^{44}Ca) Using a Multicollector TIMS Technique. *Int. J. Mass Spec.* **220**, 387–399.

Jalilehvand F., Spångberg D., Lindqvist-Reis P., Hermansson K., Persson I. and Sandström M. (2001) Hydration of the Calcium Ion. An EXAFS, Large-Angle X-ray Scattering, and Molecular Dynamics Simulation Study. *J. Am. Chem. Soc.* **123**, 431–441.

Kaufman Katz A., Glusker J. P., Beebe S. A. and Bock, C. W. (1996) Calcium Ion Coordination: A Comparison with That of Beryllium, Magnesium, and Zinc. *J. Am. Chem. Soc.* **118**, 5752–5763.

Kempe S. and Degens E. T. (1985) An Early Soda Ocean? *Chem. Geol.* **53**, 95–108.

Kim S.-T. and Neil J. R. (1997) Equilibrium and nonequilibrium oxygen isotope effects in synthetic carbonates. *Geochim. Cosmochim. Acta* **61**, 3461–3475.

Koneshan S., Rasaiah J. C., Lynden-Bell R. M., and Lee S. H. (1998) Solvent structure, dynamics, and ion mobility in aqueous solutions at 25℃. *J. Phys. Chem. B* **102** 4193–4204.

ter Kuile B. T. (1991) Mechanisms for calcification and carbon cycling in algal symbiont-bearing foraminifera. In *Biology of Foraminifera* (ed. J. L. Lee and O. R. Anderson), pp. 74–89. Academic Press.

Langmuir D. (1997) Aqueous environmental geochemistry. Prentice Hall.

Lea D. W., Martin P. A., Chan D. A., and Spero H. J. (1995) Calcium uptake and calcification rate in the planktonic foraminifer *Orbulina Universa*. *J. Foraminiferal Res.* **25**, 14–23.

Lea D. W., Pak D. K. and Spero H. J. (2000) Climate impact of late quaternary equatorial Pacific sea surface temperature variations. *Science* **289**, 1719–1724.

Nägler Th. F., Eisenhauer A., Müller A., Hemleben C., and Kramers J. (2000) The δ^{44}Ca-temperature calibration on fossil and cultured *Globigerinoides sacculifer*: New tool for reconstruction of past sea surface temperatures. *Geochem. Geophys. Geosys.* **1**, 2000GC000091.

O'Neil J. R., Clayton R. N., and Mayeda T. K. (1969) Oxygen Isotope Fractionation in Divalent Metal Carbonates. *J. Chem. Phys.* **51**, 5547–5558.

O'Neil J. R. (1986) Theoretical and experimental aspects of isotopic fractionation. In *Reviews of Mineralogy. Stable Isotopes in High Temperature Geological Processes, Vol. 16* (ed. J. W. Valley, J. R. O'Neil, and H. P. Taylor), pp. 561–570. Mineralogical Society of America.

De La Rocha C. L. and DePaolo D. J. (2000) Isotopic Evidence for Variations in the Marine Calcium Cycle Over The Cenozoic. *Science* **289**, 1176–1178.

Russell W. A., Papanastassiou D. A., and Tombrello T. A. (1978) Ca isotope fractionation on the Earth and other solar system materials. *Geochim. Cosmochim. Acta* **42**, 1075–1090.

Skulan J. L., DePaolo D. J., and Owens T. L. (1997) Biological control of calcium isotopic abundances in the global calcium cycle. *Geochim. Cosmochim. Acta* **61**, 2505–2510.

Skulan J. L. and DePaolo D.J. (1999) Calcium isotope fractionation between soft and mineralized tissues as a monitor of calcium use in vertebrates. *Biochemistry* **96**, 13709–13713.

Spångberg D., Hermansson K., Lindqvist-Reis P., Jalilehvand F., Sandström M., Persson, I. (2000) *J. Phys. Chem. B* **104**, 10467–10472.

Spero H. J. (1998) Life history and stable isotope geochemistry of planktonic foraminifera. In *Isotope Paleobiology and Paleoecology, Paleontological Society Papers*, Vol. 4 (ed. R. D. Norris and R. M. Corfield), pp. 7–36.

Spero H. J., Bijma J., Lea D. W., and Bemis B. E. (1997) Effect of seawater carbonate concentration on planktonic foraminiferal carbon and oxygen isotopes. *Nature* **390**, 497–500.

Stahl W. and Wendt L. (1968) Fractionation of calcium isotopes in carbonate precipitation. *Earth Planet. Sci. Lett.* **5**, 184–186.

Stanley S. M. and Hardie L. A. (1998) Secular oscillations in the carbonate mineralogy of reef-building and sediment-producing organisms driven by tectonically forced shifts in seawater chemistry. *Palaeogeogr. Palaeocl. Palaeoecol.* **144**, 3–19.

Swart P. K. (1983) Carbon and oxygen isotope fractionation in scleeractinian corals: A review. *Earth Sci. Rev.* **19**, 51–80.

Tsien R. W. and Tsien R. Y. (1990) Calcium channels, stores, and oscillations. *Annual Review of Cell Biology* **6**, 715–760.

Urey H. C. (1947) The Thermodynamic Properties of Isotopic Substances. *J. Chem. Soc.* **45**, 562–581

Wallmann K. (2001) Controls on the Cretaceous and Cenozoic evolution of seawater composition, atmospheric CO_2 and climate. *Geochim. Cosmochim. Acta* **65**, 3005–3025.

Williams R. J. P. (1974) Calcium ions: their ligands and their function. *Biochemical Society Symposia* **39**, 133–138.

Williams R. J. P. (1989) Calcium and cell steady states. In *Calcium Binding Proteins in Normal and Transformed Cells* (ed. R. Pochet, D. E. M. Lawson, and C. W. Heizmann), pp. 7–16. Plenum Publishing Corporation.

Zeebe R.E. (1999) An explanation of the effect of seawater carbonate concentration on foraminiferal oxygen isotopes. *Geochim. Cosmochim. Acta* **63**, 2001–2007.

Zeebe R. E. and Wolf-Gladrow D. A. (2001) CO_2 in Seawater: Equilibrium, Kinetics, Isotopes. Elsevier.

Zhu P. and MacDougall J. D. (1998) Calcium isotopes in the marine environment and the oceanic calcium cycle. *Geochim. Cosmochim. Acta* **62**, 1691–1698.

Appendix

The enrichment factor α(T) is described by a partitioning function (eq. 4.1) where ΔE is the difference of the kinetic energy (E_{kin}) between the heavy and the light isotope.

$$\alpha(\mathrm{T}) \approx \alpha_0 \cdot e^{\frac{-\Delta \mathrm{E}}{\mathrm{E}}} ; \mathrm{E}_{kin} = \frac{3}{2} \cdot \mathrm{k} \cdot \mathrm{T} \text{ and } \Delta \mathrm{E} \approx \mathrm{E}_{kin} \cdot \frac{\Delta \mathrm{m}}{\mathrm{m}} \tag{4.1}$$

it follows

$$\alpha(\mathrm{T}) = \alpha_0 \cdot e^{-\frac{2 \cdot \mathrm{E}_{kin}}{3 \cdot \mathrm{k}} \cdot \frac{\Delta \mathrm{m}}{\mathrm{m}} \cdot \frac{1}{\mathrm{T}}} \tag{4.2}$$

$\alpha(\mathrm{T}) = ({}^{44}\mathrm{Ca}/{}^{40}\mathrm{Ca})_{fluid} \,/\, ({}^{44}\mathrm{Ca}/{}^{40}\mathrm{Ca})_{solid}$. E_{kin}: kinetic energy; m: reduced atomic mass for the light and heavy isotope; k: Boltzman constant ($1.38 \cdot 10^{-23}$ J/K); T: absolute temperature in Kelvin (K).

5 δ^{44}Ca Variations of Planktonic Foraminifers from the Western Equatorial Pacific and the Southern Indian Ocean

by

A. Heuser[1], A. Eisenhauer[1], P.N. Pearson[3], F. Böhm[1], N. Gussone[1], Th.F. Nägler[3]

[1] GEOMAR, Forschungszentrum für Marine Geowissenschaften, Wischhofstr. 1-3. 24148 Kiel, Germany

[2] Department of Earth Sciences, University of Bristol, Queens Road Bristol BS8 1RJ, United Kingdom

[3] Institut für Geologie, Gruppe Isotopengeologie, Universität Bern, Erlacherstr. 9a, 3012 Bern, Switzerland

Abstract

Measurements of the calcium isotopic composition (δ^{44}Ca) of four planktonic foraminifera (*Globigerinoides trilobus, Globigerinoides ruber/subquadratus, Globigerinella spp.* and *Globigerina bulloides*) from the western equatorial Pacific and the Indian sector of the southern Ocean show variations of about 0.7 ‰ over the past 24 Ma. *G. bulloides* and *G. trilobus* fractionate Ca isotopes independent from seawater temperature changes and can be used for the reconstruction of Ca isotope composition of seawater (δ^{44}Casw). In contrast, *G. ruber/subquadratus* and *Globigerinella spp.* do fractionate Ca isotopes as a function of the seawater temperature. From these two records it is possible to evaluate temperature changes in the western equatorial Pacific Ocean over the past 24 Ma. The calculated temperatures of both records vary by about 2 °C in the studied time period. The most prominent feature of both trends is a cooling between 4 and 2 Ma of about 1 to 2 °C which could be a consequence of the closure of the Isthmus of Panama between 5 and 4 Ma and the implicated changes of ocean circulation and climate. Between 15 and 8 Ma the temperatures remained constant in western equatorial Pacific. As the two calculated temperature trends differ between 24 and 15 Ma the evolution of seawater temperatures in this region is ambiguous. The calculated $\delta^{44}Ca_{sw}$ from the *G. trilobus* and *G. bulloides* are in good agreement with previously published data but exhibit some more details due to a higher temporal resolution of our sampling (∼1 Ma).

5.1 Introduction

Foraminifers are important marine archives because the oxygen (δ^{18}O) and carbon isotope (δ^{13}C) composition as well as the element/calcium ratios (e.g. Mg/Ca and Sr/Ca) of their calcium carbonate ($CaCO_3$) shells are used as proxies for the reconstruction of past climate and environmental conditions (e.g. Farrell and Prell, 1991; Hastings et al., 1998; Lear et al., 2000; Rosenthal et al., 1997). For the reconstruction of past changes of continental erosion and chemical weathering usually strontium (Sr) and neodymium (Nd) isotopes are applied because the different rock endmembers are considerably different in their isotopic composition (e.g. Jacobsen et al. 2002; Harris, 1995; Vance and Burton, 1999). Ca isotope ratios (δ^{44}Ca) in foraminiferal tests are also supposed to serve as a proxy for continental weathering, although, the use of calcium isotope variations was limited until recently by the small extend of naturally occurring fractionation and the limited precision of the mass spectrometry (Russell et al., 1978; Heumann et al., 1970). Recent advancements in mass spectrometry (Heuser et al., 2002; Nägler et al., 2001) enhanced the precision of the δ^{44}Ca

measurements enabling detailed investigations of Ca isotope variations in foraminifers (Gussone et al, in press; De La Rocha and DePaolo, 2000).

Among other factors Ca isotope variations in foraminifers are known to be influenced by secular variations of the Ca isotope composition of the seawater (De La Rocha and DePaolo, 2000) and by seawater temperature (Nägler et al, 2000; Zhu and Macdougall, 1998). The temperature dependence of δ^{44}Ca variations in foraminiferal tests was first described by Zhu and Macdougall (1998) for the planktonic foraminifers *G. sacculifer* and *N. pachyderma*. Zhu and Macdougall compared the δ^{44}Ca of two *G. sacculifer* specimens: one that grew at present-day and one that grew at Last Glacial-Maximum (LGM) water temperatures. They found that the δ^{44}Ca of the LGM-sample is about 0.6 ‰ lighter than present-day δ^{44}Ca resulting in a gradient of 0.4 ‰/°C assuming that the seawater temperature difference between LGM (Last Glacial Maximum) and present is about 1.5 °C. The temperature dependency of *G. sacculifer* was confirmed by Nägler et al. (2000) who studied δ^{44}Ca variations of *G. sacculifer* cultured under laboratory controlled temperature conditions. They reported a gradient of about 0.24 ‰/°C. This relationship is also supported by a positive correlation of Mg/Ca ratios with their corresponding δ^{44}Ca values although there is an offset of about 2.5 °C between the two proxy records (Nägler et al., 2000). For *N. pachyderma* Zhu and Macdougall (1998) showed that the gradient for *N. pachyderma* is about 0.1 ‰/°C being smaller than the value of 0.24 ‰/°C reported by Hippler et al. (2002) for *N. pachyderma* (sinistral) from the polar North Atlantic.

In contrast to the relative large temperature-δ^{44}Ca dependency of *G. sacculifer* and *N. pachyderma* the temperature dependence of *Glabratella ornatissima* is supposed to be negligible (De La Rocha and DePaolo, 2000).

In a systematic study on the influence of seawater temperature on the δ^{44}Ca ratios of organic and inorganic $CaCO_3$ Gussone et al. (in press) investigated temperature dependent calcium isotope fractionation of laboratory cultured *Orbulina universa* and inorganically precipitated aragonite. For both they reported a δ^{44}Ca-temperature gradient of about 0.019 ‰ °C and 0.015 ‰ °C respectively, being a factor of 13 to 16 smaller when compared to *G. sacculifer*. Following a thermodynamical approach the authors proposed that the different δ^{44}Ca-temperature gradients of *O. universa* and *G. sacculifer* can be explained by different biochemical processes related to their calcite precipitation mechanisms (Gussone et al., in press).

The studies of Zhu and Macdougall (1998), Nägler et al. (2000), De La Rocha and DePaolo (2000), Hippler et al. (2002) and Gussone et al. (in press) clearly showed that before interpreting foraminiferal δ^{44}Ca records the extend of temperature dependent Ca isotope

fractionation of the foraminifer species has to be examined. Up to now exists no systematic study of the δ^{44}Ca-temperature relationship for *Globigerina bulloides, Globigerinoides ruber* and *Globigerinella* spp.

Here we present the first time data of δ^{44}Ca variations of four species of planktonic foraminifers (*G. trilobus*, *G. bulloides*, *G. ruber/subquadratus* and *Globigerinella spp.*) from the western equatorial Pacific and the Indian sector of the Southern Ocean over the past 24 Ma. The goal of this study is to verify the use of foraminifera as an archive for past δ^{44}Ca variations in seawater. This study compends and extends earlier studies from De La Rocha and DePaolo (2000) showing that the δ^{44}Ca of seawater, varied by about 0.9 ‰ during the last 80 million years (Ma).

5.2 Samples

For this study we investigated the planktonic foraminifers *Globigerinoides trilobus, Globigerinoides ruber, Globigerinella spp.* and *Globigerina bulloides*. The species *G. trilobus*, *G. ruber* and *Globigerinella spp.* were selected from ODP Leg 144 Sites 871 (Limalok Guyot) and 872 (Lo-En Guyot) in the western equatorial Pacific (871: 5°33.4'N, 172°20.7'E, 1255 m; 872: 10°5.6'N, 162°52.0'E, 1082 m), whereas *G. bulloides* was sampled from ODP Leg 183 Site 1138 in the southern Indian Ocean (53°33.1'S, 75°58,5'E, 1141 m) (Fig. 5.1). For the Leg 144 species we used a combined record of two cores (one from Hole 871A and one from Hole 872C) with an overall temporal resolution of about 1 Ma. The same samples from Leg 144 were previously used for boron isotope analysis (δ^{11}B) to reconstruct the paleo-pH of the oceans (Pearson and Palmer, 2000). Additional data and more details on the sampling locations can be found in Coffin et al. (2000), Frey et al (in press), Premoli Silva et al. (1993) and Hagerty et al. (1995). A more detailed description of the biostratigraphy and micropaleontology of Leg 144 is presented by Pearson (1995).

G. trilobus is used as a broad taxonomic concept for sacculifer-like specimens that lack the sac shaped final chamber (Hemleben, 1989; Pearson et al., 1997). A further split of these specimens into a number of morphospecies is not used.

G. ruber occurred during the Plio-Pleistocene and during the Middle Miocene, but not during the Upper and Lower Miocene. The Miocene species of *G. ruber* is a homeomorph (*G. subquadratus*, Kennett and Srinivasan, 1983) with similar carbon and oxygen isotopic characteristics (Pearson and Shackleton, 1997)

Globigerinella spp. corresponds mostly to *G. praesiphonifera* in the Miocene, which is supposed to have been evolved into modern *G. siphonifera*. In the size fraction (250 to 300

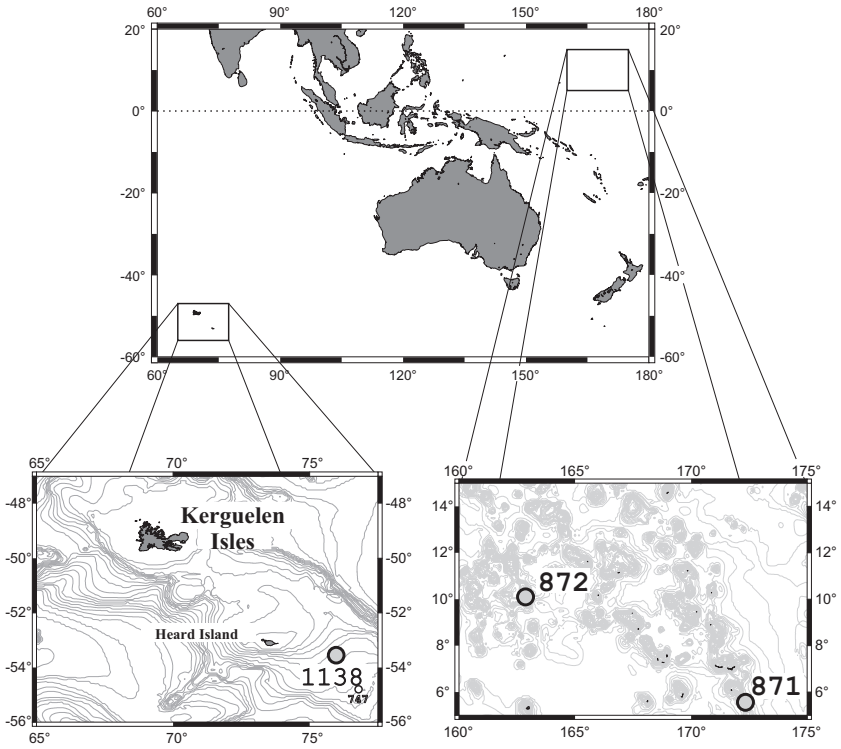

Figure 5.1: Locations of the ODP Sites 871 & 872 in the western equatorial Pacific and Site 1138 in the southern Indian Ocean.

µm) used for this study it is very difficult to distinguish morphospecies like *G. adamsi, G. calida* and *G. siphonifera*. Therefore, the term *Globigerinella spp.* is commonly used for all these species.

The analyzed size fraction of *G. bulloides* is 250 to 500 µm. During the Late Miocene (between 6 to 9 Ma) no samples are recovered due to a hiatus in sedimentation at Site 1138. The temporal resolution of the samples is about 1 Ma.

Chronostratigraphic age assignments of the samples are based on biostratigraphic data for Sites 871 and 872 (Pearson, 1995) and on combined biostratigraphic and magnetostratigraphic data for Site 1138 (Coffin et al, 2000; Vigour and Lazarus, 2002; Antretter et al, in press).

5.3 Methods

5.3.1 Sample preparation and cleaning of the foraminifers

The purpose of the cleaning procedure is to remove interfering organics and diagenetic $CaCO_3$ coatings from the foraminifer tests. About three to six individual foraminifers corresponding to a weight of about 20 to 100 µg of sample material were weighed into a teflon beaker. After adding of 100 µl ultrapure water to the foraminifers they were crushed

using a small teflon rod and then ultrasonically cleaned for 2 minutes. About 60 µl of the water were replaced by fresh water and the foraminifers then again ultrasonically cleaned for about 2 minutes, this step was repeated three times. Then 60 µl were replaced by methanol (CH_3OH) followed by further ultrasonic cleaning for about 2 minutes. Finally, the methanol containing solution was replaced by about 60 µl of ultrapure water followed by an ultrasonic cleaning for 2 minutes. This step was repeated twice.
About 60 µl of this solution was then replaced by 100 µl of a mixture of 0.1 N NaOH and a drop of H_2O_2. This solution was put on a hot plate at about 80 °C for 10 minutes and then ultrasonically cleaned for 2 minutes, this procedure was repeated twice. Then, again about 60 µl of the water was replaced by ultrapure water and again ultrasonically cleaned for another 2 minutes. This step was repeated three times.
At the end of the entire cleaning procedure the fragments of the foraminifers were dissolved using 60 µl of ultrapure 2.5 N HCl, evaporated and redissolved in ultrapure 2.5 N HCl. We used 25 µl acid for each µg of the initial sample weight resulting in a concentration of about 12.5 ng of Ca per µl of sample solution.

5.3.2 Mass spectrometry techniques and data reduction

A detailed description of the applied mass-spectrometer techniques is already presented in Heuser et al. (2002).
In order to correct for isotope fractionation during measurement procedures we added 60 µl of a $^{43}Ca/^{48}Ca$ double spike solution (Tab. 5.1) to about 16 µl of the sample solution ($\sim$ 200 ng Ca) after the cleaning procedure. The spike/sample mixture was evaporated to dryness and redissolved in 1.5 µl ultrapure 2.5 N HCl. The spike/sample mixture was loaded together with a Ta_2O_5 loading solution onto a filament (single filament Re, zone refined) using the "sandwich technique" originally presented by Birck (1985).

The measurements were carried out on a Finnigan MAT 262RPQ+ TIMS at the mass spectrometer facilities of the GEOMAR research center for marine geosciences in Kiel, Germany. Samples were automatically heated to a current of 3000 mA, corresponding to a temperature of about 1500 °C with a rate of 240 mA/min. Further heating was done manually until the intensity on the pilot mass (^{40}Ca) was about 4.5 to 5 V (for more details see Heuser et al., 2002).
For data reduction we use an iterative algorithm based on the routine previously published by Compston and Oversby (1968). This routine was modified for Ca isotope analysis by replacing the linear fractionation correction terms by exponential fractionation

Table 5.1: Ca spike concentration and isotope composition.

Isotope	Concentration (ng/g)
^{40}Ca	8.86
^{42}Ca	0.46
^{43}Ca	47.20
^{44}Ca	2.91
^{48}Ca	60.00

Isotope Ratio	Value
^{40}Ca/^{48}Ca	0.147729
^{42}Ca/^{48}Ca	0.007668
^{43}Ca/^{48}Ca	0.786624
^{44}Ca/^{48}Ca	0.048534
^{44}Ca/^{40}Ca	0.328537

correction terms (Nägler et al., 2000; Heuser et al., 2002). With this algorithm the ^{44}Ca/^{40}Ca ratio of the sample is calculated from the measured ^{44}Ca/^{48}Ca and ^{40}Ca/^{48}Ca ratio. This ^{44}Ca/^{40}Ca ratio is used for the calculation of the δ^{44}Ca value (δ^{44}Ca= $[(^{44}Ca/^{40}Ca)_{sample}/(^{44}Ca/^{40}Ca)_{standard}-1]\times 1000$).

We used the mean ^{44}Ca/^{40}Ca ratio of the two CaF_2 measurements performed at the beginning and end of the daily measurements as $(^{44}Ca/^{40}Ca)_{standard}$-ratio. A drift correction was only performed when the difference of the ^{44}Ca/^{40}Ca ratio between these two standard measurements exceeded the 1σ standard deviation ($1\sigma = \pm 4.78\times 10^{-6}$) of the long-term $(^{44}Ca/^{40}Ca)_{CaF_2}$-standard measurements. In the case of drift correction a linear drift between the two measured standards was assumed. Following the suggestion of Coplen et al. (2002) we report δ^{44}Ca values normalized to NIST SRM 915a. Our measurements originally based on the CaF_2-standard are renormalized using the following relationship: δ^{44}Ca(‰ SRM 915a)= δ^{44}Ca (‰ CaF_2) + 1.41 (SRM 915a = –1.41 (‰ CaF_2), mean of 109 measurements).

All δ^{44}Ca values are reported relative to SRM 915a and represent the mean value of at least two repeated aliquot measurements of an individual sample and statistical uncertainties represent their standard deviation of the mean ($2\sigma_{mean}$).

5.4 Results and discussion

Table 5.4 and Fig. 5.2a show the δ^{44}Ca ratios of the foraminifers from the western equatorial Pacific. All three records show δ^{44}Ca variations in the order of about 0.7 ‰ over the past

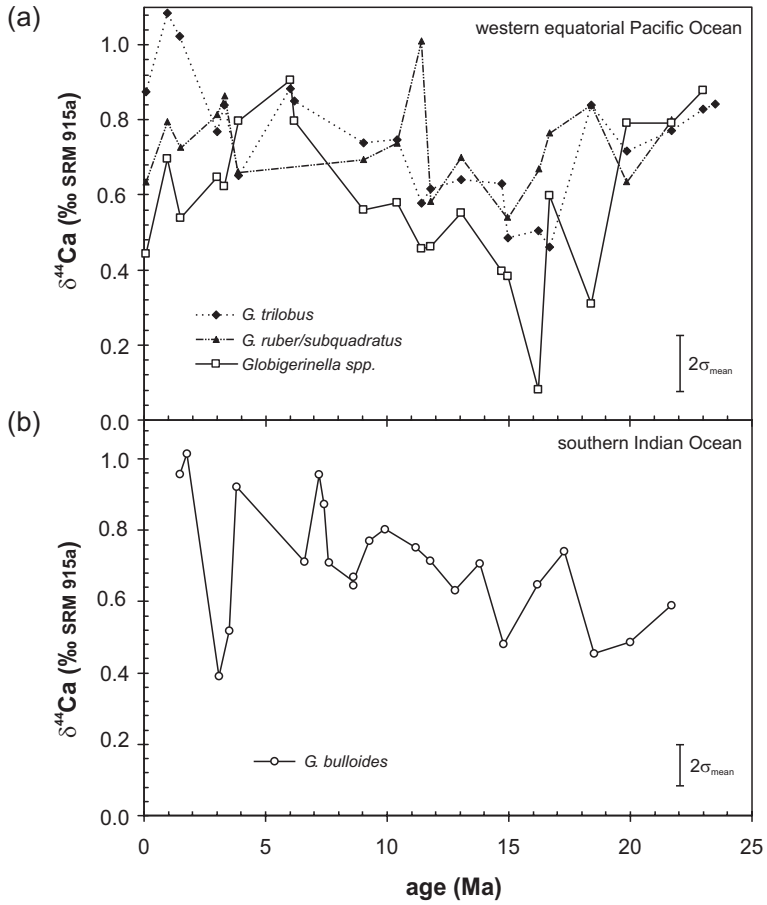

Figure 5.2: δ^{44}Ca ratios of the foraminifers from the western equatorial Pacific (*G. trilobus, G. ruber/subquadratus* and *Globigerinella*) and from the southern Indian Ocean (*G. bulloides*). Error bars represent the average $2\sigma_{mean}$ of all samples of each location.

24 Ma. Common to all three records is a decrease of the δ^{44}Ca values from 24 to 16 Ma followed by an increasing trend from about 16 to 15 Ma to the present. The δ^{44}Ca values at the minimum at ∼16 Ma differ between species. While it is +0.50 and +0.45 ‰ for *G. trilobus* and *G. ruber/subquadratus*, it is +0.1 ‰ for the *Globigerinella spp.*-record. During the entire Miocene (24 to 5 Ma) theδ^{44}Ca patterns of all three species are relatively similar although the *Globigerinella spp.* values are slightly lighter (0.2 ‰) than the δ^{44}Ca values of the other two species. This general accordance of the δ^{44}Ca values is lost in the Pliocene/Pleistocene where the trends remain similar the absolute δ^{44}Ca values diverge to a larger extend. The δ^{44}Ca values of *Globigerinella spp.* are about 0.2 ‰ lighter than *G. ruber/subquadratus* and the δ^{44}Ca values of *G. trilobus* are about 0.3 ‰ heavier than *G. ruber/subquadratus*.

Table 5.2: δ^{44}Ca-ratios of foraminifers from ODP Sites 871A & 872C

Hole	Core	Depth (cm)	Age (Ma)	*G. trilobus*			*G. ruber/subquadratus*			*Globigerinella spp.*		
				δ^{44}Ca	±	n	δ^{44}Ca	±	n	δ^{44}Ca	±	n
871A	1H-1	124–126	0.085	0.87	0.05	3	0.63	0.05	2	0.44	0.13	4
871A	2H-2	59–61	0.98	1.09	0.03	2	0.79	0.15	3	0.70	0.23	5
871A	2H-6	59–61	1.49	1.03	0.11	6	0.73	0.19	3	0.54	0.27	5
871A	3H-2	123–125	3	0.77	0.13	3	0.81	0.30	6	0.65	0.10	3
872C	3H-2	59–61	3.31	0.84	0.14	5	0.86	0.16	4	0.62	0.21	4
872C	3H-5	118–120	3.87	0.65	0.03	3	0.66	0.19	4	0.80	0.14	4
871A	3H-5	60–62	6	0.89	0.10	3	–			0.91	0.13	5
871A	3H-5	123–125	6.2	0.85	0.15	4	–			0.80	0.25	4
872C	5H-2	14–16	9.02	0.74	0.10	3	0.69	0.09	3	0.56	0.16	4
872C	5H-6	59–61	10.39	0.75	0.10	3	0.74	0.11	3	0.58	0.21	4
872C	6H-5	20–22	11.4	0.58	0.15	4	1.01	0.20	5	0.46	0.20	4
871A	4H-5	59–61	11.81	0.62	0.15	3	0.58	0.08	3	0.46	0.16	4
871A	6H-6	60–62	13.06	0.64	0.16	5	0.70	0.29	5	0.55	0.25	4
871A	7H-2	124–126	14.73	0.63	0.14	6	–			0.40	0.04	3
871A	7H-5	59–61	14.96	0.49	0.15	5	0.54	0.20	5	0.38	0.24	5
871A	8H-2	59–63	16.23	0.51	0.18	6	0.67	0.12	6	0.08	0.06	3
872C	11H-1	20–22	16.7	0.46	0.19	3	0.77	0.21	6	0.60	0.24	3
872C	11H-6	20–22	18.38	0.84	0.07	3	0.84	0.06	2	0.31	0.10	4
872C	12H-2	78–80	19.85	0.72	0.18	2	0.64	0.03	3	0.79	0.10	2
872C	13H-3	20–22	21.7	0.77	0.09	3	0.80	0.20	4	0.79	0.25	3
872C	13H-5	20–22	23	0.83	0.22	3	–			0.88	0.29	3
872C	14H-4	20–22	23.51	0.84	0.17	6	–			–		

The δ^{44}Ca record of *G. bulloides* (Table 5.3 and Fig. 5.2b) from the southern Indian Ocean shows a δ^{44}Ca minimum at about 15 Ma similar to the samples from the western equatorial Pacific. In addition there is also an increasing δ^{44}Ca trend from about 15 Ma to 1.5 Ma. Differing from the Pacific δ^{44}Ca records two more minima of the δ^{44}Ca can be seen at about 18 Ma and at 3 Ma.

5.4.1 Factors influencing the δ^{44}Ca of the foraminifers

The δ^{44}Ca records of the three species from the western equatorial Pacific (Fig. 5.2a) show similarities concerning their patterns although the *Globigerinella spp.* record tends to show lower values than the other two records. Latter difference may be related to species dependent reaction to temperature fluctuations, pH changes or changes in seawater chemistry. In particular δ^{44}Ca-temperature relationships have been found to be considerably different between species (Gussone et al., 2002; Nägler et al., 2000). In order to understand our data and to possibly use the measured δ^{44}Ca records of all four species for the reconstruction of past δ^{44}Ca seawater variations the influence of seawater temperature and other environmental conditions on the foraminifer records has to be studied in detail.

5.4.1.1 δ^{44}Ca-temperature relationship

In a first attempt to understand the δ^{44}Ca/temperature relationship of the studied species we calculate the fractionation factor α for the youngest samples in the sediment cores (Tab. 5.4):

$$\alpha = \frac{(^{44}Ca/^{40}Ca)_{cc}}{(^{44}Ca/^{40}Ca)_{sw}} = \frac{\delta^{44}Ca_{cc} + 1000}{\delta^{44}Ca_{sw} + 1000} \text{with cc = calcite, sw = seawater} \qquad (5.1)$$

For this purpose we use the δ^{44}Ca value of the IAPSO seawater salinity standard (δ^{44}Ca=+1.82 ‰) to represent modern seawater. In contrast to the other species the fractionation factor α cannot be calculated for the youngest sample of *G. bulloides* (1.5 Ma) because this sample is already older than the assumed residence time of Ca in the oceans which is supposed to be about 1 million years (Broecker and Peng, 1982; Zhu and Macdougall, 1998). Instead we use the $\delta^{44}Ca_{sw}$ value of *G. trilobus* of the western equatorial Pacific Ocean at 1.5 Ma ($\delta^{44}Ca_{sw}$ = +1.97 ‰). For the determination of the fractionation factor α we generally assume constant temperatures in the Pacific from 1.5 Ma to 0.085 Ma and a homogeneous distribution of $\delta^{44}Ca_{sw}$ in the oceans.

In Fig. 5.3 the α-values are shown as a function of the seawater temperature (Levitus and

Table 5.3: δ^{44}Ca ratios of *G. bulloides* from ODP Site 183-1138

sample	core	depth (mbsf)	age (Ma)	δ^{44}Ca (‰SRM 915a)	±	n
3327	7R-2	57.67	1.5	0.96	0.04	3
3330	8R-3	67.92	1.8	1.02	0.05	4
3360	9R-2	76	3.1	0.39	0.11	3
3392	10R-3	87	3.5	0.52	0.09	2
3444	11R-1	93.34	3.8	0.92	0.07	4
3491	12R-2	104.1	6.6	0.71	0.13	3
3564	13R-1	112.94	7.2	0.96	0.13	5
3574	13R-4	117.38	7.4	0.87	0.15	6
3619	14R-2	123.78	7.6	0.71	0.11	2
3660	15R-2	133	8.6	0.64	0.06	3
3664	15R-2	134	8.6	0.67	0.06	3
3691	16R-3	144.6	9.3	0.77	0.18	4
3769	17R-5	157.12	9.9	0.80	0.04	2
3876	19R-1	169.8	11.2	0.75	0.13	6
3879	19R-4	174.3	11.8	0.71	0.08	4
3923	20R-2	180.98	12.8	0.63	0.12	4
3949	21R-2	190.59	13.8	0.71	0.18	3
3971	22R-1	199.5	14.8	0.48	0.06	4
3990	23R-1	209.11	16.2	0.65	0.08	3
4011	24R-1	217.9	17.3	0.74	0.16	2
4029	25R-1	227.5	18.5	0.45	0.14	4
4094	26R-1	237.12	20.0	0.49	0.13	4
4085	27R-2	248.22	21.7	0.59	0.11	3

Table 5.4: α-values of the most recent foraminifers

species	age (Ma)	α
G. trilobus	0.085	0.99906
G. ruber/subquadratus	0.085	0.99881
Globigerinella spp.	0.085	0.99862
G. bulloides	1.5	0.99901

Boyer, 1994) together with previously published α-values of other foraminifera cultured under controlled laboratory conditions (Gussone et al., in press).

Using the calculated α-values it is hardly possible to make an inference concerning the δ^{44}Ca/temperature relationship for *G. trilobus* because the α-value lies within the intersection of the different temperature dependent fractionation trends (*G. sacculifer* and *O. universa*). Thus, we cannot distinguish whether this species follows the steep fractionation curve of *G. sacculifer* showing a large δ^{44}Ca-temperature gradient or the shallow fraction-

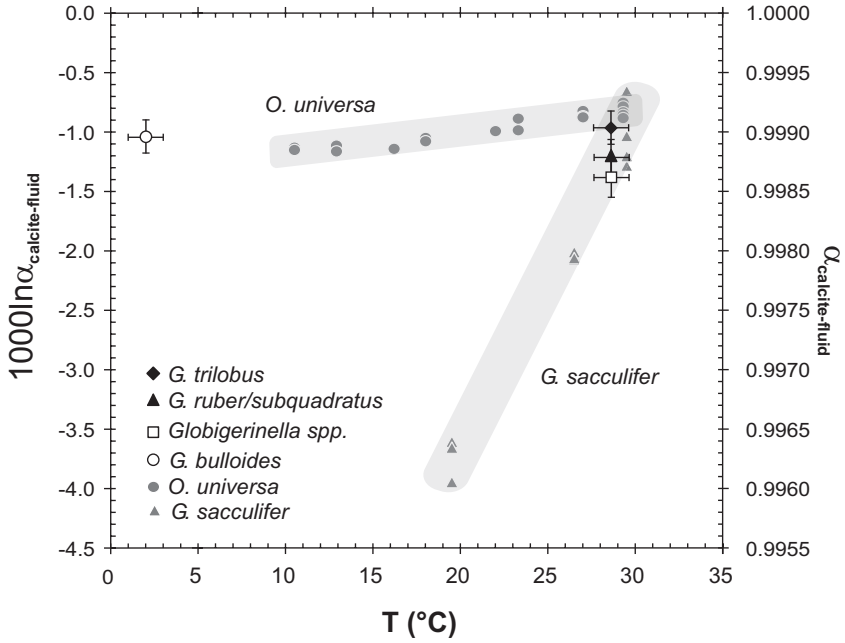

Figure 5.3: Fractionation factors (α-values) of *G. ruber/subquadratus, G. trilobus* and *Globigerinella spp.* are plotted versus temperature of the foraminiferal habitat. In addition the α-values of *G. sacculifer* (Nägler et al. (2000)) and of *O. universa* (Gussone et al. (in press)) can be seen together with our data. Note, that the *Globigerinella spp.* and *G. ruber/subquadratus* data fall along the *G. sacculifer* line. The *G. trilobus* data plot within the intersection of the *O. universa* and *G. sacculifer* data.

ation trend of *O. universa* showing a weak δ^{44}Ca-temperature gradient.

For *G. bulloides* the α-value indicates a weak temperature dependent Ca isotope fractionation similar to the Ca isotope fractionation trend of *O. universa*. The temperature of 2 °C is at the lower limit where *G. bulloides* lives (3–25 °C; Hilbrecht, 1996) and therefore, it can be excluded that the calculated α-value is at an intersection of a parallel shifted *G. sacculifer*-like trend with the *O. universa* trend. Otherwise the δ^{44}Ca of *G. bulloides* living at higher temperatures would show positive fractionation ($1000\ln\alpha > 0$, see Fig. 5.3). The propagated temperature independence is supported by the comparison of the δ^{44}Ca values of *G. bulloides* from Site 1138 with the δ^{18}O record of benthic foraminifers (Fig. 5.4) from Site 747 (Wright and Miller, 1992) located about 150 km southeast of Site 1138. The δ^{18}O record indicates a warming between 24 and 15 Ma followed by a cooling trend from 15 to about 10 Ma (Mid-Miocene cooling event). In contrast, the δ^{44}Ca data, if interpreted as a temperature signal, indicate a cooling between 18 and 15 Ma followed by a continuous warming from 15 to about 4 Ma. This contradictionary observation may support the inference that the δ^{44}Ca record of *G. bulloides* is not controlled by water temperature rather than by other environmental mechanisms.

The α-values of *G. ruber/subquadratus* and *Globigerinella spp.* plot on the steep frac-

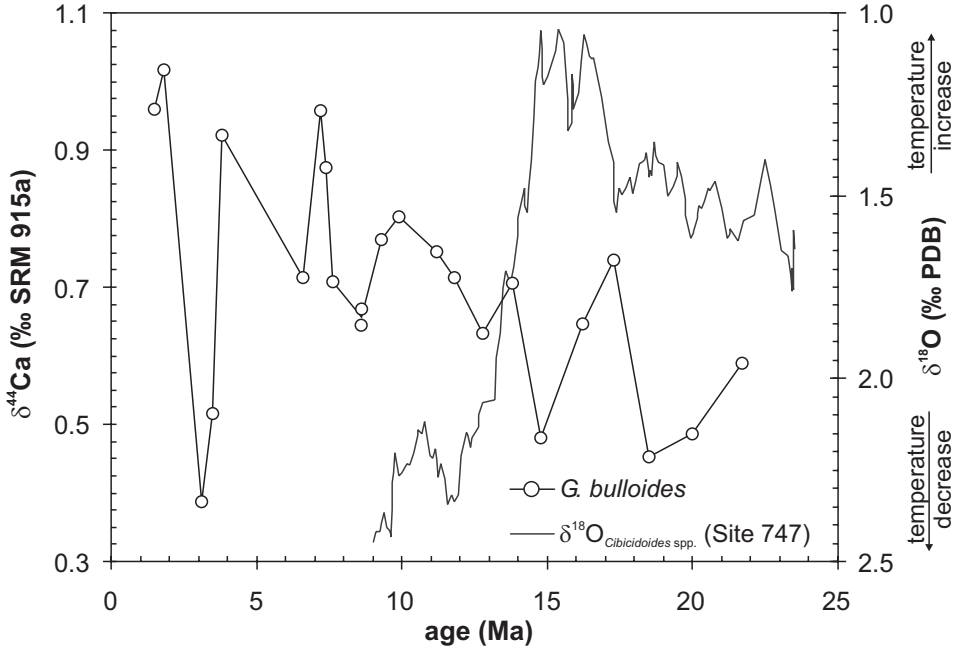

Figure 5.4: Plot of δ^{44}Ca (open circles) of *G. bulloides* (Site 1138) and δ^{18}O of *Cibicidoides spp.* (Site 747).

tionation curve of *G. sacculifer*. Therefore, these two species may show a temperature dependent fractionation comparable to those of *G. sacculifer* and may then be used to reconstruct seawater temperatures of the western equatorial Pacific over the past 24 Ma. The difference of the α-values of *G. ruber/subquadratus* and *Globigerinella spp.* has then either to be explained by species-specific temperature dependent fractionation or by temperature differences due to different calcification depths. It is known that the calcification depth of *Globigerinella spp.* is below *G. ruber/subquadratus* (Pearson and Shackleton, 1995). Pearson and Shackleton (1995) reported that the δ^{18}O values of *Globigerinella spp.* are about (0.33 ± 0.09)‰ heavier than the δ^{18}O values of *G. ruber/subquadratus* corresponding to a temperature difference in the order about 1.5 ℃ using the relationship between δ^{18}O and temperature reported for the planktonic foraminifer *O. universa* (T=–4.8·δ^{18}O (‰), (Bemis et al., 1998)). The offset of the $\delta^{44}Ca_{cc}$ record of *Globigerinella spp.* being in average about 0.2 ‰ lighter than the $\delta^{44}Ca_{cc}$ record of *G. ruber/subquadratus* could be a consequence of the different calcification depths.

5.4.1.2 δ^{44}Ca-pH relationship

There are two lines of evidence suggesting that the δ^{44}Ca of foraminifers is independent from pH variations of seawater. First evidence comes from Gussone et al. (in press) who studied *O. universa* cultured in seawater with varying CO_3^{2-} concentrations being a direct

function of the pH (Spero et al., 1997; Zeebe, 1999). They found no significant relationship between CO_3^{2-} concentration and δ^{44}Ca. Although this finding is certainly correct for *O. universa* it may not necessarily be pertinent to other foraminiferal species.
Second evidence comes from direct comparison of the δ^{44}Ca record with the corresponding δ^{11}B record of Pearson and Palmer (2000) from the same samples (Fig. 5.5). The δ^{11}B record of foraminifers can be interpreted as pH proxy for seawater (Spivack et al., 1993; Sanyal et al., 1995, 1996; Hemming et al. 1992) but was alternatively also interpreted as a proxy for continental weathering (Lemarchand et al. 2000). As the residence time of boron in the oceans is in the order of about 10 to 20 Ma (Broecker and Peng, 1982; Spivack and Edmond, 1987; Vengosh et al., 1991; Lemarchand et al., 2000) the observed short term variations of the δ^{11}B on timescales of a few million years should represent changes of the seawater-pH. However, from Fig. 5.5 it can be seen that there is no clear relationship between the short term changes of the δ^{11}B/pH record and the δ^{44}Ca records.

5.5 Reconstruction of past δ^{44}Ca of seawater and past seawater temperatures

Our investigations clearly showed that the foraminiferal records are independent from pH variations but that there is a clear species dependency of the δ^{44}Ca ratio on seawater temperature. The species *G. ruber/subquadratus* and *Globigerinella spp.* show a temperature dependent fractionation behavior which is closely related to the one of *G. sacculifer*. In contrast, the δ^{44}Ca records of the two other species *G. bulloides* and *G. trilobus* are supposed to show a weak *O. universa*-like behavior of their Ca isotope fractionation. The strongly temperature dependent fractionation *G. ruber/subquadratus* and *Globigerinella spp.* and the weak fractionation behavior of *G. bulloides* and *G. trilobus* can either be applied for secular changes of the $\delta^{44}Ca_{sw}$ in the past and for reconstructions of past seawater temperature fluctuations.

5.5.1 Reconstruction of past δ^{44}Ca of seawater

Past δ^{44}Ca of seawater ($\delta^{44}Ca_{sw}$) can be reconstructed from the δ^{44}Ca values of the foraminiferal calcite ($\delta^{44}Ca_{cc}$) and their corresponding fractionation factor α (equation 5.1). A precondition for such a reconstruction is that the $\delta^{44}Ca_{cc}$ signal was not superimposed by other factors influencing Ca isotope fractionation, e.g. seawater temperature or pH. From equation (5.1) follows:

$$\delta^{44}Ca_{sw} = \frac{\delta^{44}Ca_{cc} + 1000}{\alpha} - 1000 \qquad (5.2)$$

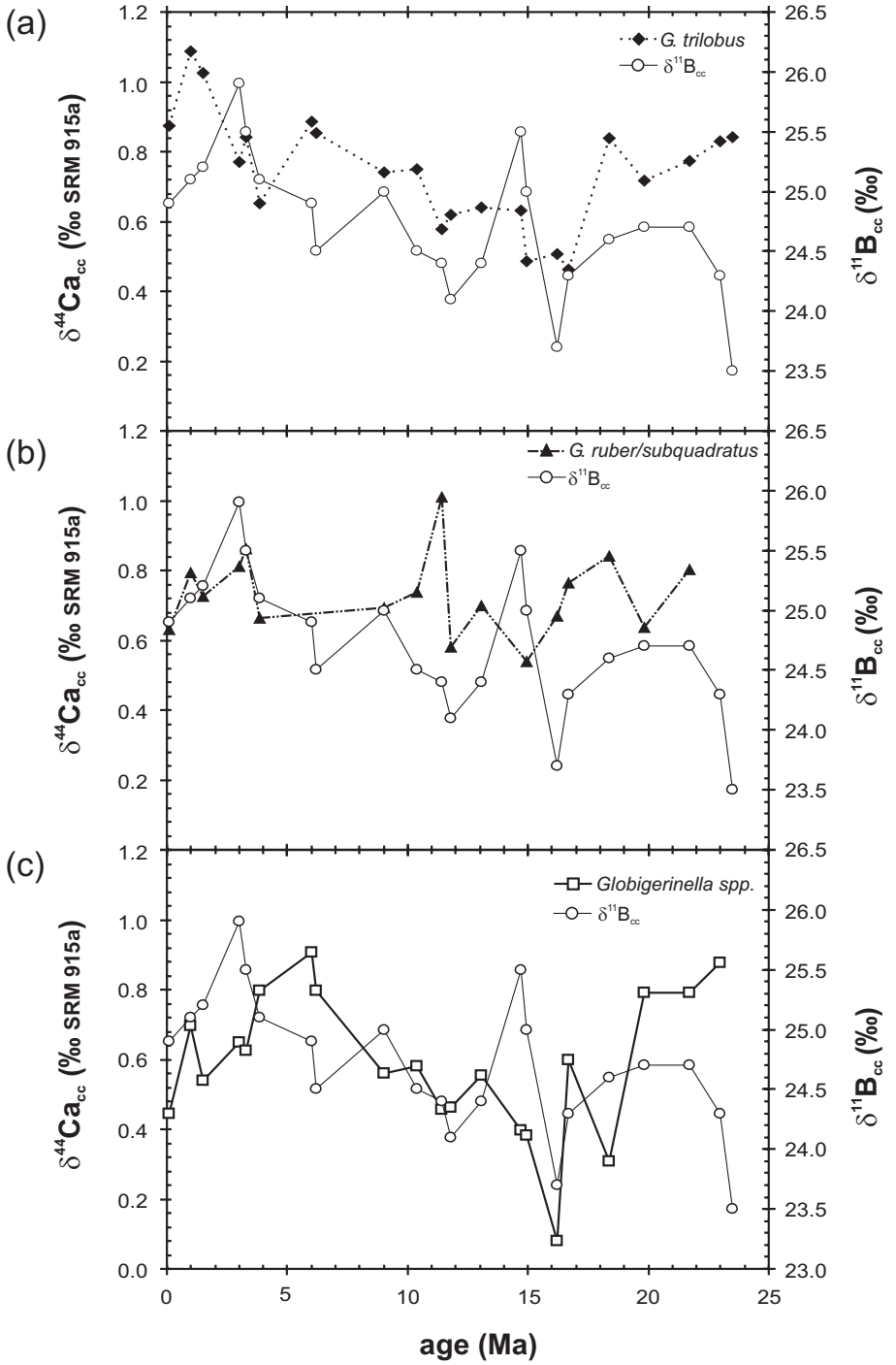

Figure 5.5: Comparison of δ^{11}B values (open circles) with the $\delta^{44}Ca_{cc}$ values of (a) *G. trilobus* (filled diamonds), (b) *G. ruber/subquadratus* (filled triangles) and (c) *Globigerinella spp.* (open squares).

Table 5.5: $\delta^{44}Ca_{sw}$ calculated from the $\delta^{44}Ca_{cc}$ of *G. trilobus* and *G. bulloides*.

G. trilobus		*G. bulloides*	
age (Ma)	$\delta^{44}Ca_{sw}$	age (Ma)	$\delta^{44}Ca_{sw}$
0.085	1.82	1.5	1.95
0.98	2.03	1.8	2.01
1.49	1.97	3.1	1.38
3.00	1.71	3.5	1.51
3.31	1.79	3.8	1.91
3.87	1.60	6.6	1.70
6.00	1.83	7.2	1.95
6.20	1.80	7.4	1.86
9.02	1.69	7.6	1.70
10.39	1.69	8.6	1.63
11.40	1.52	8.6	1.66
11.81	1.56	9.3	1.76
13.06	1.59	9.9	1.79
14.73	1.58	11.2	1.74
14.96	1.43	11.8	1.70
16.23	1.45	12.8	1.62
16.70	1.41	13.8	1.70
18.38	1.78	14.8	1.47
19.85	1.66	16.2	1.64
21.70	1.72	17.3	1.73
23.00	1.78	18.5	1.44
23.51	1.79	20	1.48
		21.7	1.58

In a first order approach using the α-values for the most recent sample of *G. trilobus* and *G. bulloides* (Table 5.4) and assuming, that the specific fractionation factor was constant throughout time we calculated the $\delta^{44}Ca_{sw}$ for all samples of these species (Table 5.5 and Fig. 5.6). Both $\delta^{44}Ca_{sw}$ records show a good agreement (Fig. 5.6) providing further evidence for a temperature independent Ca isotope fractionation of *G. bulloides* and *G. trilobus*.

Furthermore the two $\delta^{44}Ca_{sw}$ records of *G. bulloides* and *G. trilobus* are in good agreement with $\delta^{44}Ca_{sw}$ data from De La Rocha and DePaolo (2000). Please note that the $\delta^{44}Ca$ ratios presented by De La Rocha and DePaolo (2000) are $\delta^{44}Ca_{cc}$ ratios of marine carbonates and originally were normalized to an ultrapure $CaCO_3$ sample being different from SRM 915a. For a better comparability we renormalized the $\delta^{44}Ca$ data to the SRM 915a standard and then calculated the $\delta^{44}Ca_{sw}$ data using equation 5.2. Fig. 5.7 shows the comparison of

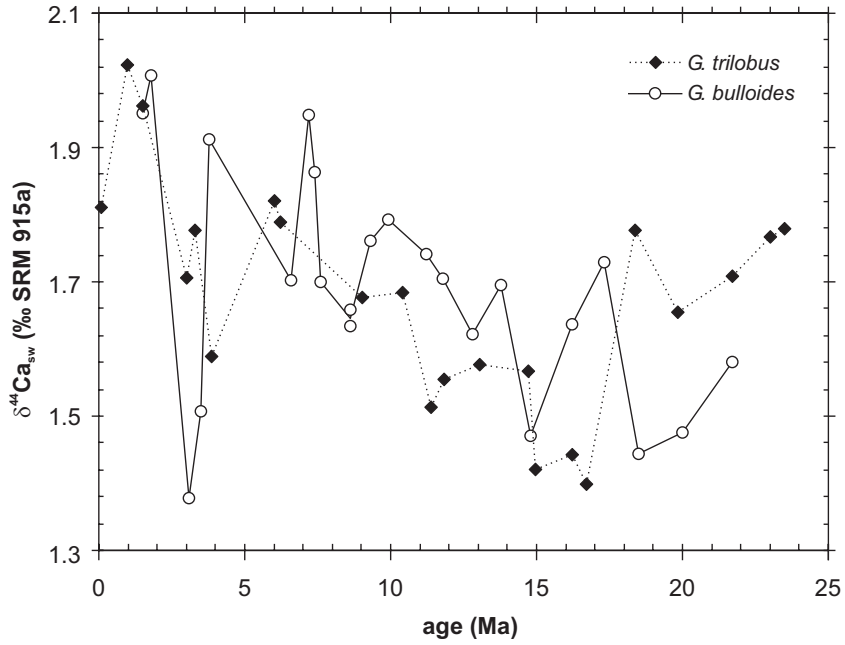

Figure 5.6: δ^{44}Ca values of seawater ($\delta^{44}Ca_{sw}$) calculated from the δ^{44}Ca record of *G. trilobus* and *G. bulloides*.

$\delta^{44}Ca_{sw}$ records of *G. bulloides* and *G. trilobus* with the $\delta^{44}Ca_{sw}$ record from De La Rocha and DePaolo (2000). Due to our higher temporal resolution more details of the Ca isotope evolution of seawater during the Miocene can be observed.

5.5.2 Calculation of seawater temperatures for the western equatorial Pacific

Following our approach that the two species *G. ruber/subquadratus* and *Globigerinella spp.* show a temperature dependent Ca isotope fractionation we can evolve equations for the linear correlation of α-value and temperature for *G. ruber/subquadratus* and *Globigerinella spp.* from Fig 5.3:

$$\alpha(T)_{G.ruber/subq.} = -0.000267 \cdot T(\text{°C}) + 0.991183 \tag{5.3}$$

$$\alpha(T)_{Globigerinellaspp.} = -0.000267 \cdot T(\text{°C}) + 0.990994 \tag{5.4}$$

In equations (5.3) and (5.4) the slope of the equations are adopted from the linear correlation of α-value and temperature of *G. sacculifer*. Rewriting of equations (5.3) and (5.4)

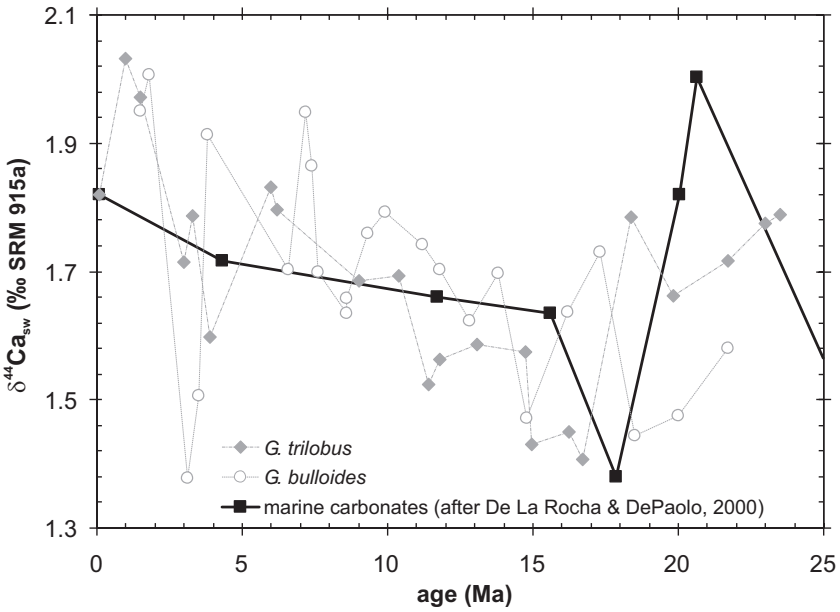

Figure 5.7: Comparison of $\delta^{44}Ca_{sw}$ from this study with the δ^{44}Ca record of De La Rocha and DePaolo (2000). Please note, that the $\delta^{44}Ca_{cc}$ record of De La Rocha and DePaolo (2000) was renormalized to SRM 915a and the $\delta^{44}Ca_{sw}$ record was then calculated using equation (5.2).

results in:

$$T(\text{°C}) = \frac{\alpha(T)_{G.ruber/subq.} - 0.991183}{-0.000267} \tag{5.5}$$

$$T(\text{°C}) = \frac{\alpha(T)_{Globigerinella} - 0.990994}{-0.000267} \tag{5.6}$$

We calculated the α-values for the *Globigerinella spp.* and *G. ruber/subquadratus* samples using the $\delta^{44}Ca_{sw}$ record of *G. trilobus* and then calculated the temperatures (Table 5.6).

The temperature reconstructions based on the $\delta^{44}Ca_{cc}$ ratios of *G. ruber/subquadratus* and *Globigerinella spp.* (Fig. 5.8) show variations of about 3 °C in the temperature range from 28 to 31 °C over the past 24 Ma. This observation is in general agreement with the paleoceanographic reconstructions of Kennett et al. (1985). Reconstructions of circulation patterns of surface and sub-surface waters in the Pacific Ocean at 22, 16 and 8 Ma show warm currents in the equatorial Pacific coming from the Caribbean through the open Isthmus of Panama (Kennett et al., 1985). At the transition from the Miocene to Pliocene/Pleistocene both temperatures records show a decrease of about 1 to 2 °C.

Fig. 5.9 shows a comparison of the calculated temperatures with the global evolution of benthic δ^{18}O (Zachos et al., 2001). Although the δ^{18}O data mainly represent deep sea temperatures and continental ice volume (Zachos et al., 2001) and the δ^{44}Ca records represent ocean surface rather than deep ocean temperatures an agreement of the δ^{18}O trend and the

Table 5.6: Temperatures derived from the $\delta^{44}Ca_{sw}$ records of *G. ruber/subquadratus* and *Globigerinella spp.*

Age	*G. ruber/subquadratus*		*Globigerinella spp.*	
(Ma)	T_{calc} (°C)	±	T_{calc} (°C)	±
0.085	28.6	0.3	28.6	0.4
0.98	28.4	0.4	28.8	0.5
1.49	28.4	0.5	28.4	0.6
3	29.7	0.7	29.8	0.4
3.31	29.6	0.5	29.4	0.5
3.87	29.5	0.4	30.8	0.4
6	–		30.3	0.4
6.2	–		30.0	0.6
9.02	29.3	0.3	29.5	0.4
10.39	29.5	0.4	29.6	0.5
11.4	31.1	0.5	29.8	0.5
11.81	29.4	0.4	29.6	0.5
13.06	29.7	0.7	29.9	0.6
14.73	–		29.3	0.4
14.96	29.7	0.5	29.8	0.6
16.23	30.1	0.5	28.6	0.4
16.7	30.6	0.6	30.7	0.6
18.38	29.5	0.3	28.2	0.3
19.85	29.2	0.4	30.5	0.5
21.7	29.6	0.5	30.3	0.6
23	–		30.4	0.7

δ^{44}Ca derived temperatures can be observed. Both temperature trends show a generally decreasing seawater temperature between 24 Ma and the present. However, the decreasing trend of the δ^{44}Ca temperatures is superimposed by frequent temperature excursions.

As the comparison of the calculated temperatures with the global benthic δ^{18}O data is critical, a comparison with local planktonic δ^{18}O is more reliable. Fig. 5.10 shows a comparison of the temperatures calculated from the δ^{44}Ca records with δ^{18}O-data of *G. ruber* from Site 871 (Pearson and Shackleton, 1995). In order to correct the δ^{18}O data for changes of δ^{18}O of seawater ($\delta^{18}O_{sw}$) caused by fluctuations of the global ice volume we subtracted the $\delta^{18}O_{sw}$ data of Billups and Schrag (2002). The δ^{44}Ca based temperatures and the δ^{18}O record show a good agreement not arguing against a temperature dependent Ca isotope fractionation of *Globigerinella spp.* and *G. ruber/subquadratus*.

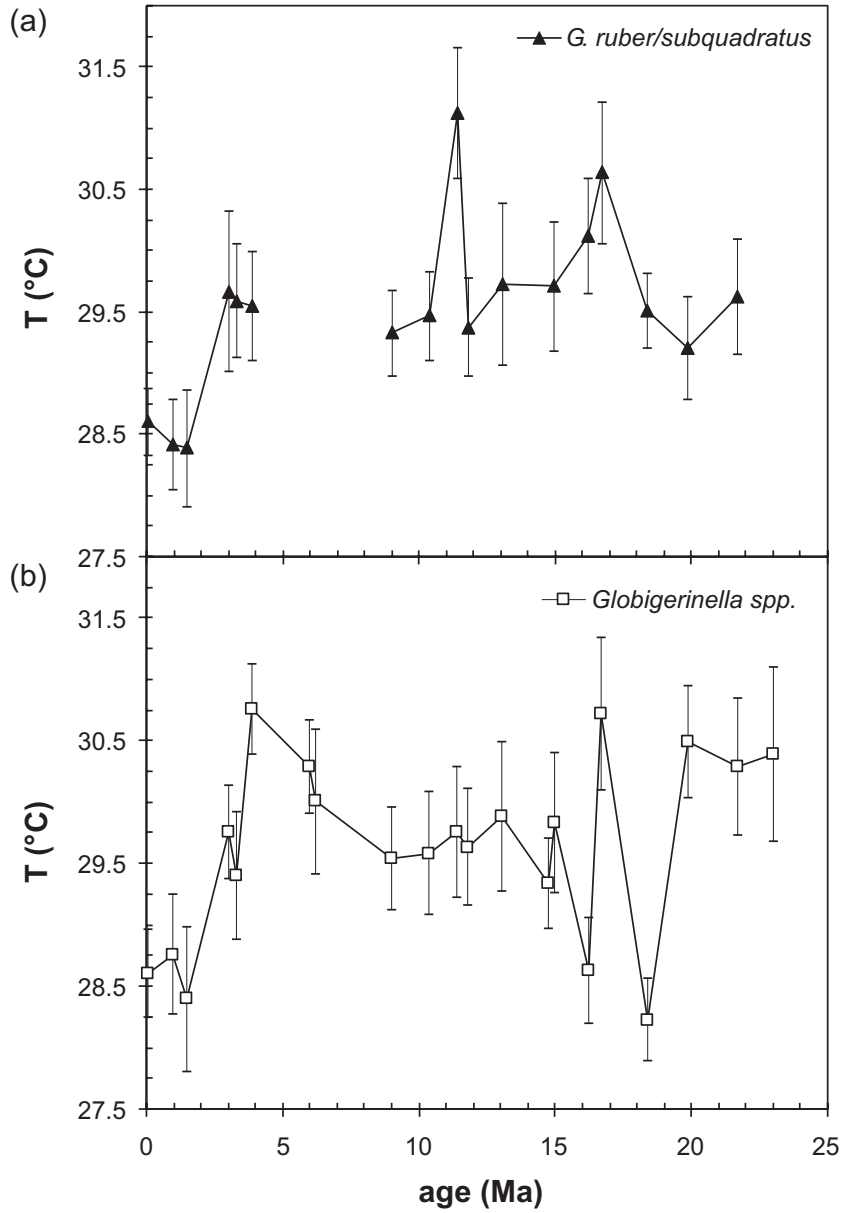

Figure 5.8: Calculated temperatures from the $\delta^{44}Ca_{cc}$ of (a) *G. ruber/subquadratus* and (b) *Globigerinella spp.*

5.6 Conclusions

Variations of δ^{44}Ca of foraminiferal calcite are caused by variations of the δ^{44}Ca of seawater and by changes of the seawater temperature. The extend of the fractionation by the latter effect is species dependent and was found in this study to be negligible for *G. bulloides* and *G. trilobus*. Consequently, both species can be used to reconstruct the past δ^{44}Ca of seawater. The variations of seawater δ^{44}Ca are superimposed by temperature dependent Ca isotope fractionation in the δ^{44}Ca records of *G. ruber/subquadratus* and *Globigerinella*

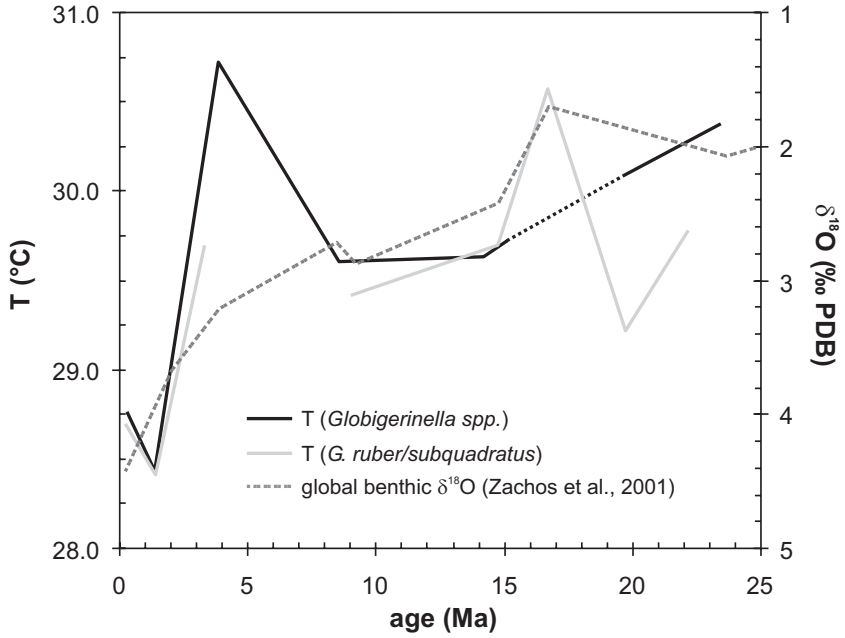

Figure 5.9: Comparison of the smoothed temperature trends of *G. ruber/subquadratus* and *Globigerinella spp.* with the global benthic δ^{18}O data of Zachos et al. (2001).

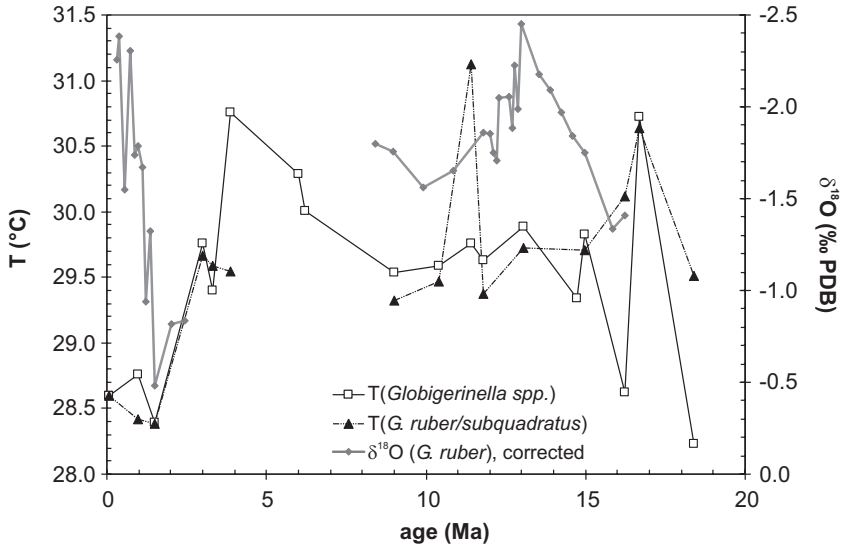

Figure 5.10: Comparison of the calculated temperatures of *G. ruber/subquadratus* and *Globigerinella spp.* with the local δ^{18}O record of *G. ruber*. The δ^{18}O record is corrected for the evolution of $\delta^{18}O_{sw}$ which is mainly affected by changes in global ice volume. The corrected δ^{18}O data reflects local changes in near surface seawater temperatures.

spp.. The temperature dependent Ca isotope fractionation of *G. ruber/subquadratus* and *Globigerinella spp.* is supported by a relatively good agreement of the δ^{44}Ca based temperatures with the global benthic δ^{18}O record and local planktonic δ^{18}O data. Nevertheless, more reliable evidences for this temperature dependence and the extend of the temperature dependence are needed which can best be obtained by culture experiments as previously done for *O. universa* and *G. sacculifer*.

Acknowledgements

Financial support to A Heuser was provided by the Graduiertenkolleg "Dynamik globaler Kreisläufe" from the DFG (GRK 171) and by the state government of Schleswig-Holstein. This study was also supported by a DFG grant to A. Eisenhauer (Ei272/12- 1). We thank Barbara Bock for helpful discussions and constructive criticism.

References

Antretter, M., Inokuchi, H., Zhao, X. (in press) Paleomagnetic and Rock Magnetic Properties of Sediment Samples from Ocean Drilling Program Leg 183, Kerguelen Plateau, Holes 1138A and 1140A. In *Proc. ODP, Sci. Results, 183 [online]* (eds. F. A. Frey, M.F. Coffin, P.J. Wallace and P. G. Quilty) Available from WWW: http://www-odp.tamu.edu/publications/183_SR/004/004.htm [Cited 2002-12-17].

Bemis B.E., Spero H.J., Bijma J. and Lea D.W. (1998) Reevaluation of the oxygen isotopic composition of planktonic foraminifera: Experimental results and revised paleotemperature equations. *Paleoceanography* **13**, 150–160.

Birck, J. (1986) Precision K-Rb-Sr isotopic analysis: application to Rb-Sr chronology. *Chem. Geol.* **56**, 73–83.

Billups K. and Schrag D. P. (2002) Paleotemperatures and ice volume of the past 27 Myr revisited with paired Mg/Ca and ^{18}O/^{16}O measurements on benthic foraminifera. *Paleoceanography* **17**, 10.1029/2000PA000567.

Broecker, W. H. and T.-H. Peng (1982) *Tracers in the Sea*, Eldigio Press.

Coffin M. F., Frey F. A., Wallace P. J., et al. (2000) *Proc. ODP, Init. Repts.* **183**.

Compston, W. and Oversby V. (1968) Lead Isotopic Analysis Using A Double Spike. *J. Geophys. Res.* **74**, 4338–4348.

Coplen T. B., Hopple J.A., Böhlke J. K., Peiser H. S., Rieder S. E., Krouse H. R., Rosman K.J.R., Ding T., Vocke Jr. R. D., Révész K. M., Lamberty A., Taylor P., and De Bièvre P. (2002) Compilation of Minimum and Maximum Isotope Ratios of Selected

Elements in Naturally Occurring Terrestrial Materials and Reagents. *Water-Resources Investigations Report* **98**, USGS.

De La Rocha C. L. and DePaolo D. J. (2000) Isotopic Evidence for Variations in the Marine Calcium Cycle Over the Cenozoic. *Science* **289**, 1176–1178.

Farrell J. and Prell W. (1991) Pacific $CaCO_3$ and $\delta^{18}O$ since 4 Ma, Paleoceanic and paleoclimatic implications. *Paleoceanography* **6**, 485–498.

Frey F. A., Coffin M. F., Wallace P. J. and Quilty P. G. (in press) *Proc. ODP, Sci. Results, 183 [online].* Available from WWW: http://www-odp.tamu.edu/publications/183_SR/183sr.htm. [Cited 2002-10-15].

Gussone N., Eisenhauer A., Heuser A., Dietzel M., Bock B., Böhm F., Spero H. J., Lea D. W., Bijma J., Zeebe R. and Nägler T. F. (in press) Model for Kinetic Effects on Calcium Isotope Fractionation (δ^{44}Ca) in Inorganic Aragonite and Cultured Foraminifer (*Orbulina universa* and *Globigerinoides sacculifer*), *Geochim. Cosmochim. Acta.*

Haggerty J. A., Premoli Silva I., Rack F., and McNutt M. K. (1995). *Proc. ODP, Sci. Results, 144.*ODP, College Station, TX.

Hastings D. W., Russell A. D., and Emerson S. R. (1998) Foraminiferal magnesium in *G. sacculifer* as paleotemperature proxy. *Paleoceanography* **13**, 161–169.

Hemming N. G. and Hanson G. N. (1992) Boron isotopic composition and concentration in modern marine carbonates. *Geochim. Cosmochim. Acta* **56**, 537–543.

Harris N. (1995) Significance of weathering Himalayan metasedimentary rocks and leucogranites for the Sr isotope evolution of seawater during the early Miocene. *Geology* **23**, 795–798.

Heumann K. and Lieser K. (1973) Untersuchung von Isotopenfeinvariationen des Calciums in der Natur an rezenten Carbonaten und Sulfaten. *Geochim. Cosmochim. Acta* **37**, 1463–1471.

Heumann K., Lieser K., and Elias H. (1970) Difficulties in Measuring the Isotopic Abundances of Calcium with a Mass Spectrometer. In *Recent Developments in Mass Spectrometry* (eds. K. Ogata and T. Hayakawa). University of Tokyo Press, pp. 457–460.

Heuser A., Eisenhauer A., Gussone N., Bock B., Hansen B. T. and Nägler Th. F. (2002) Measurement of Calcium Isotopes (δ^{44}Ca) Using a Multicollector TIMS Technique. *Int. J. Mass. Spec.* **220**, 387–399.

Hilbrecht, H. (1996) Extant planktic foraminifera and the physical environment in the Atlantic and Indian Oceans. In *Mitteilungen aus dem Geologischen Institut der Eidgen. Technischen Hochschule und der Universität Zürich, Neue Folge, No. 300*, Zürich.

Hippler D., Gussone N., Darling K., Eisenhauer A., and Nägler Th. F. (2002) δ^{44}Ca in

N. pachy (left): a new SST-proxy in polar regions. *Geochim. Cosmochim. Acta Spec. Suppl.* **66**(15A), A331.

Jacobson A. D., Blum J. D., Chamberlain C. P., Poage M. A., and Sloan V. F. (2002) Ca/Sr and Sr isotope systematics of a Himalayan glacial chronosequence: Carbonate versus silicate weathering rates as a function of landscape surface age. *Geochim. Cosmochim. Acta* **66**, 13–27.

Kennett J. P. and M. S. Srinivasan (1983) *Neogene planktonic foraminifera*. Hutchinson Ross Publishing Company.

Lear C. H., Elderfield H., and Wilson P. A. (2000) Cenozoic deep-sea temperatures and global ice volumes from Mg/Ca in benthic foraminiferal calcite. *Science* **287**, 269–272.

Lemarchand D., Gailiardet J. , Lewin É and Allé gre C. J. (2000) The influence of rivers on Marine boron isotopes and implications for reconstructing past ocean pH. *Nature* **408**, 951–954.

Levitus S. and Boyer T. (1994) *World Ocean Atlas 1994 Volume 4: Temperature, NOAA Atlas NESDIS 4*. Natl. Oceanic and Admos. Admin., Silver Spring, MD.

Nägler T. F., Eisenhauer A., Müller A., Hemleben C. and Kramers J. (2000) The δ^{44}Ca-temperature calibration on fossil and cultured *Globigerinoides sacculifer*: New tool for reconstruction of past sea surface temperatures. *Geochem. Geophys. Geosyst.* **1**, 2000GC000091.

Pearson P. N. (1995) Planktonic Foraminifer Biostratigraphy and the Development of Pelagic Caps on Guyots in the Marshall Island Group. *Proc. ODP, Sci. Res.* **144**, 21–59.

Pearson P. N. and Palmer M. R: (2000) Atmospheric carbon dioxide concentrations over the past 60 million years. *Nature* **406**, 695–699.

Pearson P. N., Shackleton N. J., and Hall M. A. (1997) Stable isotopic evidence for the sympatric divergence of *Globigerinoides trilobus* and *Orbulina universa* (planktonic foraminifera). *J. Geol. Soc. London* **154**, 295–302.

Premoli Silva I., Haggerty J. A., and Rack F. R. (1993) *Proc. ODP, Init. Rep., Vol. 144*. ODP, College Station, Texas.

Rosenthal Y., Boyle E. A., and Slowey N. (1997) Temperature control on the incorporation of magnesium, strontium, fluorine and calcium into benthic foraminiferal shells from Little Bahama Bank: Prospect for thermocline paleoceanography. *Geochim. Cosmochim. Acta* **61**, 3633–3643.

Sanyal A., Hemming N. G., Hanson G. N. and Broecker W. S. (1995) Evidence for a higher pH in the glacial ocean from boron isotopes in foraminifera. *Nature* **373**, 234–236.

Sanyal A., Hemming N. G., Broecker W. S., Lea D. W., Spero H. J., and Hanson G. N. (1996) Oceanic pH control on the boron isotopic composition of foraminifera: Evidence from culture experiments. *Paleoceanography* **11**, 513–517.

Skulan J. L., DePaolo D. J., and Owens T. L. (1997) Biological control of calcium isotopic abundances in the global calcium cycle. *Geochim. Cosmochim. Acta* **61**, 2505–2510.

Spero H. J., Bijma J., Lea D. W., and Bemis B. E. (1997) Reassessing foraminiferal carbon and oxygen isotope data: Effects of sea water carbonate chemistry. *Nature* **390**, 497–500.

Spivack A. J. and Edmond J. M. (1987) Boron isotope exchange between seawater and the oceanic crust. *Geochim. Cosmochim. Acta* **51**, 1033–1043.

Spivack A. J., You C.-F. and Smith J. H. (1993) Foraminiferal Boron Isotope Ratios as a Proxy for Surface Ocean pH over the past 21 Myr. *Nature* **363**, 149–151.

Vance D. and Burton K. (1999) Neodymium isotopes in planktonic Foraminifera: a record of the response of continental weathering and ocean circulation rates to climate change. *Earth Planet. Sci. Lett.* **173**, 365–379.

Vengosh A., Kolodny Y., Starinsky A., Chivas A. R., and McCulloch M. T. (1991) Coprecipitation and isotopic fractionation of boron in modern biogenic carbonates. *Geochim. Cosmochim. Acta* **55**, 2901–2910.

Vigour R. and Lazarus D. (2002) Biostratigraphy of Late Miocene-Early Pliocene Radiolarians from ODP Leg 183 Site 1138. In *Proc. ODP, Sci. Results, Vol. 183 [online]* (eds. F. A. Frey, M. F. Coffin, P. J. Wallace, and P. G. Quilty). Available from WWW: http://www-odp.tamu.edu/publications/183_SR/007/007.htm [Cited 2002-12-17].

Wright J. D. and Miller K.G. (1992) Miocene stable isotope stratigraphy, Site 747, Kerguelen Plateau. In *Proc. ODP, Sci. Res., Leg 120.* (eds. S. W. Wise and R. Schlich). ODP, College Station, Texas, pp. 855–866.

Zachos J. C., Pagani M., Sloan L. C., Thomas E. and Billups K. (2001) Trends, Rhythms, and Aberrations in Global Climate 65 Ma to Present. *Science* **292**, 686–693.

Zeebe R. (1999) An explanation of the effect of seawater carbonate concentration on foraminiferal oxygen isotopes. *Geochim. Cosmochim. Acta* **63**, 2001–2007.

Zhu P. and Macdougall J. (1998) Calcium isotopes in the marine environment and the oceanic calcium cycle. *Geochim. Cosmochim. Acta* **62**, 1691–1698.

6 Evolutionary Controlled Changes on Ca Isotope Fractionation

The proposed temperature controlled δ^{44}Ca of *G. ruber/subquadratus* and *Globigerinella* is mainly based on the "one point evidence" of Fig. 5.3. The data from this study as well as literature data of δ^{44}Ca of foraminifers suggest that the fractionation factor α is species specific (Tab. 6.1 and Fig. 6.1). This let me hypothesize that the fractionation factors α are not constant throughout time rather than dependent on relative changes of the individual calcification process of the species. Biochemically controlled calcification is determined by the foraminifer genes which may have changed due to selection and mutation with their evolution throughout times.

In contrast to other isotope systems like boron, oxygen and carbon Ca isotope fractionation may be very sensitive to changes of the calcium carbonate precipitation mechanism because it is controlled by kinetic isotope fractionation rather than by equilibrium fraction-

Table 6.1: Ca isotope fractionation factors ($\alpha_{calcite-fluid}$) of various foraminifers

species	α	T (°C)	type	source
G. trilobus	0.99905	28.6	natural	this study
G. ruber	0.99881	28.6	natural	this study
Globigerinella spp.	0.99862	28.6	natural	this study
G. bulloides	0.99898	2	natural	this study
G. sacculifer	0.99796	26.5	cultured	Nägler et al. (2000)
G. sacculifer	0.99897	29.3	cultured	Nägler et al. (2000)
G. sacculifer	0.99914		natural	Zhu and Macdougall (1998)
G. sacculifer	0.99855		natural	Zhu and Macdougall (1998)
O. universa	0.99904	22	cultured	Zhu (1999)
O. universa	0.99903	22	cultured	Gussone et al. (2002)
O. universa	0.99919	29.3	cultured	Gussone et al. (2002)
N. pachyderma (s)[1]	0.99836	3.4	natural	Hippler (pers. comm)
N. pachyderma (s)[2]	0.99852	3.4	natural	Hippler (pers. comm)
N. pachyderma (s)	0.99846	0.28	natural	Gussone (prev. unpublished)
N. pachyderma (s)	0.99863		natural	Zhu and Macdougall (1998)
N. pachyderma (s)	0.99904		natural	Zhu and Macdougall (1998)
Alveolinella sp.	0.99957		natural	Skulan et al. (1997)
G. ornatissima	0.99877	9.8	natural	De La Rocha and DePaolo (2000)

[1] arctic; [2] antarctic

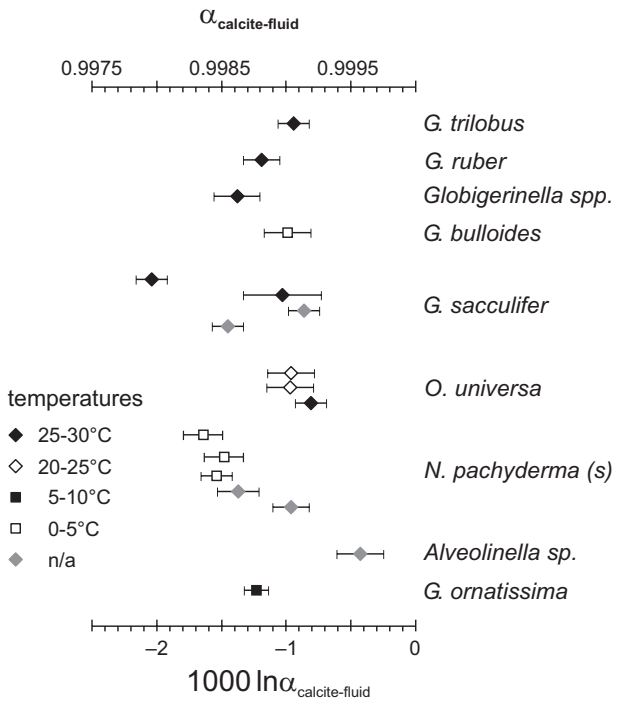

Figure 6.1: α-values of different planktonic foraminifers.

ation (Heumann and Lieser, 1973; O'Neil et al., 1986, Gussone et al., in press). Equilibrium fractionation for C and O isotopes is associated with covalent bonding and occurs already at the formation and transition of the dissolved carbonate species like CO_2(aq), HCO_3^- and CO_3^{2-} in the bulk solution. Isotope fractionation of C and O isotopes is relatively large when these molecules form in a distinct bulk solution. For example at the transition from CO_2(aq) to HCO_3^- oxygen isotope fractionation is in the order of about 23 ‰ and O isotope fractionation at the transition from HCO_3^- to CO_3^{2-} is 16 ‰ (Zeebe, 1999). However, kinetic O isotope fractionation during $CaCO_3$ precipitation is relatively small. That C and O isotope fractionation is less controlled by mineralogical effects during precipitation is also supported by the observation that O and C isotopic difference between calcite and aragonite only amounts to about 1 ‰ and 1.7 ‰, respectively (Böhm et al., 2000; Romanek et al., 1992). This is much less than the fractionation processes related to the formation of HCO_3^- and CO_3^{2-} molecules in the bulk solution.

In the bulk solution Ca isotopes occur as hydrated Ca^{2+} ions and no isotope fractionation occurs as a function of varying speciation. Because Ca isotopes are controlled by kinetic fractionation only during $CaCO_3$ precipitation from the bulk solution Ca isotope fraction reacts much more sensitive to changes of the calcification process. This has been extensively discussed in Gussone et al. (in press) who showed that different biochemical

calcification processes in foraminifer control their fractionation factor differing by one order of magnitude between *G. sacculifer* and *O. universa*. Pearson et al. (1997) used the fossil record from Site 871 to date this separation of *G. trilobus* and *O. universa* from their ancestral lineage back to the middle Miocene (~ 15.1 Ma). From a genetic point of view, both foraminifers evolved from a common ancestor at about 19 Ma (de Vargas et al., 1997). Evolutionary changes of the biochemical processes controlling $CaCO_3$ precipitation in foraminifer are therefore a likely candidate to influence Ca isotope fractionation.

Evolutionary changes of foraminiferal species are well known to have occurred throughout the Phanerozoic (e.g. Loeblich and Tappan, 1964; Pflug 1965, Kennet and Srinivasan, 1983). However, to our knowledge no information are available about the evolutionary history of changes of biochemical controlled calcification processes and their effects on the Ca-isotope fractionation.

It seems possible that the Miocene *G. subquadratus* being the ancestor of *G. ruber* (Kennett and Srinivasan, 1983) had a different Ca fractionation factor than modern *G. ruber*. From *Globigerinella spp.* it is known that there was an evolution since the Oligocene (Kennett and Srinivasan, 1983). *G. praesiphonifera* evolved from *G. obesa* at the transition from the Oligocene to Miocene and further evolved into modern *G. siphonifera* (=*G. aequilateralis*) during the late Miocene.

Currently, foraminiferal species are distinguished primarily on morphological concepts although several studies showed that this classical species definition is critical with regards to molecular approaches (De Vargas et al., 1999; De Vargas et al., 2002; Darling et al. 1999; Huber et al. 1997; Kucera and Darling, 2002). De Vargas et al. (2002) found four genotypes for *Globigerinella siphonifera*. The extend of the genetic differences between these four genotypes is in the range of species level. De Vargas et al. (2002) detected that each of these genotypes is adapted to specific environment characterized by typical ranges of e.g. salinity, temperature and pH. Genotypes with significant genetic differences have also been reported for *G. ruber* (Darling et al., 1997). Differing from *G. siphonifera* and *G. ruber* there are only small genetic differences within the *G. sacculifer* cluster. This is also true for *G. bulloides*, where only slight genetic differences between transitional zone and subtropical specimens were observed (Darling et al., 1999). A good overview on the relations between morphologic evolution and genetic evolution of foraminifera was given by De Vargas et al. (1997). Our data indicate a divergence of the records starting at about 3 Ma. We propose that a change of the fractionation factor at this time leads to a shift between the $\delta^{44}Ca_{sw}$ record of *G. trilobus* relative to the $\delta^{44}Ca_{sw}$ records of *G. ruber/subquadratus* and *Globigerinella spp.*

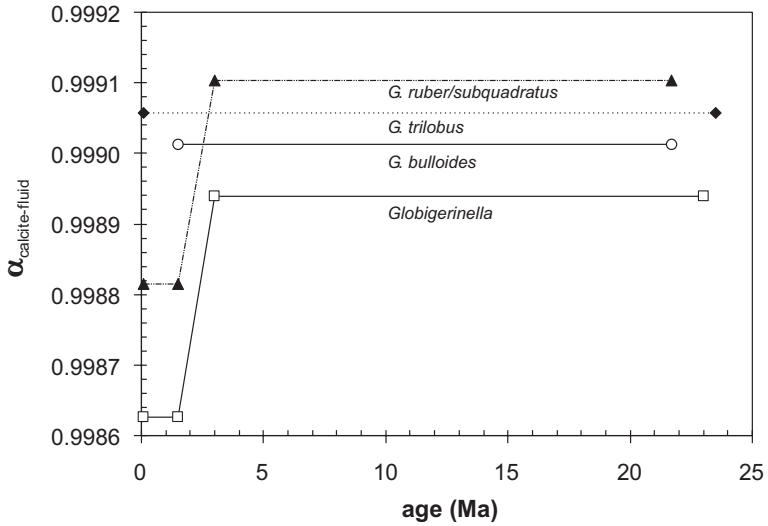

Figure 6.2: Proposed change of the α-values of *G. ruber/subquadratus* and *Globigerinella* spp. between 3 and 1.5 Ma.

In order to reconcile the four records the fractionation factor for *Globigerinella* in the time interval before 3 Ma had to be about 0.99894, slightly higher than in the time interval from the present to about 3 Ma ($\alpha = 0.99863$) (Fig. 6.2). Similarly, for *G. ruber/subquadratus* we assume that the fractionation factor dropped at about 3 Ma from 0.99910 to 0.99881 (Fig. 6.2). In contrast to these species we infer that the fractionation factors for *G. trilobus* and *G. bulloides* must have remained constant for the last 24 Ma. Applying this corrections to the *Globigerinella* and *G. ruber* records the $\delta^{44}Ca_{sw}$ records are consistent within their statistical uncertainties (Fig. 6.3). However, records still show discrepant values before about 16 Ma. It may be speculated that this observation also reflects an evolutionary change of the calcification processes resulting in an earlier change of the fraction factor α.

References

Böhm F., Joachimski M.M., Dullo W.-Chr., Eisenhauer A., Lehnert H., Reitner J., and Wörheide, G. (2000): Oxygen isotope fractionation in marine aragonite of coralline sponges. *Geochim. Cosmochim. Acta* **64**, 1695–1703

Darling K. F., Wade C. M., Kroon D., and Leigh Brown A. J. (1997) Planktic foraminiferal molecular evolution and their polyphyletic origins from benthic taxa. *Mar. Micropaleontol.* **30**, 251-266.

Darling K. F., Wade C. M., Kroon D., Leigh Brown A. J., and Bijma J. (1999) The diversity and distribution of modern planktic foraminiferal small subunit robosomal RNA genotypes and their potential as tracers of present and past ocean circulations.

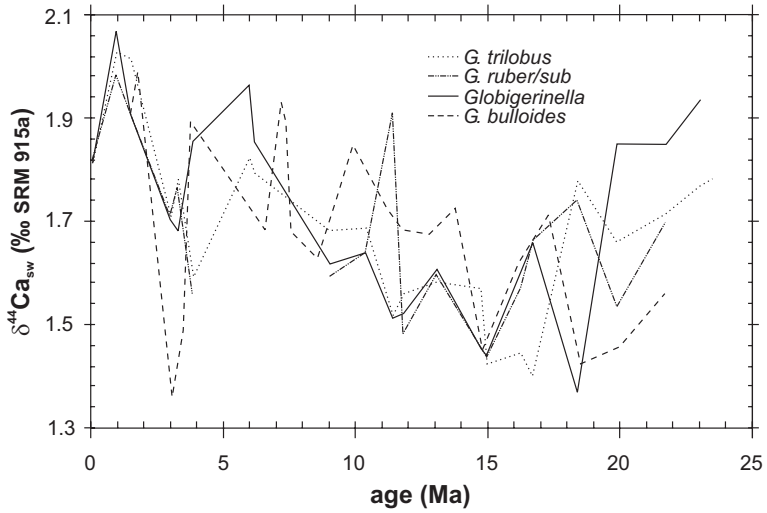

Figure 6.3: $\delta^{44}Ca_{sw}$ records assuming a change of a between 1.5 and 3 Ma of *G. ruber/subquadratus* and *Globigerinella spp.* shifting $\delta^{44}Ca_{sw}$ towards the *G. trilobus*-record. This leads to matching records of all four studied species.

Paleoceanography **14**, 3- 12.

De La Rocha C. L. and DePaolo D. J. (2000) Isotopic Evidence for Variations in the Marine Calcium Cycle Over the Cenozoic, *Science* **289**, 1176-1178.

de Vargas C., Zaninetti L., Hilbrecht H., and Pawlowski J. (1997) Phylogeny and Rates of Molecular Evolution of Planktonic Foraminifera: SSU rDNA Sequences Compared to the Fossil Reocord. *J. Mol. Evol.* **45**, 285-294.

de Vargas C., Norris R., Zaninetti L., Gibb S. W., and Pawlowski J. (1999) Molecular evidence of cryptic speciation in planktonic foraminifers and their relation to ocean provinces. *Proc. Nat. Acad Sci.* **96**, 2864-2868.

de Vargas C., Bonzon M., Rees N. W., Pawlowski J., and Zaninetti L. (2002) A molecular approach to biodiversity and biogeography in the planktonic foraminifer *Globigerinella siphonifera* (dOrbigny). *Mar. Micropaleontol.* **45**, 101-116.

Gussone, N., Eisenhauer A., Heuser A., Dietzel M., Bock B., Böhm F., Spero H. J., Lea D. W., Bijma J., Zeebe R. and Nägler T. F. (in press) Model for Kinetic Effects on Calcium Isotope Fractionation (δ^{44}Ca) in Inorganic Aragonite and Cultured Foraminifer (*Orbulina universa* and *Globigerinoides sacculifer*), *Geochim. Cosmochim. Acta.*

Hippler D., Gussone N., Darling K., Eisenhauer A., and Nägler Th. F. (2002) δ^{44}Ca in *N. pachy* (left): a new SST-proxy in polar regions. *Geochim. Cosmochim. Acta Spec. Suppl.* **66** (15A), A331.

Huber B. T., Bijma J., and Darling K. (1997) Cryptic speciation in the living planktonic foraminifer *Globigerinella siphonifera* (d'Orbigny). *Paleobiology* **23**, 313–338.

Kennett J. P. and M. S. Srinivasan (1983) *Neogene plankonic foraminifera*. Hutchinson Ross Publishing Company.

Kucera M. and Darling K. F. (2002) Cryptic species of planktonic foraminifera: their effect on paleoceanographic reconstructions. *Phil. Trans. R. Soc. Lond. A* **360**, 695–717.

Lemarchand D., Gailiardet J., Lewin É and Allègre C. J. (2000) The influence of rivers on marine boron isotopes and implications for reconstructing past ocean pH. *Nature* **408**, 951–954.

Loeblich A. R. J. and Tappan H. (1964) Foraminiferal classification and evolution. *J. Geol. Soc. India* **5**, 5–40.

Nägler T. F., Eisenhauer A., Müller A., Hemleben C. and Kramers J. (2000) The δ^{44}Ca-temperature calibration on fossil and cultured *Globigerinoides sacculifer*: New tool for reconstruction of past sea surface temperatures, *Geochem. Geophys. Geosyst.* **1**, 2000GC000091.

O'Neil J. R. (1986) Theoretical and experimental aspects of isotopic fractionation. In *Reviews of Mineralogy. Stable Isotopes in High Temperature Geological Processes, 16* (eds. J. W. Valley, J. R. O'Neil, and H. P. Taylor), pp. 561–570. Mineralogical Society of America.

Pearson P. N. (1995) Planktonic Foraminifer Biostratigraphy and the Development of Pelagic Caps on Guyots in the Marshall Island Group, *Proc. Ocean Drill. Program Sci. Results* **144**, 21–59.

Pearson P. N., Shackleton N. J., and Hall M. A. (1997) Stable isotopic evidence for the sympatric divergence of Globigerinoides trilobus and Orbulina universa (planktonic foraminifera). *J. Geol. Soc. London* **154**, 295–302.

Pflug H. (1965) Foraminiferen und aehnliche Fossilreste aus dem Kambrium und Algonkium. *Paleontographica A* **125**, 46–59. Romanek C.S., Grossman E.L. and Morse J.W. (1992): Carbon isotopic fractionation in synthetic aragonite and calcite: Effects of temperature and precipitation rate. *Geochim. Cosmochim. Acta* **56**, 419–430

Skulan J. L., DePaolo D. J., and Owens T. L. (1997) Biological control of calcium isotopic abundances in the global calcium cycle. *Geochim. Cosmochim. Acta* **61**, 2505–2510.

Spero H. J., Bijma J., Lea D. W., and Bemis B. E. (1997) Reassessing foraminiferal carbon and oxygen isotope data: Effects of sea water carbonate chemistry. *Nature* **390**, 497–500.

Zhu P. and Macdougall J. (1998) Calcium isotopes in the marine environment and the oceanic calcium cycle, *Geochim. Cosmochim. Acta* **62**, 1691–1698.

Zhu P. (1999) Calcium isotopes in the Marine Environment. Ph. D. Thesis, University of California, San Diego.

Conference-Abstracts

EUG XI Meeting 2001, Strassbourg

Determination of δ^{44}Ca-ratios on *G. bulloides* (ODP Leg 183 Site 1138) using a new TIMS multicollector technique

A. Heuser[1], A. Eisenhauer[1], N. Gussone[1], B. Bock[1], F. Böhm[1], Th.F. Nägler[2]

[1] GEOMAR Forschungszentrum für marine Geowissenschaften, Wischhofstr. 1–3, 24148 Kiel, Germany

[2] Mineralogisch-Petrographisches Institut, Universität Bern, Erlachstr. 9a, 3012 Bern, Switzerland

During the last years the precision of calcium isotope measurements (δ^{44}Ca) has considerably improved due to technical improvement in mass spectrometer instrumentation, and the application of the double spike technique. Recent progress in Ca-isotope measurements showed that calcium isotopic variations can be used in order to reconstruct past sea surface temperature (Nägler et al., 2000) and past global fluctuations of continental weathering fluxes (De La Rocha & DePaolo, 2000).

Here we present a rapid method for the determination of calcium isotope compositions by thermal ionisation mass spectrometry (TIMS). The main improvement is the use of a multicollector analyzer and the use of a ^{43}Ca/^{48}Ca double spike. The analyses were performed on a MAT262 RPQ^{+} using a two step dynamic mode. In the first step masses 40, 41, 42 and 43 are measured simultaneously and in the second step masses 44 and 48 are measured simultaneously. Interferences of ^{40}K are monitored on mass 41 and can generally be neglected. Comparison of the result from this new method to results from simple peak jumping indicate that the new method show comparable and precision. Measured ratios are corrected for the double spike by an external numerical algorithm using an iterative approach (Compston & Oversby 1969). The δ^{44}Ca-ratios are normalized to the ^{44}Ca/^{40}Ca ratio of NIST SRM 915a (pure $CaCO_3$). The long term reproducibility was determined by repeated measurements of this standard and amounts to $\pm\,0.08\,‰$(δ-units).

The new technique has been applied to δ^{44}Ca variations of planktonic foraminifera (*G. bulloides*) from ODP Leg 183 Site 1138 (Kerguelen Plateau). The results show that the δ^{44}Ca ratios vary during the last 22 Ma within a range of about 1 ‰. The δ^{44}Ca values decrease from the present to a δ^{44}Ca-minimum at about 16 Ma. This observation can be interpreted in terms of global SST-cooling or an increase of ocean calcium concentration due to enhanced rates of continental weathering.

References:

Compston W. and Oversby V. (1969) Lead Isotopic Analysis Using A Double Spike. *J. Geophys. Res.* **74**, 4338–4348.

De La Rocha C.L. and DePaolo D.J. (2000) Isotopic Evidence for Variations in the Marine Calcium Cycle Over the Cenozoic. *Science* **289**, 1176–1178.

Nägler Th.F., Eisenhauer A., Müller A., Hemleben C., and Kramers J. (2000) The δ^{44}Ca-temperature calibration on fossil and cultured *Globigerinoides sacculifer*: New tool for reconstruction of past sea surface temperatures. *Geochem. Geophys. Geosyst.* **1**, 2000GC000091.

AGU Spring Meeting 2001, Boston

A Calcium Isotope Record from the Miocene of the Kerguelen Plateau (Southern Indian Ocean) - Global or Local Signal?

A. Heuser[1], F. Böhm[1], A. Eisenhauer[1], W.-Chr. Dullo[1], Leg 183 Shipboard Scientific Party

[1] GEOMAR Forschungszentrum, Wischhofstr. 1–3, 24148 Kiel, Germany

The Kerguelen Plateau is a mostly drowned oceanic plateau in the Indian sector of the Southern Ocean. It formed during the late Cretaceous as a temporarily subaerial volcanic plateau. Today most of the plateau is situated south of the polar front and many parts are at water depths of less than 2000 m. Several holes drilled during ODP Legs 119, 120 and 183 offer the opportunity to study Miocene sedimentary sequences from a southern high latitude setting.

The Miocene of the Kerguelen Plateau shows a pronounced facies shift from carbonate dominated sediments in the Early and Middle Miocene to opaline and volcanoclastic domination in the Pliocene and Pleistocene. The facies transition started during the Late

Miocene, when around 11 Ma carbonate accumulation rates began to decline. A short period of lowered carbonate contents at about 8.5 to 9.5 Ma may be an expression of the Late Miocene "carbonate crash". During the transitional time hiatuses were widespread and there appears to exist no sedimentary record from about 4.5 to 7 Ma, when a major hiatus formed at all investigated sites. Almost pure diatom oozes were deposited at the southern sites during the latest Miocene and in the Pliocene. At the more northern sites, however, there is sufficient carbonate during this time to allow almost continuous sampling of carbonate components from Early Miocene through Pleistocene. We collected planktonic foraminifera from the most continuous record, cored at ODP Site 1138, at a resolution of about 1 Ma from Late Miocene to Pleistocene for determination of calcium and strontium isotope ratios.

Our calcium isotope record correlates well with the data of De La Rocha & DePaolo (2000). Our better temporal resolution allows to date the Middle Miocene calcium isotope minimum as 15 Ma. Comparison with a benthic foraminifera oxygen isotope record from the nearby ODP site 747 (Wright & Miller, 1992) shows a parallel rise of calcium and oxygen isotopes from the minimum at 15 Ma to a Late Miocene maximum at about 7 Ma. Comparing calcium and strontium isotope records, we find that the the minimum further correlates with the well known Middle Miocene inflection in the seawater strontium isotope curve.

During the Pliocene/Pleistocene cooling no correlation between oxygen and calcium isotopes can be observed. Thus, it is not possible to explain our observations by local temperature effects. More likely, the calcium isotope record reflects global changes in the oceanic calcium reservoir through changing weathering fluxes or dissolution and deposition of calcium carbonates. If this is the case, global events like the Late Miocene "carbonate crash" or the Miocene/Pliocene lowering of the carbonate compensation depth should have left traces in the calcium isotope record as recorded in planktonic foraminifera.

References:

De La Rocha C.L. and DePaolo D.J. (2000) Isotopic Evidence for Variations in the Marine Calcium Cycle Over the Cenozoic. *Science* **289**, 1176–1178

Wright J.D. and Miller K.G. (1992) Miocene stable isotope stratigraphy, Site 747, Kerguelen Plateau. *Proc. ODP Sci. Res.* **120**, 855–866

AGU Fall Meeting 2001, San Francisco

Comparison of δ^{44}Ca Records of Foraminifers From the Indian Ocean and the Western Equatorial Pacific Ocean

A. Heuser[1,2], A. Eisenhauer[2], P.N. Pearson[3], N. Gussone[2], B. Bock[2], F. Böhm[2], Th.F. Nägler[4]

[1] Graduiertenkolleg "Dynamik globaler Kreisläufe im System Erde", Wischhofstr. 1–3, 24148 Kiel, Germany

[2] GEOMAR, Forschungszentrum für marine Geowissenschaften, Wischhofstr. 1–3, 24148 Kiel, Germany

[3] Department of Earth Sciences, University of Bristol, Queens Road, Bristol BS8 1RJ, United Kingdom

[4] Institut für Isotopengeologie der Universität Bern, Erlachstr. 9a, 3012 Bern, Switzerland

We present a comparison of the calcium isotope record (δ^{44}Ca) of different species of planktonic foraminifers from the southern Indian Ocean (ODP Site 1138; *G. bulloides*) and the western Equatorial Pacific (ODP Site 871A and 872C; *G. ruber* and *G. trilobus*). For the latter two sites most recently a detailed δ^{11}B-record was presented by Pearson et al., 2000. The δ^{44}Ca records of both cores show decreasing δ^{44}Ca values between 21 Ma and 16 Ma. The minimum at 16 Ma is followed by rapidly increasing values until 13 Ma and then a slow increase to the present seawater values. These results are in general accord with earlier findings of De La Rocha & DePaolo (2000), although there are some discrepancies concerning core chronologies. Unfortunately, direct comparison of the δ^{44}Ca values is hindered by the use of different standard materials and normalizing procedures.

Because of our high temporal resolution of about 1 sample/Ma details of the calcium isotope evolution of the oceans can be seen. The *G. bulloides* record shows a drop of the δ^{44}Ca of 0.5 ‰ whereas the *G. ruber* record shows a drop of 0.3 ‰ at about 3 Ma. Another drop occurred between 10 and 9 Ma but with a smaller amplitude (0.15 ‰ *G. ruber* and 0.2 ‰ *G. bulloides*). Presumably, the amplitude of the observed variations depends on foraminiferal species and/or location. The δ^{44}Ca of *G. ruber* and of *G. bulloides* show maximum variations of 0.6 ‰ and about 0.7 ‰, respectively, over the studied time interval. First measurements of *G. trilobus* show a δ^{44}Ca increase of about 1.0 ‰ between 16 and 12 Ma. The records of *G. ruber* and *G. trilobus* (ODP sites 871A and 872C) show the same trend and similar δ^{44}Ca values between 19 and 16 Ma. Between 4 Ma and today the trends are similar, but the δ^{44}Ca values show an offset of about 0.25 ‰.

The trends of our δ^{44}Ca records can be interpreted in terms of changing global conditions, e.g. changing weathering rates, global temperature changes, ocean pH-variations and of oscillations of input and output calcium fluxes.

References:

De La Rocha C.L. and DePaolo D.J. (2000) Isotopic Evidence for Variations in the Marine Calcium Cycle Over the Cenozoic. *Science* **289**, 1176–1178.

Pearson P.N. and Palmer M.R. (2000) Atmospheric carbon dioxide concentrations over the past 60 million years. *Nature* **406**, 695–699.

AGU Fall Meeting 2002, San Francisco

A Reconstruction of Seawater δ^{44}Ca from Foraminiferal Records of the Western Equatorial Pacific Ocean

A. Heuser[1], A. Eisenhauer [1], P.N. Pearson[2], F. Böhm [1], N. Gussone [1]

[1] GEOMAR, Forschungszentrum für marine Geowissenschaften, Wischhofstr. 1–3, 24148 Kiel, Germany

[2] Department of Earth Sciences, University of Bristol, Queens Road, Bristol BS8 1RJ, United Kingdom

We present δ^{44}Ca records of three different foraminifera species (*G. ruber/subquadratus, G. trilobus* and *Globigerinella spp.*) from the western equatorial Pacific (ODP Site 871 and 872) corresponding to the last 23 Ma. Assuming a constant calcium isotope fractionation factor (α) between seawater and the foraminiferal calcium carbonate the δ^{44}Ca of the past seawater ($\delta^{44}Ca_{sw}$) can be reconstructed. The $\delta^{44}Ca_{sw}$ records of *G. ruber/subquadratus* and of *Globigerinella spp.* are similar. The two records show a decrease of the $\delta^{44}Ca_{sw}$ between 25 and 16 Ma of about 0.5 ‰ followed by an increase of about 0.5 ‰ between 16 and 3 Ma. Between 3 Ma and the present the $\delta^{44}Ca_{sw}$ decreases again by about 0.25 ‰. The $\delta^{44}Ca_{sw}$ calculated from *G. trilobus* record shows a similar trend between 22 and 6 Ma but is isotopically lighter by about $\sim$0.2 ‰ compared to the other two records: The $\delta^{44}Ca_{sw}$ of Site 871 is positively related to its $^{87}Sr/^{86}Sr$ record. This indicates that the $\delta^{44}Ca_{sw}$ is triggered by the balance of the input of continental weathering products and submarine volcanism and the output of biogenically driven calcium carbonate precipitation.

From *G. sacculifer* being closely related to *G. trilobus* it is known that calcium isotope

fractionation is temperature dependent (Nägler et al. 2000; Gussone et al. 2002). Thus the differences between the $\delta^{44}Ca_{sw}$ from *G. trilobus* and the mean of the $\delta^{44}Ca_{sw}$ of *G. ruber/subquadratus* and *Globigerinella spp.* can be interpreted as a temperature related signal. Using the known correlation of the fractionation factor (α) and temperature (T) of *G. sacculifer* the calculated temperature varies between 26.5 °C and 29 °C over the past 23 Ma. The calculated temperatures the *G. trilobus* record shows a cooling trend between 23 and 16 Ma followed by slight warming between 16 and 3 Ma. Between 3 and 1.5 Ma a rapid warming can be observed. These observed temperature variations are in the order of 1–2 °C. In contrast, the $\delta^{18}O$ record of Site 871 and the global evolution of the $\delta^{18}O$ record of benthic foraminifers show a cooling between 16 Ma and 1.5 Ma being in contradiction to the $\delta^{44}Ca$ based temperature reconstructions of the *G. trilobus* record.

References:

Gussone, N., Eisenhauer, A., Dietzel, M., Heuser, A., Spero, H., Bijma, J., Böhm, F., Nägler, Th. F., *Geophysical Research Abstracts* **4**, 2002 (EGS02-A-02944)

Nägler T. F., Eisenhauer A., Müller A., Hemleben C., and Kramers J. (2000) The $\delta^{44}Ca$-temperature calibration on fossil and cultured *Globigerinoides sacculifer*: New tool for reconstruction of past sea surface temperatures. *Geochem. Geophys. Geosyst.* **1**, 2000GC000091

Ca double spike correction using Excel97/2k

The listing below shows the definition of the function "CaCalc(*arguments*)" programmed in VBA for MS Excel97/2k. This function is the iterative algorithm for the Ca double spike correction (fig. 2.5). The function requires the input of 5 arguments separated by a semicolon: a spike number, the measured $^{43}Ca/^{48}Ca$, $^{44}Ca/^{48}Ca$ and $^{40}Ca/^{48}Ca$ ratios of the spiked sample and a logical value (True/False). The logical value is used for the output of either the $\delta^{44}Ca$ value (True) or of the $^{44}Ca/^{40}Ca$ ratio (False). Each used Ca double spike gets a number and its composition has to be defined within the program.
Short overview of the parts of the listing:

lines	event
1+2	Definition of the function 'CaCalc'
4–28	Declaration of the variables and the type of the variables
30	Definition of the value for the end of the iteration
34–38	"Russell"-values as starting parameters for the iterative routine
40–60	Definition of the Ca double spike compositions; as we have two different $^{43}Ca/^{48}Ca$ double spikes the numbers "1" and "3" are defined
63	setting of the cycles counter
67	Fig. 2.5 equation: (11)
68	Fig. 2.5 equation: (12)
69	Fig. 2.5 equation: (13)
71–72	Fig. 2.5 equation: (1)
73	Fig. 2.5 equation: (2)
74	Fig. 2.5 equation: (3)
75	Fig. 2.5 equation: (4)
76	Fig. 2.5 equation: (5)
77	Fig. 2.5 equation: (6)
78–79	Fig. 2.5 equation: (7)
80–81	Fig. 2.5 equation: (8)
82	Fig. 2.5 equation: (9)
84	Fig. 2.5 equation: (10)
95	End of the iterations if one the defined conditions is fulfilled
99+101	Output of the result either as δ-value (line 99) or as $^{44}Ca/^{40}Ca$-ratio (line 101).

```
Static Function CaCalc(Spike As Byte, Mix_4348 As Double,
   Mix_4448 As Double, Mix_4048 As Double, Delta As Boolean)

'Dimensionierung der Variablen
Dim MixCalc_4348 As Double
Dim MixCalc_4448 As Double
Dim MixCalc_4048 As Double
Dim MixCalc_4440 As Double
Dim Spike_4348 As Double
Dim Spike_4448 As Double
Dim Spike_4048 As Double
Dim Spike_4440 As Double
Dim PureSample_4348 As Double
Dim PureSample_4448 As Double
Dim PureSample_4048 As Double
Dim PureSample_4440 As Double
Dim PureSample_4348_recalc As Double
Dim PureSample_4448_recalc As Double
Dim PureSample_4048_recalc As Double
Dim PureSample_4440_recalc As Double
Dim beta As Double
Dim fu As Double
Dim Q40 As Double
Dim Qmean As Double
Dim DeltaQ As Double
Dim Q4840 As Double
Dim Q4844 As Double
Dim Krit As Double

'Kriterium fuer Beendung der Iteration
Krit = 0.000000001
Dim Counter As Single

'Russell-Werte
PureSample_4448 = 11.27268628
PureSample_4348 = 0.731146432
PureSample_4048 = 531.5409762
PureSample_4440 = 0.021207558

'Spike-Daten und Wert auf den normalisiert wurde
Select Case Spike
Case 1 'Bern
    If Mix_4348 = 0 Then Mix_4348 = 0.786624
    Spike_4348 = 0.78664337
    Spike_4448 = 0.048534265
    Spike_4048 = 0.147728596
    Spike_4440 = 0.328536698
Case 3 'Kaiser-Karl
    If Mix_4348 = 0 Then Mix_4348 = 0.750546274
    Spike_4348 = 0.750546274
    Spike_4448 = 0.044730243
    Spike_4048 = 0.151914776
    Spike_4440 = 0.294443004
Case Else
```

```
55      If Mix_4348 = 0 Then Mix_4348 = 0.786624
        Spike_4348 = 0.78664337
        Spike_4448 = 0.048534265
        Spike_4048 = 0.147728596
        Spike_4440 = 0.328536698
60  End Select

    'Schleifenzaehler fuer Abbruch der Iteration
    Counter = 0

65  'Iteration
    Do
        Q4844 = (Mix_4448 - Spike_4448) / (PureSample_4448 - Mix_4448)
        Q4840 = (Mix_4048 - Spike_4048) / (PureSample_4048 - Mix_4048)
        Qmean = (Q4844 + Q4840) / 2
70      DeltaQ = Q4844 - Q4840
        MixCalc_4348 = (Spike_4348 + Qmean * PureSample_4348) / _
                       (1 + Qmean)
        beta = Log(MixCalc_4348 / Mix_4348) / Log(43 / 48)
        MixCalc_4048 = Mix_4048 * (40 / 48) ^ beta
75      MixCalc_4448 = Mix_4448 * (44 / 48) ^ beta
        MixCalc_4440 = MixCalc_4448 / MixCalc_4048
        Q40 = Qmean * PureSample_4048 / Spike_4048
        PureSample_4440_recalc = (1 + 1 / Q40) * MixCalc_4440 - _
                                 (1 / Q40) * Spike_4440
80      fu = Log(PureSample_4440_recalc / PureSample_4440) / _
             Log(44 / 40)
        PureSample_4448_recalc = PureSample_4448 * (44 / 48) ^ fu
        PureSample_4348_recalc = PureSample_4348 * (43 / 48) ^ fu
        PureSample_4048_recalc = PureSample_4048 * (40 / 48) ^ fu
85      Mix_4448 = MixCalc_4448
        Mix_4348 = MixCalc_4348
        Mix_4048 = MixCalc_4048
        PureSample_4448 = PureSample_4448_recalc
        PureSample_4348 = PureSample_4348_recalc
90      PureSample_4048 = PureSample_4048_recalc
        PureSample_4440 = PureSample_4440_recalc
        Counter = Counter + 1

    'Ende Iteration bei Erfuellung eines der Kritrien
95  Loop Until Abs(DeltaQ) < Krit Or Counter = 10

    'eigentliches Ergebnis
    If Delta = "Wahr" Then
    CaCalc = (PureSample_4440_recalc * 47.153 - 1) * 1000
100 Else:
    CaCalc = PureSample_4440_recalc
    End If
    End Function
```

Danksagung

Ich bedanke mich bei all denen, die mir mittelbar und unmittelbar auf vielfältige Weise bei dieser Arbeit geholfen haben.
Meinem Betreuer Prof. Anton Eisenhauer danke ich für seine Unterstützung und Betreuung meiner Arbeit. Die viele intensiven und meist fruchtbaren Diskussionen haben entscheidend zum Gelingen dieser Arbeit beigetragen. Auch für die Finanzierung einer halben Stelle im Anschluss an mein Stipendium bedanke ich mich herzlich.
Nikolaus Gussone als Leidensgenossen in Sachen Calcium-Isotope danke ich für die sehr gute Zusammenarbeit und die unzähligen interessanten Diskussionen und Gespräche nicht nur über Calcium-Isotope.
Ein ganz großes "Dankeschön" auch an Barbara Bock, die immmer ein offenes Ohr für Probleme und Nöte hatte und unermüdlich meine Manuskripte Korrektur gelesen hat. Auch für ihre Unterstützung bei meinen ersten "Gehversuchen" am TIMS sei ihr herzlich gedankt.
Thomas Nägler (Bern) danke ich für seine große Unterstützung vor allem zu Beginn der Arbeit. Seine Erfahrungen mit Calciumisotopen-Messungen waren eine sehr große Hilfe. Bedanken möchte ich mich bei ihm auch für das Bereitstellen eines fertigen $^{43}Ca/^{48}Ca$ Doppelspikes.
Florian Böhm danke ich für das zur Verfügung Stellen von Proben vom Kerguelen-Plateau, viel konstruktive Kritik und für die vielen Diskussionen über Foraminiferen, $\delta^{18}O$ und alles was "Paläo" im Namen trägt.
Paul Pearson (Bristol) danke ich für die Bereitstellung des umfangreichen Probenmaterials aus dem westlichen äquatorialen Pazifik.
Ich danke Dorothee Hippler (Bern), Prof. Peter Stille und Anne-Désirée Schmitt (Strasbourg) für die gute Kooperation und einigen sehr wertvollen Diskussionen beim Kieler Calciumisotopen-Workshop.
Volker Karpen gilt ein besonderer Dank für die sehr gute Zusammenarbeit in Sachen"TEX/LATEX & KOMA-Script". Ohne ihn, hätte ich mich wohl mit der Textverarbeitung eines namhaften Software-Herstellers rumgeärgert.
Bedanken möchte ich mich auch bei meinen GK-Mitstreitern Sandra Bollwerk, Barbara Teichert, Béatrice Cailleau, Britta Lissinna, Evguenia Kandiano, Michael Abratis, Alex Schimanski, Thomas Walter, Volker Karpen, Nico Urbanski, Dirk Rickert, Ralf Schmidt, u.v.m. für viele (nette) GK-Stammtische, die unzähligen Grill-Happenings und das meist gute (Arbeits)Klima.
Last but not least danke ich meinen Eltern ganz herzlich für ihre große und vielfältige

Unterstützung und ihr Interesse an meiner Arbeit.

Diese Arbeit wurde im Rahmen des Graduiertenkollegs “Dynamik globaler Kreisläufe im System Erde” von der deutschen Forschungsgemeinschaft gefördert.